THE UNIVERSITY of TEXAS

SCHOOL OF HEALTH INFORMATION SCIENCES AT HOUSTON

Nuclear Magnetic Resonance

For students of HI 6001-125

“Computational Structural Biology”

Willy Wriggers, Ph.D.

http://biomachina.org/courses/structures/06.html

Introduction / Medical Applications

NMR History

1946 Bloch, Purcell	First nuclear magnetic resonance
1955 Solomon	NOE (nuclear Overhauser effect)
1966 Ernst, Anderson	Fourier transform NMR
1975 Jeener, Ernst	Two-dimensional NMR
1985 Wüthrich	First solution structure of a small protein from NOE-derived distance restraints
→ NMR is about 25 years younger than X-ray crystallography	
1987/8	3D NMR + ^{13}C, ^{15}N isotope labeling
1996/7	New long-range structural parameters:
	- residual dipolar couplings (also: anisotropic diffusion)
	- cross-correlated relaxation
	TROSY (molecular weight > 100 kDa)
2003	First solid-state NMR structure of a small protein

Nobel prizes

1944 Physics	Rabi (Columbia)
1952 Physics	Bloch (Stanford), Purcell (Harvard)
1991 Chemistry	Ernst (ETH)
2002 Chemistry	Wüthrich (ETH)
2003 Medicine	Lauterbur (Urbana), Mansfield (Nottingham)

Spin and Magnetic Moment

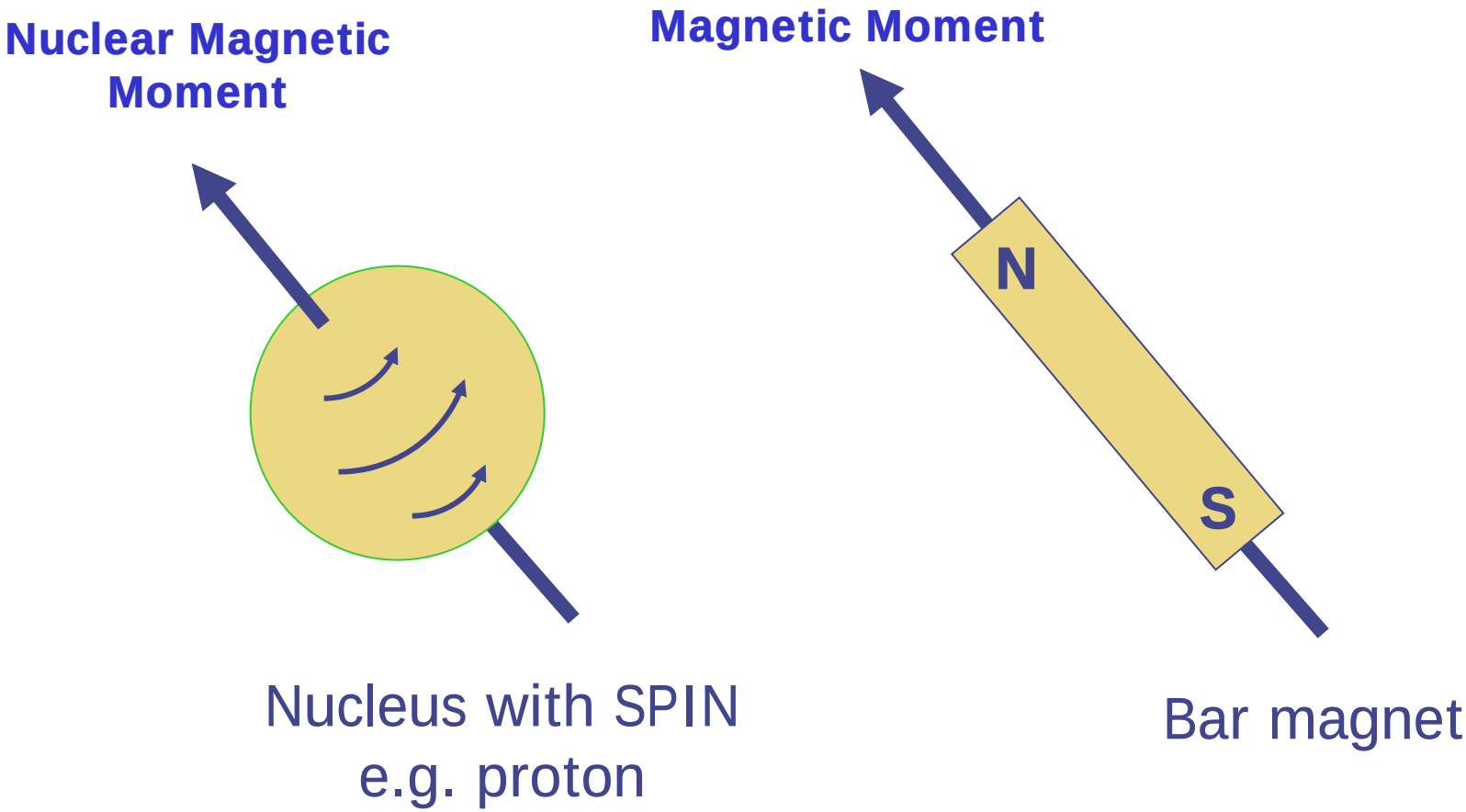

Effect of External Field

Zero External Magnetic Field

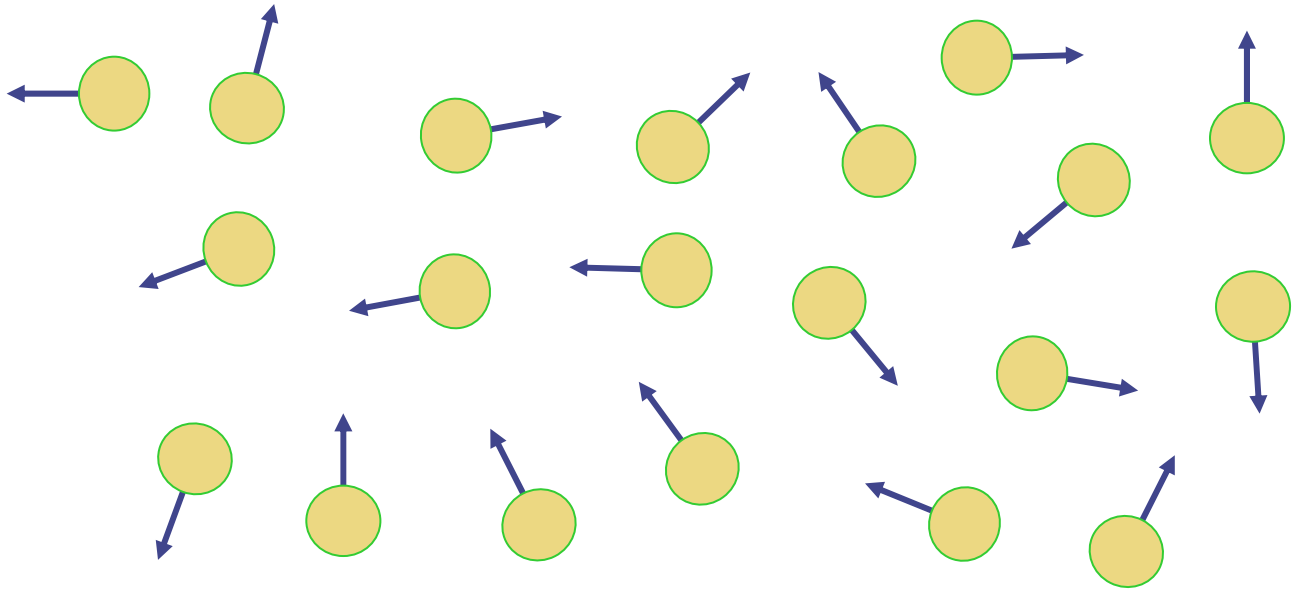

Point in random directions.

Effect of External Field

Strong External Magnetic Field

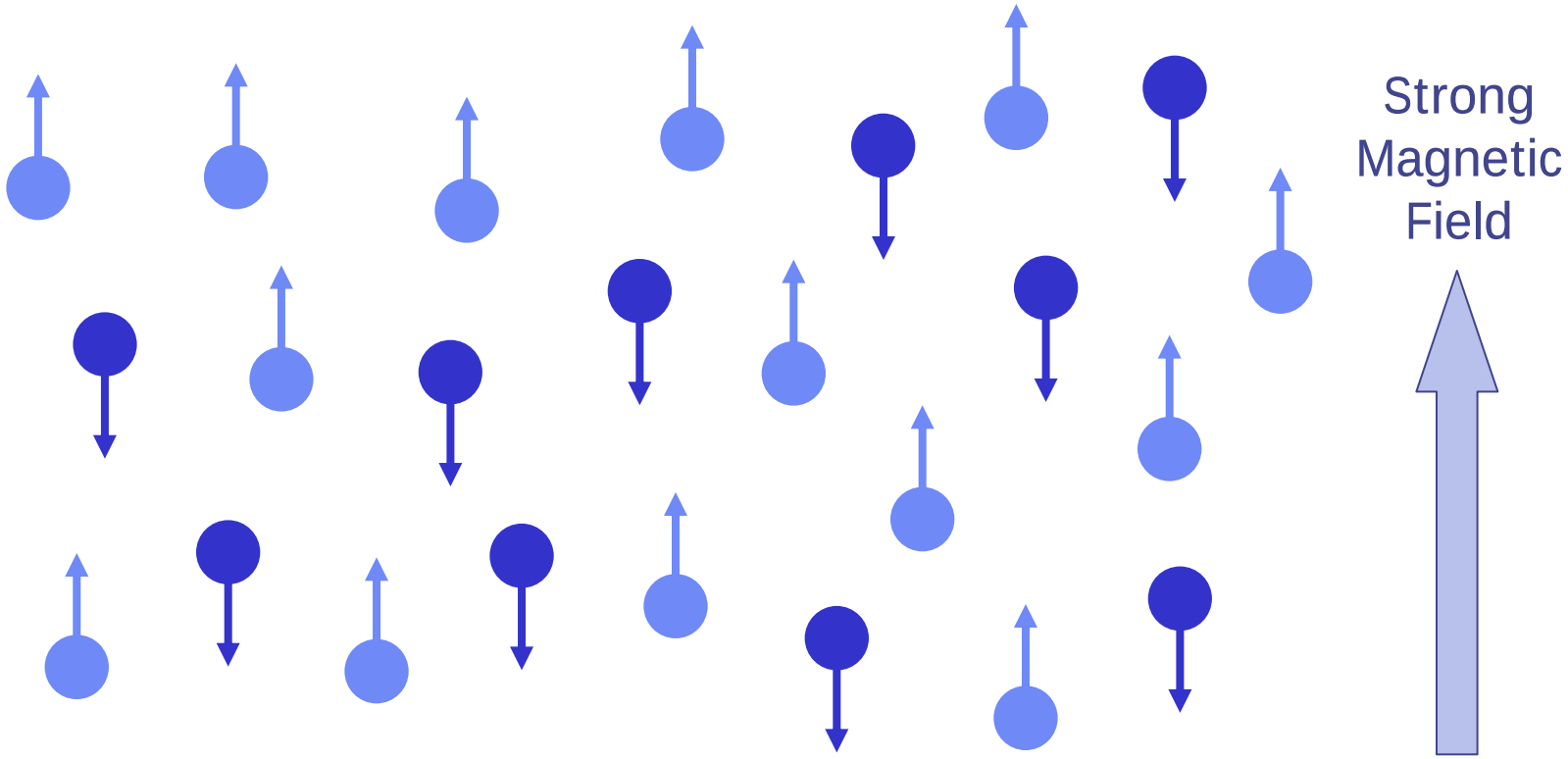

Some line up. Some line down. Just the majority line up.
Out of 1 million ~ 500,002 UP – 499,998 DOWN.

Magnetic Resonance Imaging (MRI)

Hydrogen Nucleus

- **The proton.**
- **Biggest nuclear magnetic moment of any stable nucleus.**
- **Most abundant nucleus in the human body.**
- **Water and lipid (fat).**
- **MRI gives a distribution of water and fat in the patient.**

Magnetic Resonance Imaging (MRI)

Flipping Spins

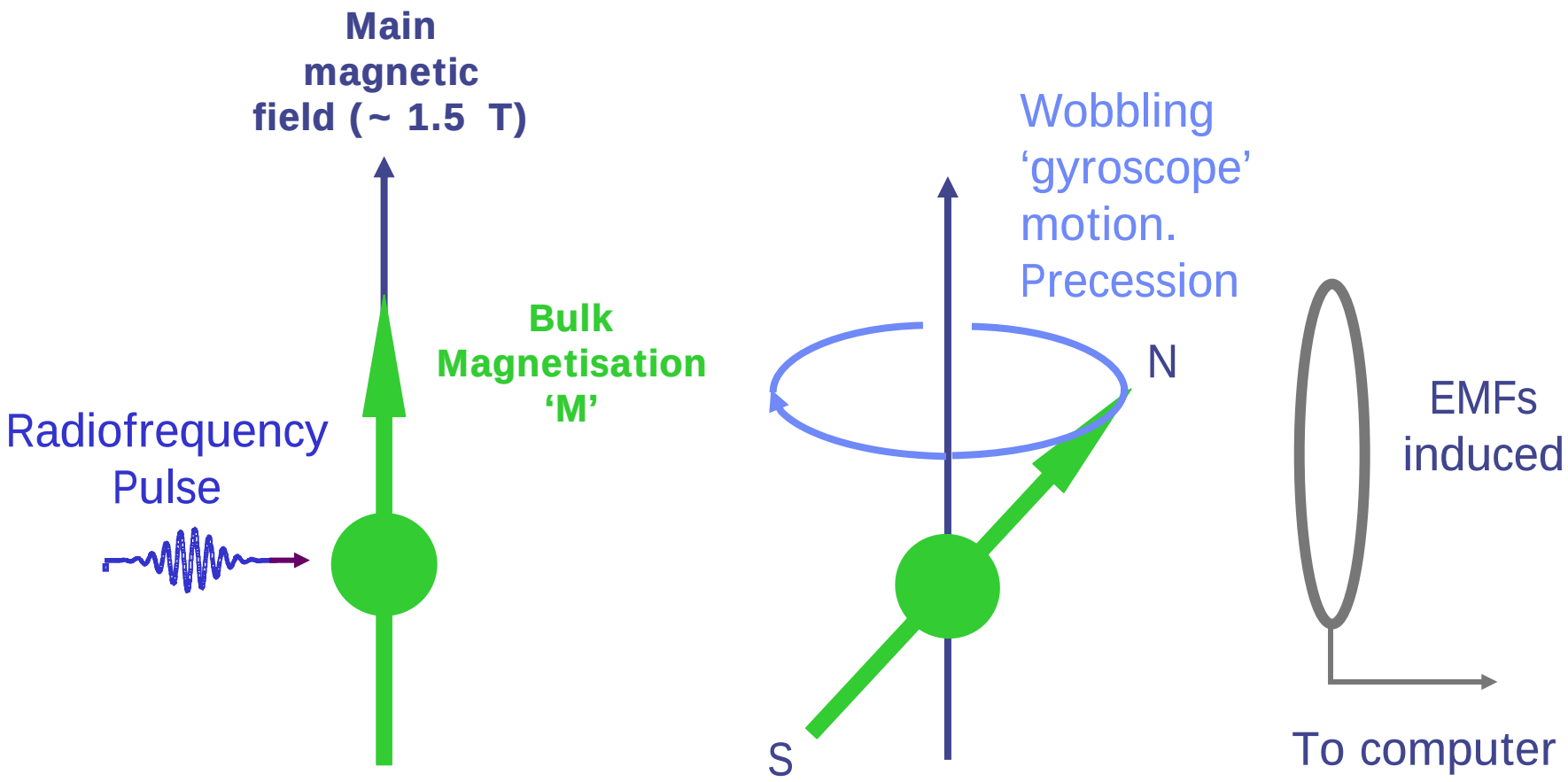

Magnetic Resonance Imaging (MRI)

Larmor Frequency

Rate of ‘wobbling’ depends on
big magnetic field strength.

$$\omega = \gamma B$$

γ = gyromagnetic ratio
(42.57 MHz per Tesla for protons)

1 Tesla ≈ 10,000 x Earth’s magnetic field.

Magnetic Resonance Imaging (MRI)

Frequency Encoding of Spatial Dimensions

No gradient

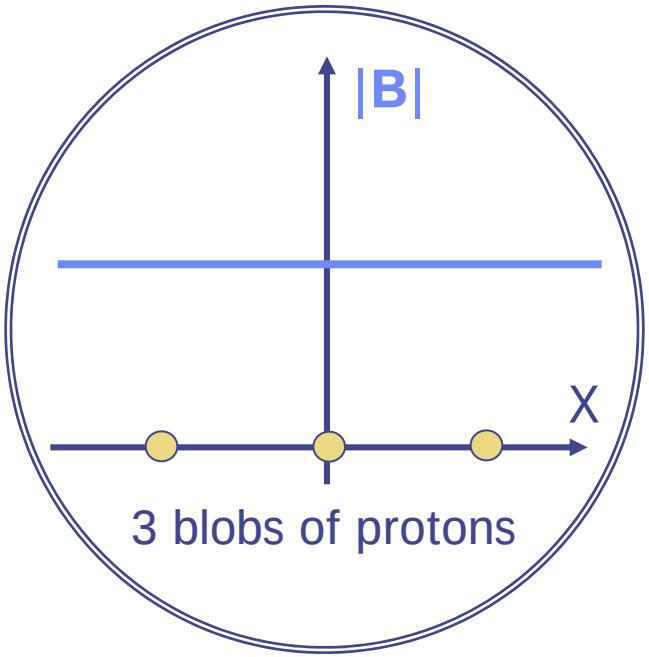

All 3 ‘see’ the same **B**
& wobble at same rate

With gradient

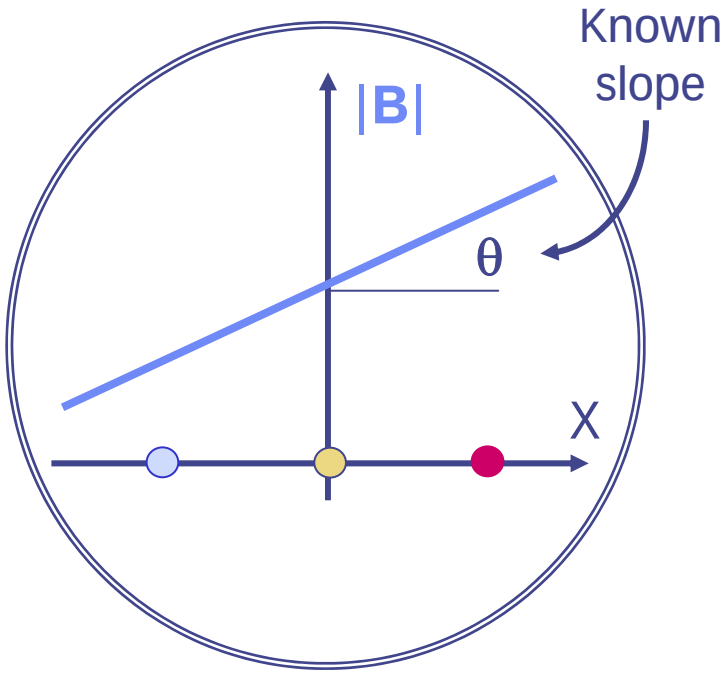

Each ‘see’ a different **B**
& wobble at 3 different rates

Magnetic Resonance Imaging (MRI)

Nuclear Relaxation and Image Contrast

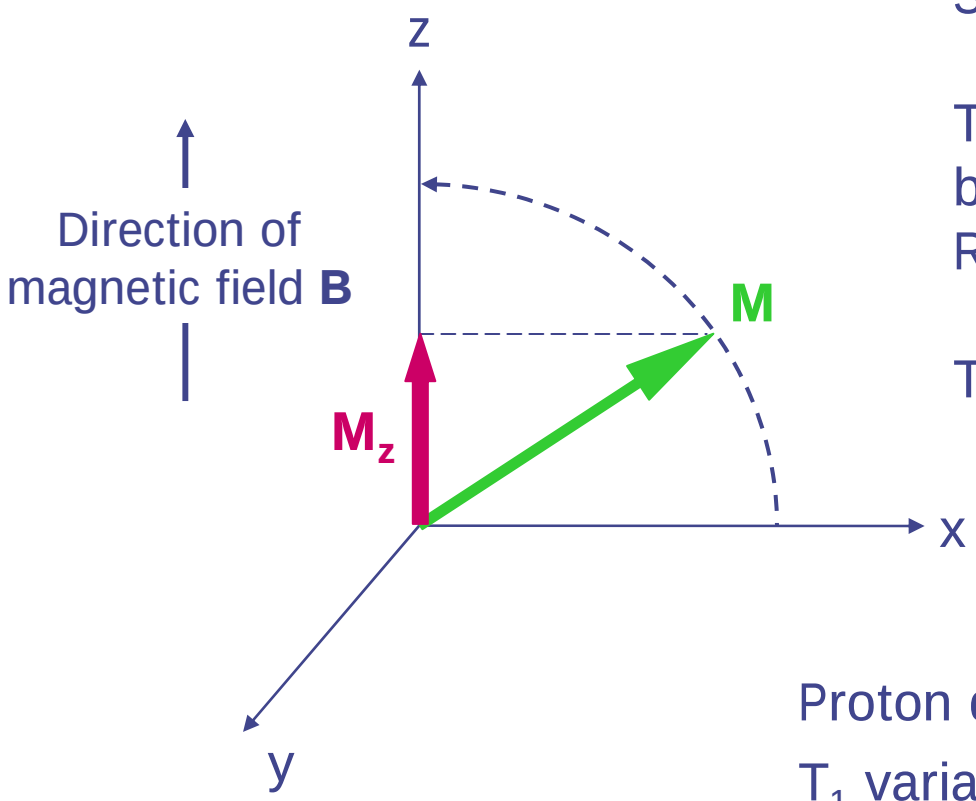

Spin-Lattice (or T_1) Relaxation.

Tipping back up of the bulk magnetisation (**M**). Re-aligns with **B**.

T_1 ~ 1 second for tissues.

Proton density variations < 10%

T_1 variations can be ~ 700%

Magnetic Resonance Imaging (MRI)

Axial Brain Images

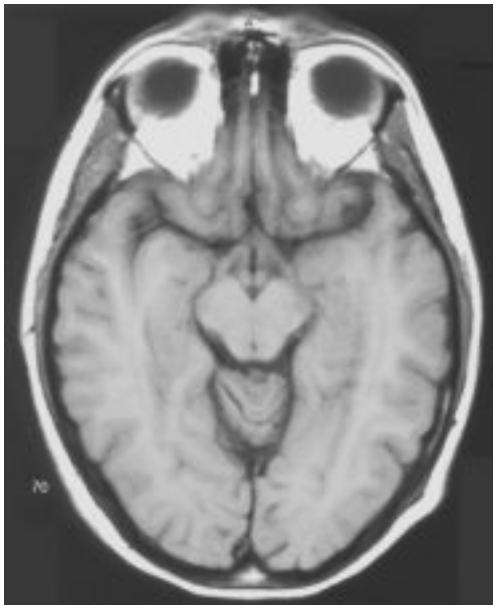

T_1-weighted

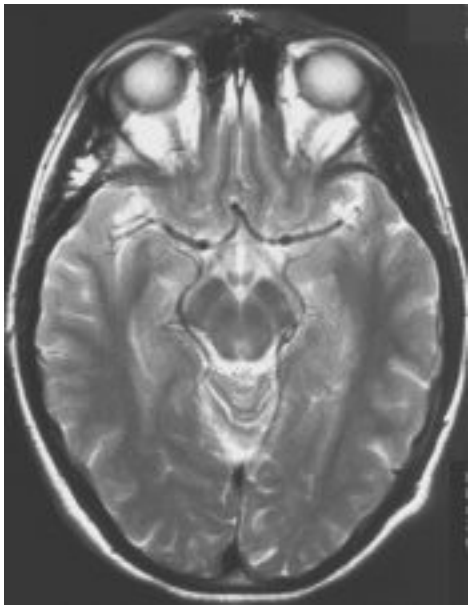

T_2-weighted

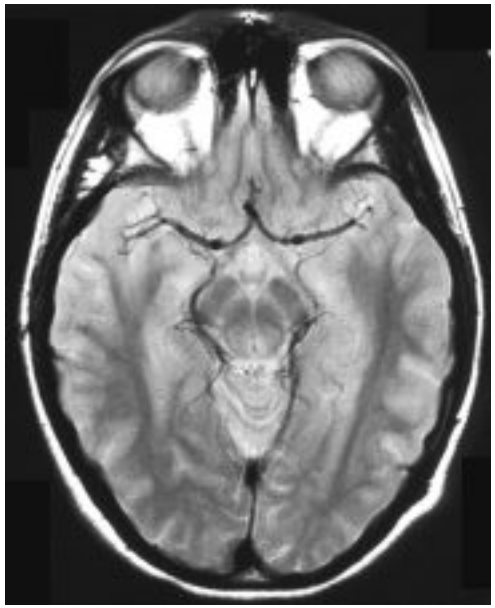

Proton density weighted

MRI Scanner

- Big superconducting magnet (~ 1.5 tesla).
- Gradient coils.
- Radiofrequency coils.

Why Biomolecular NMR?

- Structure determination of biomacromolecules
  - → no crystal needed, native-like conditions
  - → nucleic acids: difficult to crystallize, affected by crystal packing
- Characterization of dynamics and mobility, enzyme kinetics, folding
  - → picosecond to seconds time scales
  - → … with residue, e.g. amino acid, resolution !!!
- Ligand binding and molecular interactions in solution

- molecular weight: X-ray: >200 kDa, NMR < 50-100 kDa, 900 kDa!?
- → NMR and X-ray crystallography are complementary

	Proteins	Protein/DNA Protein/RNA	DNA/ RNA	Carbo- hydrates
X-ray	17821	857	688	14
NMR	2784	95	547	4

PDB Holding List 7-Oct-2003

Why Biomolecular NMR?

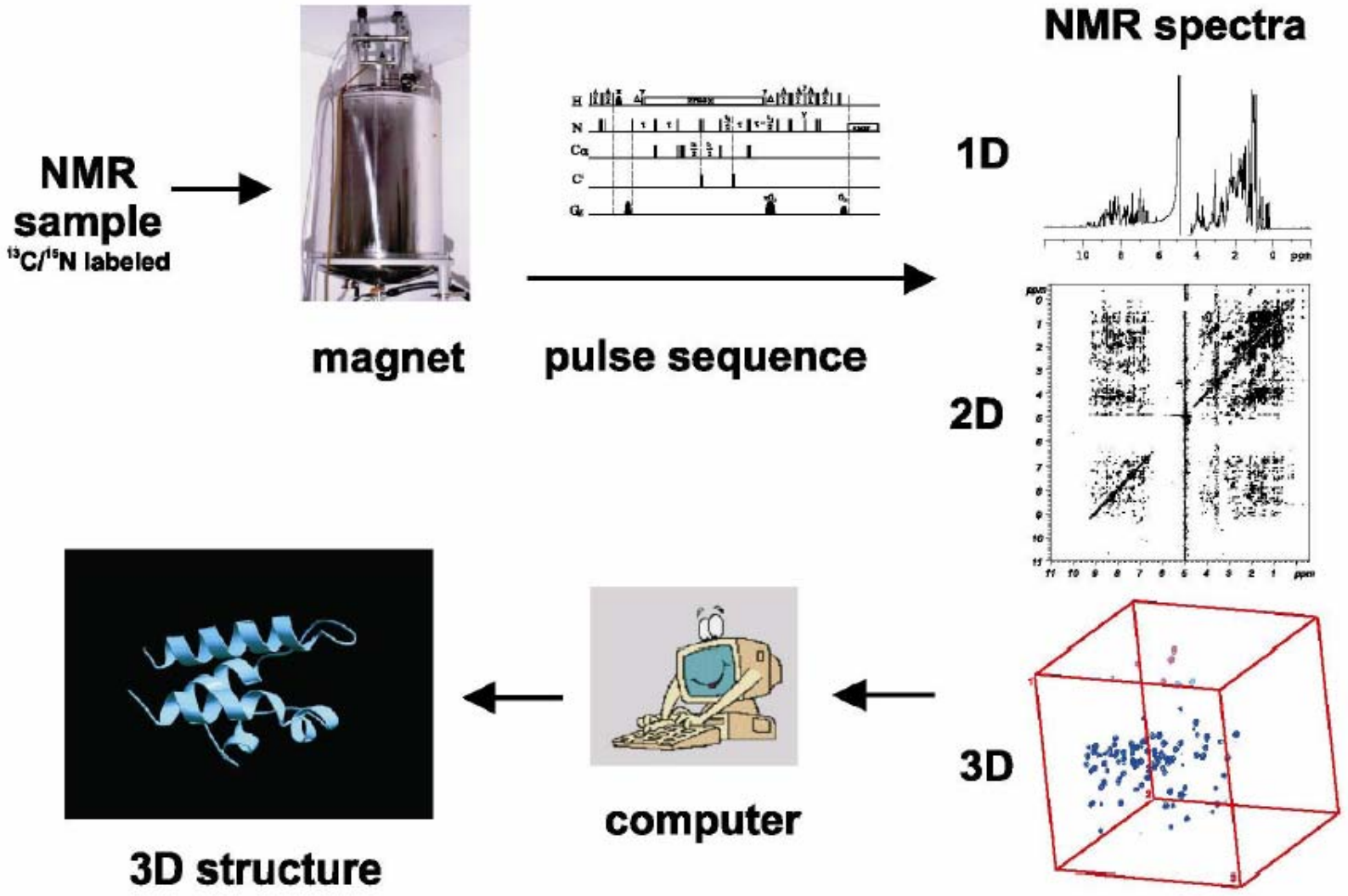

Basic Physics Concepts

Angular Momentum

A rotating object possesses angular momentum

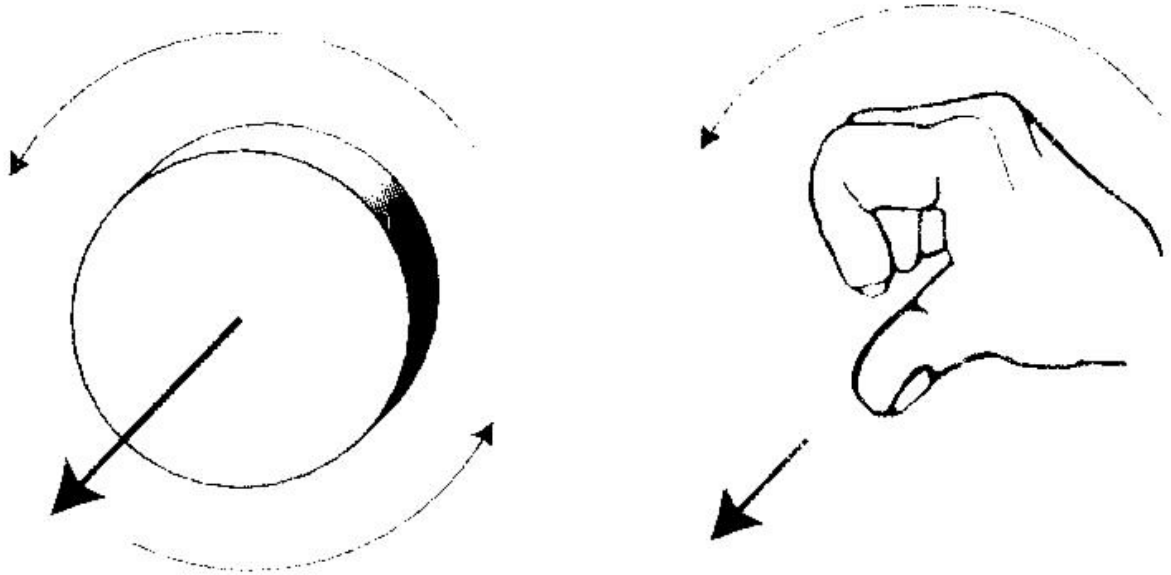

Right hand rule

Angular Momentum is *Quantized*

Example: Rotational energy of a molecule

At the level of atoms and molecules, only specific rotational states are “allowed”

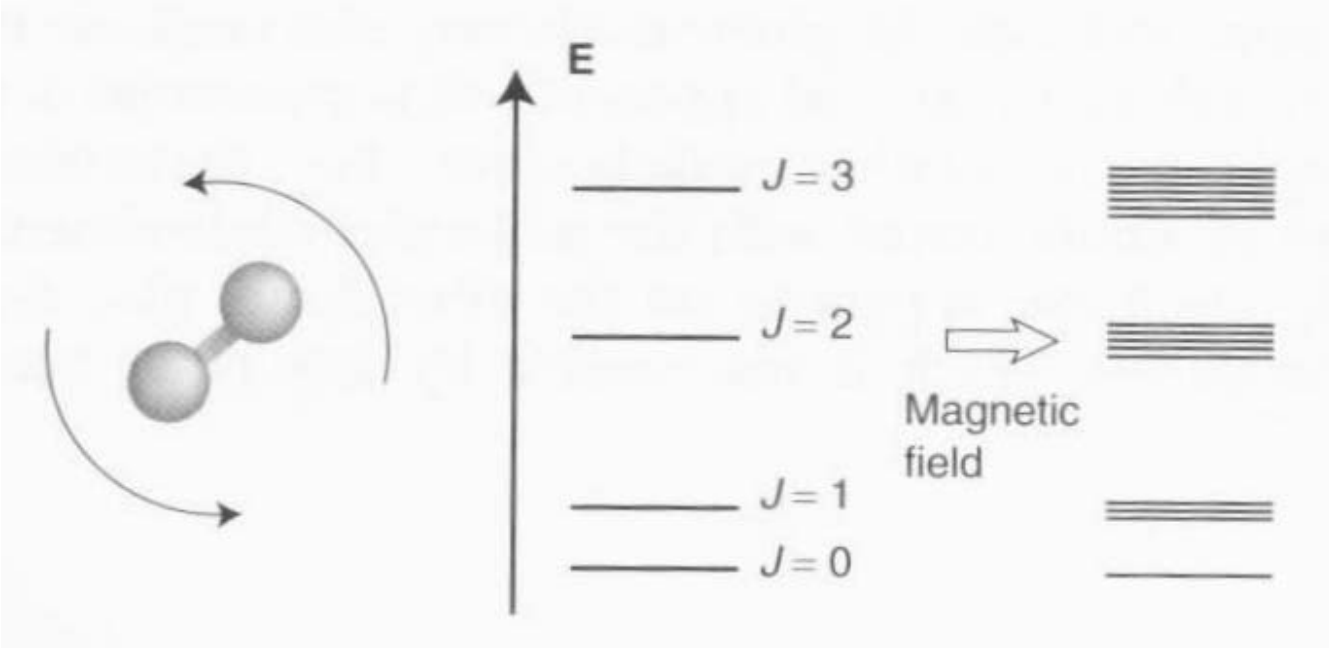

Diatomic molecule

http://instruct1.cit.cornell.edu/courses/biobm730

Spin Angular Momentum

- really an *intrinsic* property (not due to rotation)
- is quantized
- particles with spin I have 2I + 1 sublevels (degenerate without B or E field)
- bosons = particles with integer spin
- fermions = particles with half-integer spin
- arises from quantizing the electromagnetic field (Dirac)

Neutrons and Protons

3 quarks, stuck together by gluons

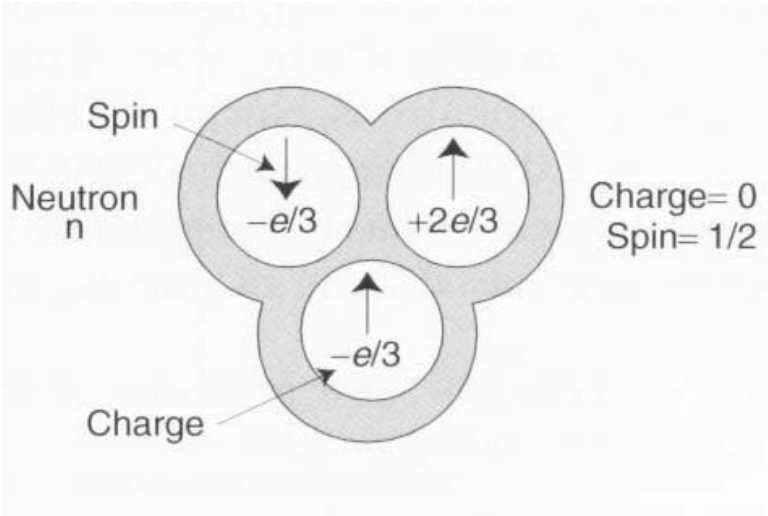

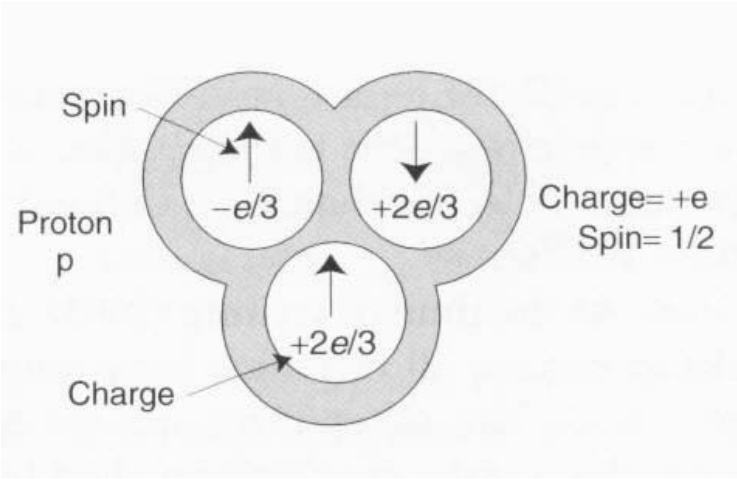

Nuclear Spin Energy Levels

no magnetic field

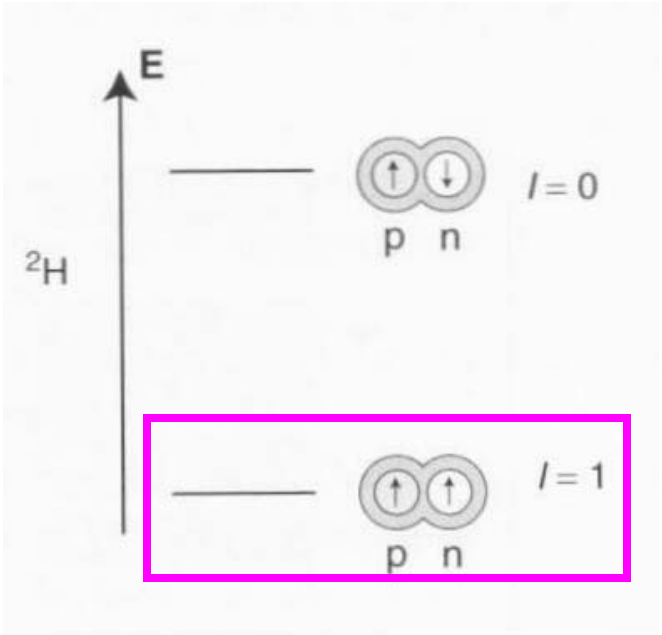

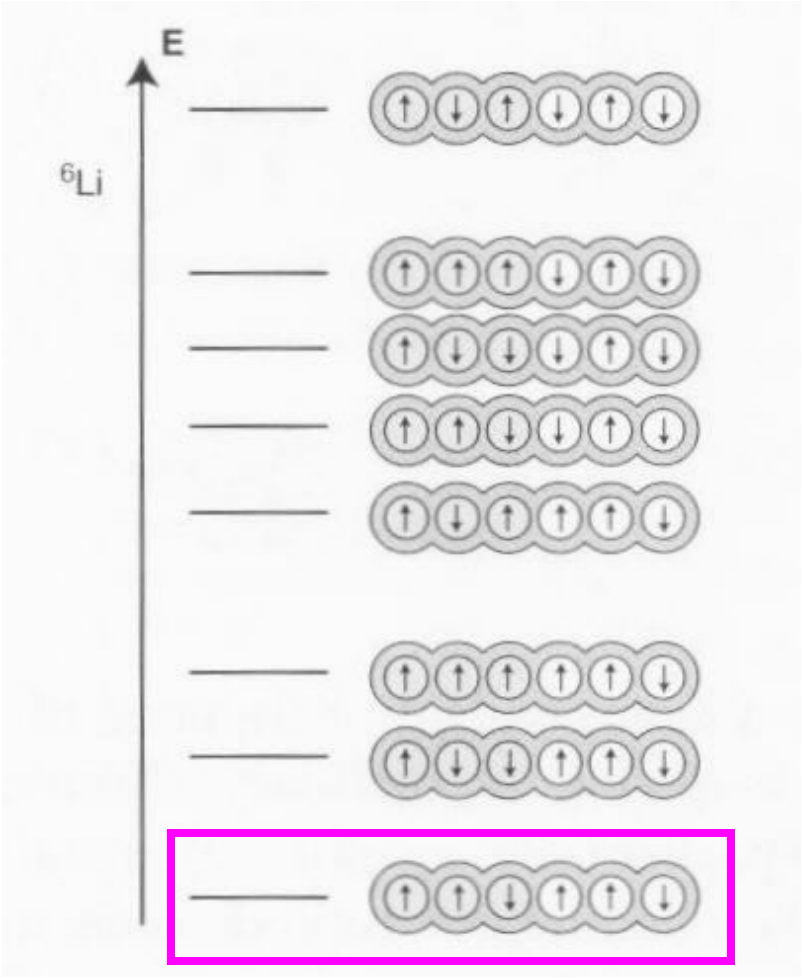

Ground state nuclear spin ~ empirical property of each isotope

Determining Spin of Isotopes

mass number	atomic number (Z)	I	NMR detectable
odd	even or odd	1/2, 3/2, 5/2 ...	yes
even	even	0	no
even	odd	1, 2, 3 ...	yes

Possible number of spin states = 2I + 1

^{1}H:	I = 1/2	2(1/2) + 1 = 2	m = ±1/2
^{14}N:	I = 1	2(1) + 1 = 3	m = -1, 0, 1

NMR-Active Nuclei in Proteins

Naturally abundant

1H, spin ½

31P, spin ½

Enriched via bacterial expression (isotope labeling)

2H, spin 1

13C, spin ½

15N, spin ½

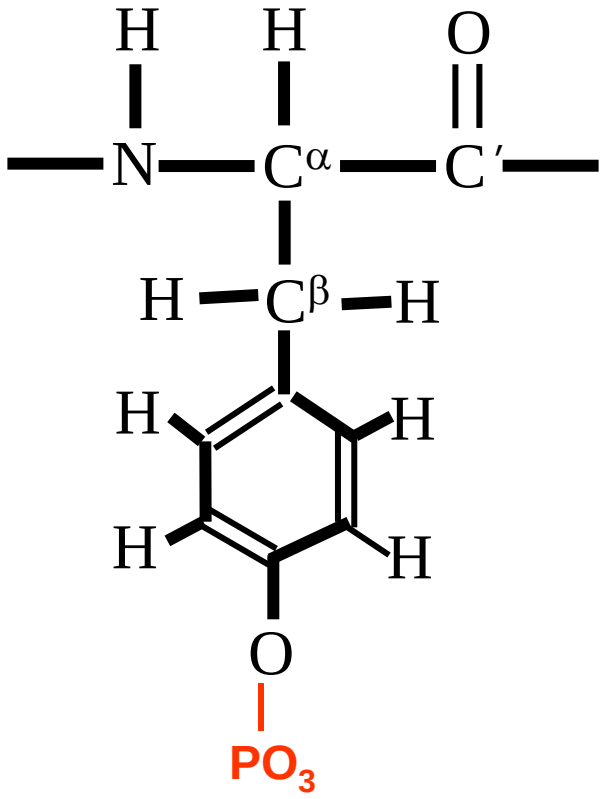

The Gyromagnetic Ratio

For spin angular momentum of the nucleus,

$$\vec{\mu} = \frac{g_N \mu_N \vec{I}}{\hbar}$$

where g_N is the nuclear g-factor and μ_N is the nuclear magneton

Defining the "gyromagnetic ratio" of μ and I:

$$\frac{g_N \mu_N}{\hbar} = \gamma$$

the relationship between angular momentum and magnetic moment becomes:

$$\vec{\mu} = \gamma \vec{I}$$

Hence, the angular momentum and magnetic moment vectors associated with nuclear spin are pointed in the same direction and are related by a constant.

Gyromagnetic Ratio, γ

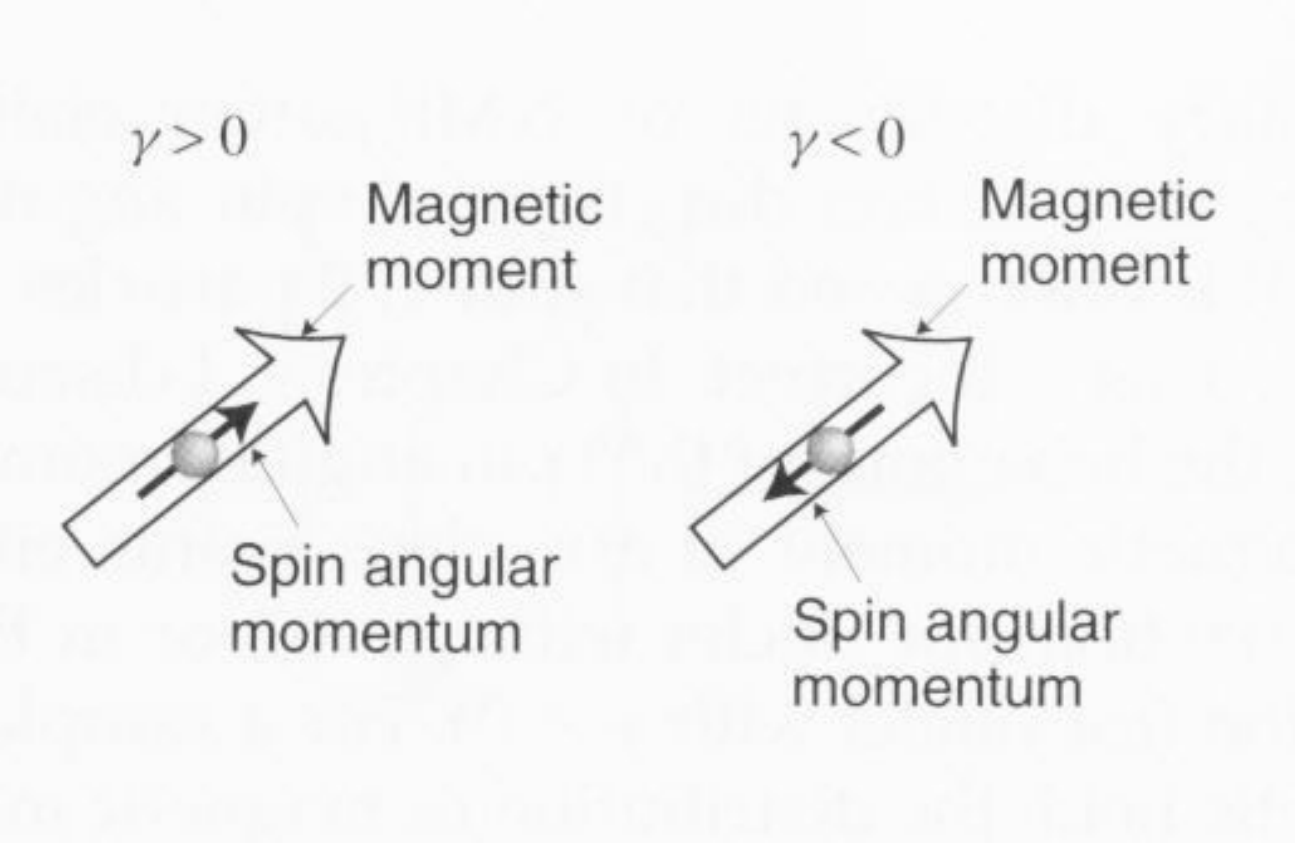

http://instruct1.cit.cornell.edu/courses/biobm730

Magnetic Energy

$$E = -\vec{\mu} \cdot \vec{B}$$

- Magnetic energy depends on the relative orient

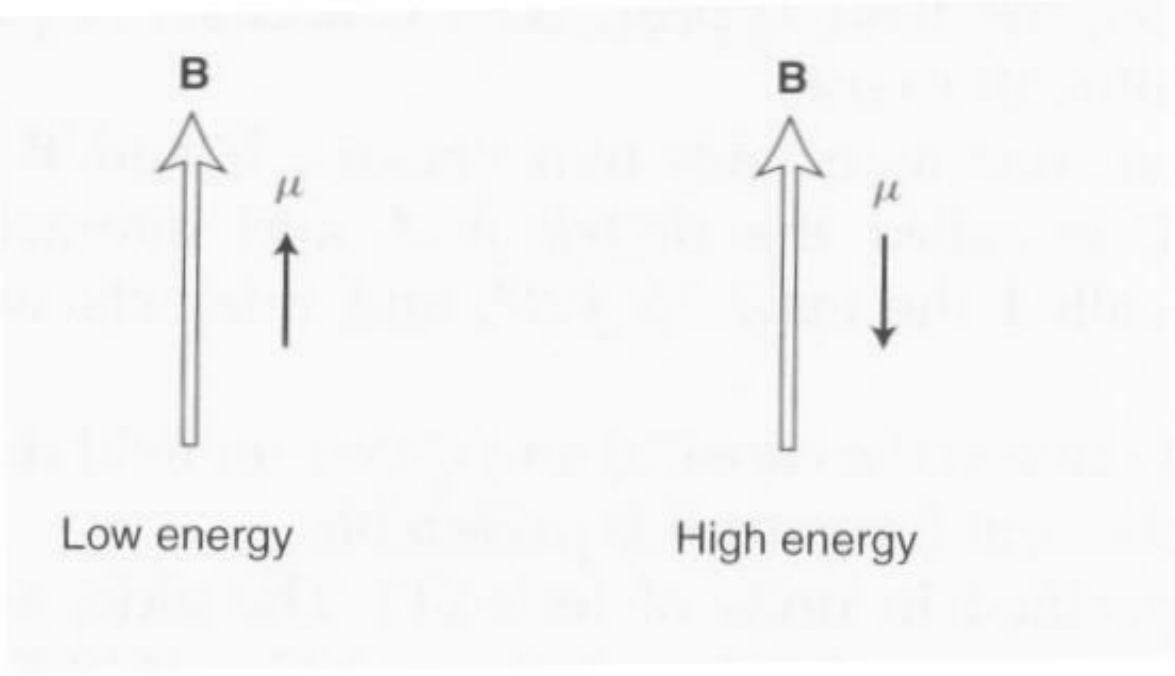

Angular Momentum and Projection Quantum Number

Magnitude of the angular momentum vector is fixed by the value of the nuclear spin quantum number

$$\left|\vec{\mathrm{I}}\right| = \hbar\sqrt{\mathrm{I}(\mathrm{I}+1)}$$

and that the z-component of the angular momentum vector is given by

$$I_z = \hbar m$$

where m is the magnetic quantum number:

m = (-I, -I+1, ..., I-1, I)

I_z has 2I+1 possible values

Example

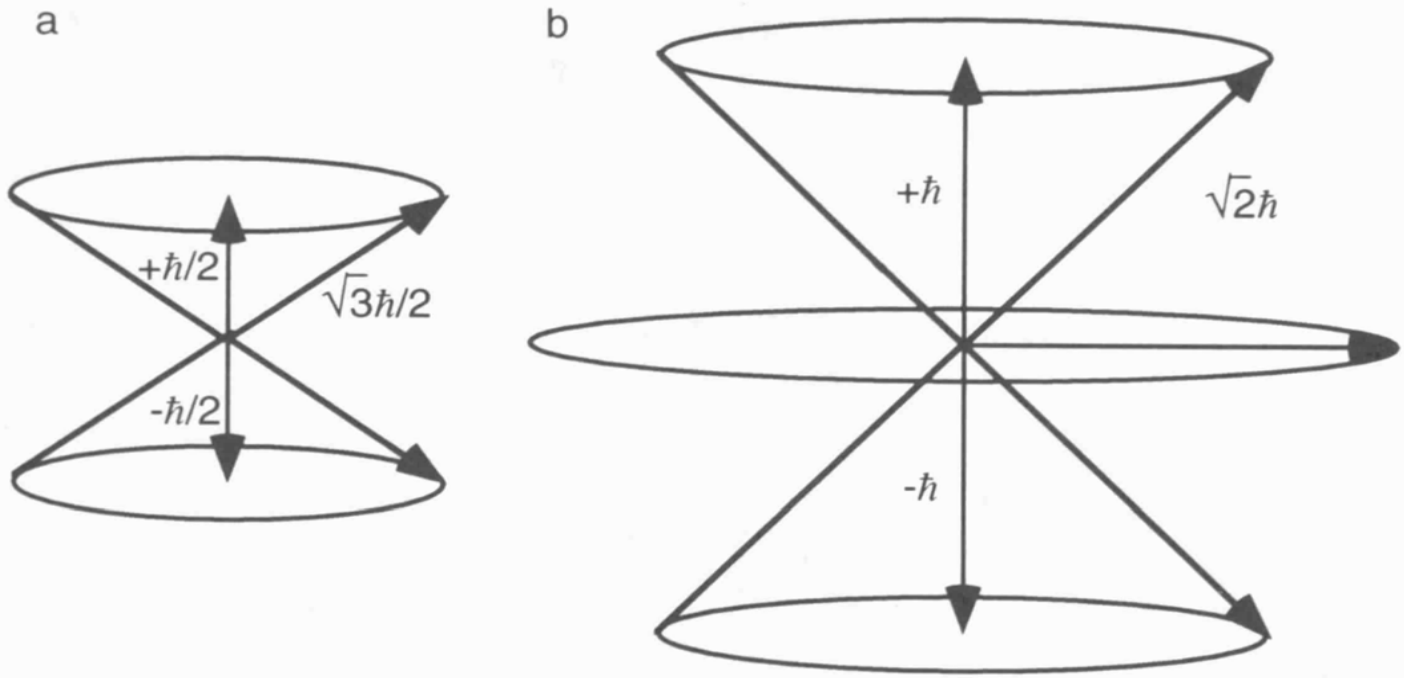

FIGURE 1.1 Angular momentum. The angular momentum vectors, **I**, and the allowed z components, I_z, for (a) a spin-$\frac{1}{2}$ particle and (b) a spin-1 particle are shown. The location of **I** on the surface of the cone of precession cannot be specified because of quantum-mechanical uncertainties in the I_x and I_y components.

Effect of an External Magnetic Field

- No magnetic field:

  (2I+1) spin states are degenerate (*i.e.* they all have the same energy).

- With magnetic field:

  Spin states separate in energy (larger values of m have lower energy)

- The separation of energy levels in a magnetic field is called the nuclear Zeeman effect. The energy of a spin state is given by:

$$E = -\vec{\mu} \cdot \vec{B}; \quad \vec{\mu} = \gamma \vec{I}$$

Magnetic Quantum Number and Interaction Energy

$$\left|\vec{\mathrm{I}}\right| = \hbar\sqrt{\mathrm{I}(\mathrm{I}+1)};\quad I_z = \hbar m$$

Thus, the discrete values of I_z are always smaller than |**I**|. The minimum energy occurs when the projection of μ onto **B** is the greatest. Hence, the energies of the *m* allowed spin states are proportional to their projection onto $\mathbf{B}_o$:

$$E_m = -mB_o\gamma\hbar$$

where:

Em	=	Energy of the state
m	=	magnetic quantum number
Bo	=	magnetic field strength
γ	=	gyromagnetic ratio
ħ	=	Planck's constant/2π

Degeneracy Lifted

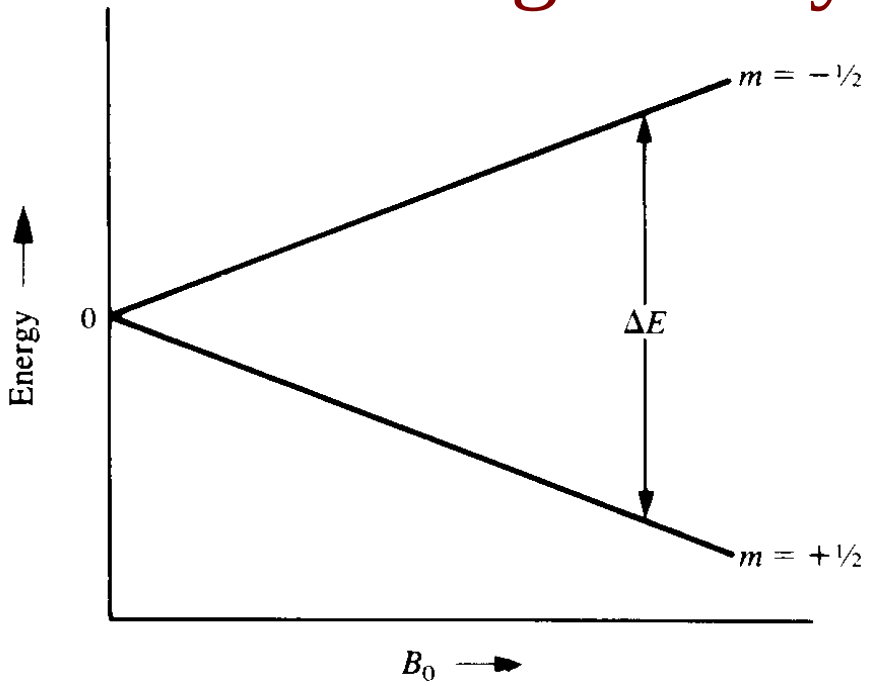

Depends on
1) the type of nucleus (γ)
2) the spin state (*m*)
3) strength of magnet (B_o)

selection rule for transitions between energy levels:
$\Delta m = \pm 1$

For spin ½ $\quad \Delta E = -[(-1/2) - (+1/2)]B_o\gamma\hbar = B_o\gamma\hbar$

Planck's Law $\quad \Delta E = h\upsilon = \hbar\omega = \underbrace{B_o\gamma\hbar}$

from above

Energy Levels and Populations

The Boltzmann equation tells us the population of a state if we know its energy:

$$\frac{N_\alpha}{N_\beta} = e^{\frac{E_\beta - E_\alpha}{k_B T}}$$

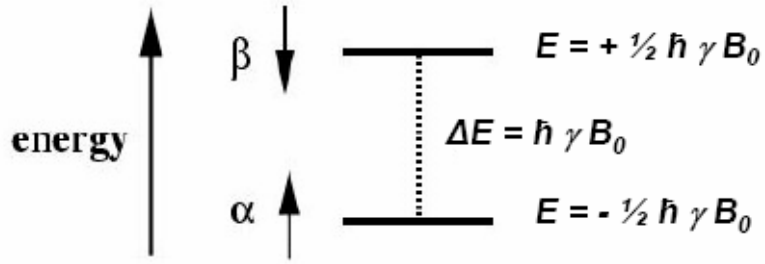

Boltzmann distribution: $\frac{N(\alpha)}{N(\beta)} = e^{\frac{2\mu B_0}{kT}} \sim 1 + \frac{2\mu B_0}{kT} = \frac{1.00001}{1}$

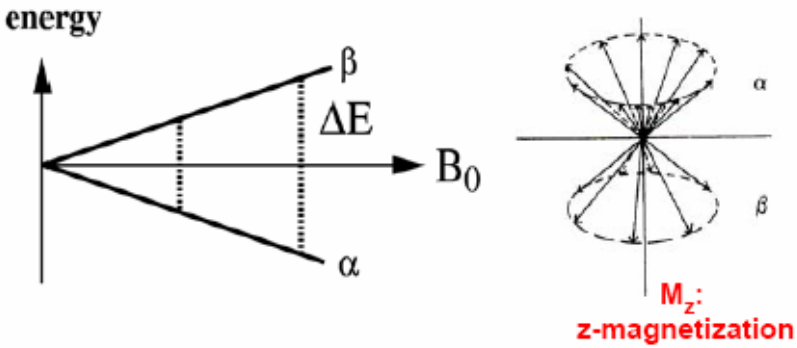

- In an ensemble of spin ½ nuclei the α (up) and β (down) energy levels are populated according to Boltzmann statistics.
- This leads to a small effective magnetization along the *z*-axis (B_0).
- No *x*- or *y*-magnetization is observed since the spin vectors are not *phase coherent*, i.e. they precess independent from each other around B_0 and their x,y components thus average to zero.

Interaction with RF Radiation

Electromagnetic Radiation

Electromagnetic radiation is composed of magnetic and electronic waves:

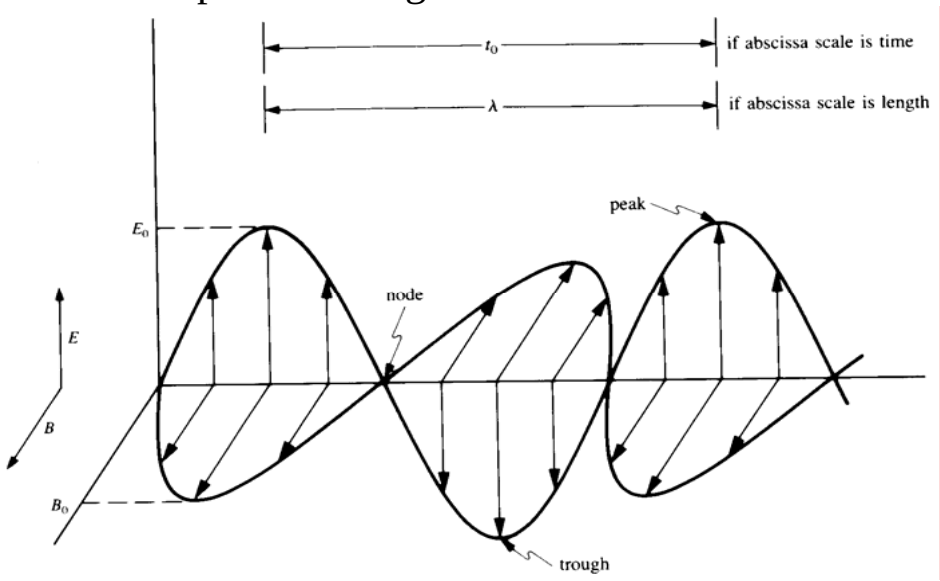

From: R.S. Macomber (1988) NMR spectroscopy: Essential Theory and Practice

- The frequency is defined as $\nu = 1/t_o$, where t_o is the peak-to-peak time.
- A wave travels λ (distance) in t_o, so that the speed of the radiation (c, the speed of light, $3x10^8$ m/s) is defined as:

$$c = \frac{\lambda}{t_o} = \lambda\nu \quad \therefore \text{ wavelength and frequency are inversely related}$$

Electromagnetic Radiation

Radiofrequency energy (ΔE for nuclear spin state transitions):

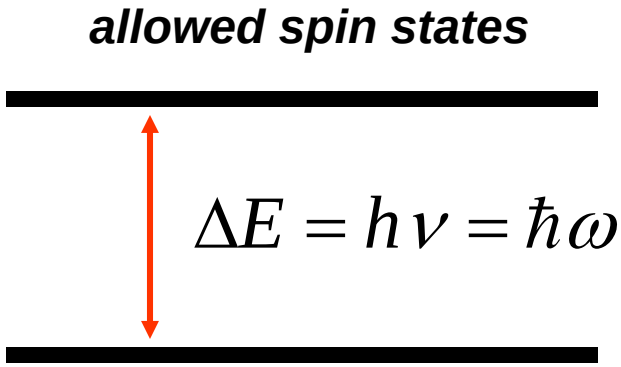

$\lambda = 10^{11}$ to 3×10^{7} nm

$\nu = 10^{6}$ to 10^{10} Hz

By setting the frequency of electromagnetic radiation (ν, or equivalently ω) to the resonance condition, transitions between nuclear spin states can be induced

(*i.e.* one can do NMR spectroscopy!).

The Electromagnetic Spectrum

NMR resonance frequency: $\omega = \gamma B_0$

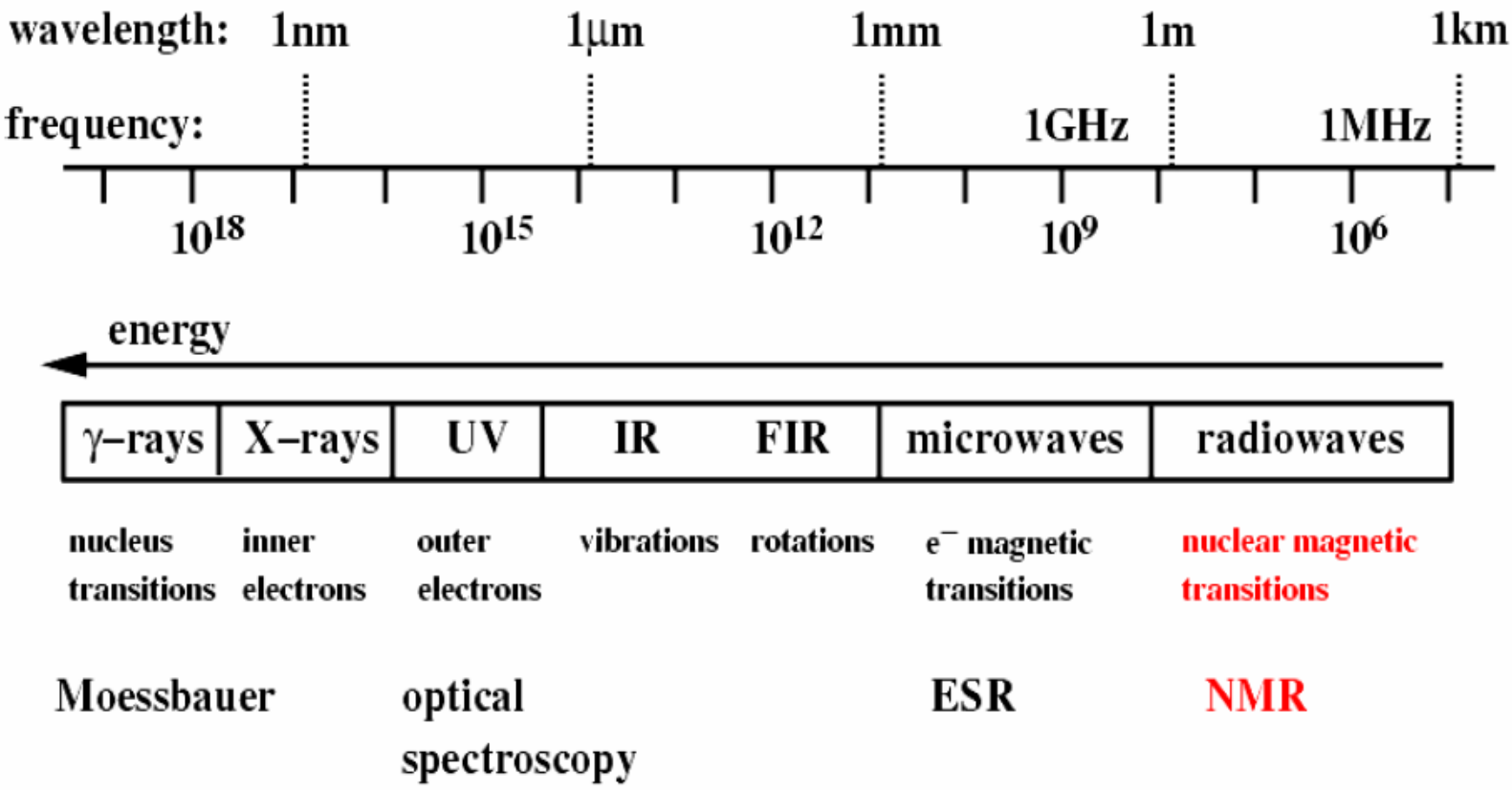

Resonance (ω_o), B_o and γ

Resonance condition: $\Delta E = h\nu = \hbar\omega = B_o\gamma\hbar$

Resonance (Larmor) frequency for exciting nuclear spin transition:

$$\omega_o = B_o\gamma$$

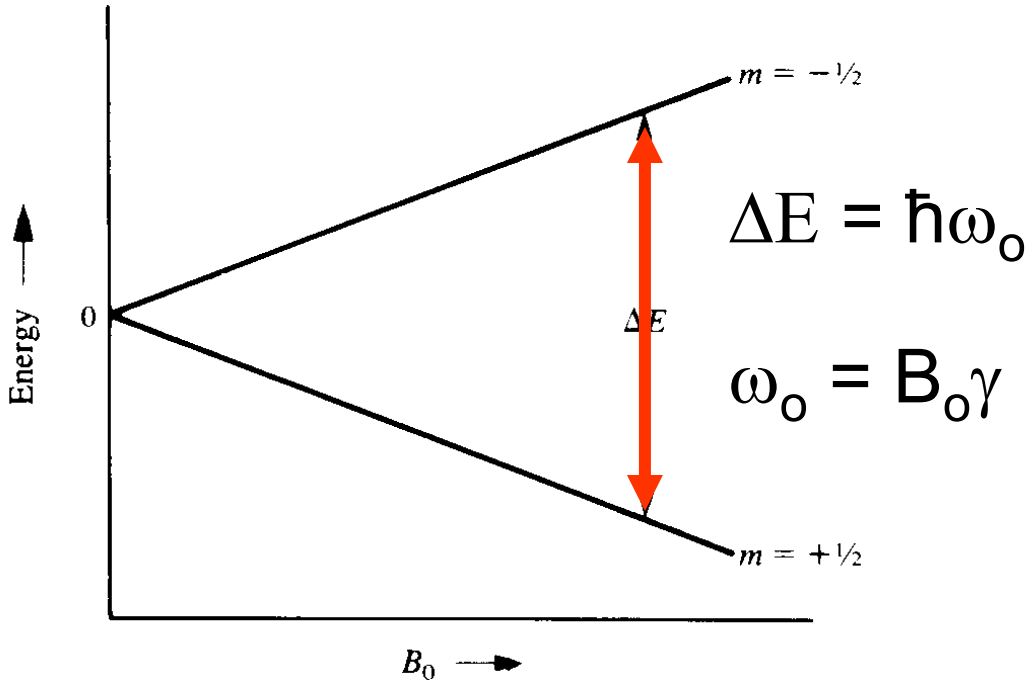

$\Delta E = \hbar\omega_o$

$\omega_o = B_o\gamma$

Bulk Magnetization

$$\vec{\mu} = -\gamma \hat{I}$$

The magnetic moment (μ) is a vector parallel to the spin angular momentum. The gyromagnetic ratio (γ) is a physical constant particular to a given nucleus.

Unfortunately, the vast majority of the magnetic moments cancel one another. The "Boltzmann excess" in the α state add together to create bulk angular momentum and magnetization.

$$\vec{\mathbf{J}} = \sum \hat{\mathbf{I}}$$

$$\vec{\mathbf{M}} = \sum \vec{\boldsymbol{\mu}}$$

Bulk Magnetization

Individual magnetic moments:

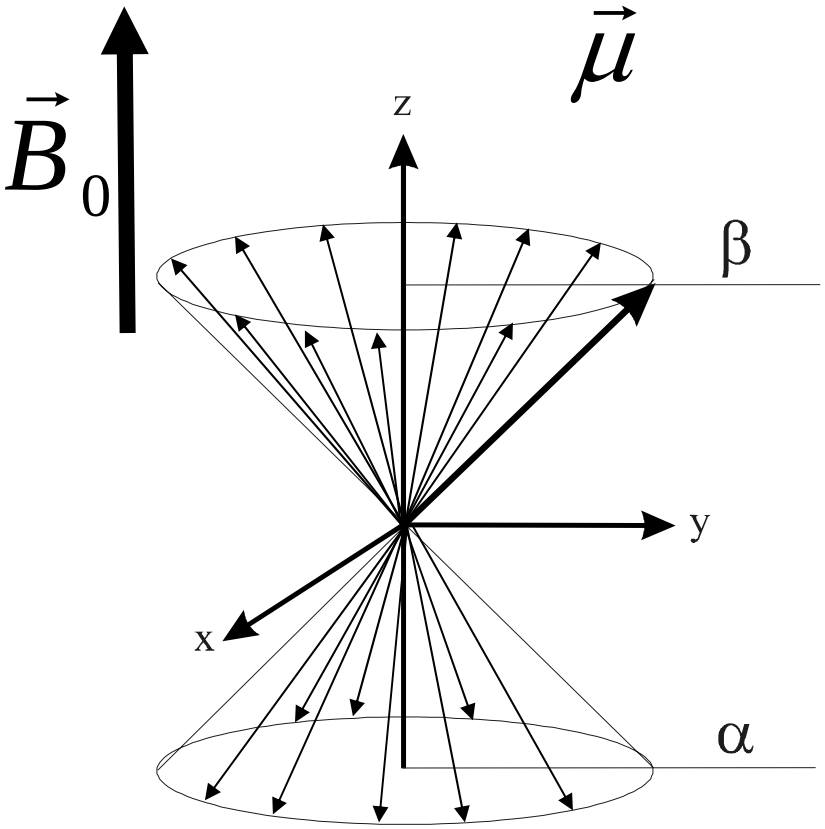

$$\vec{\mu} = -\gamma \hat{I}$$

Bulk Magnetization:

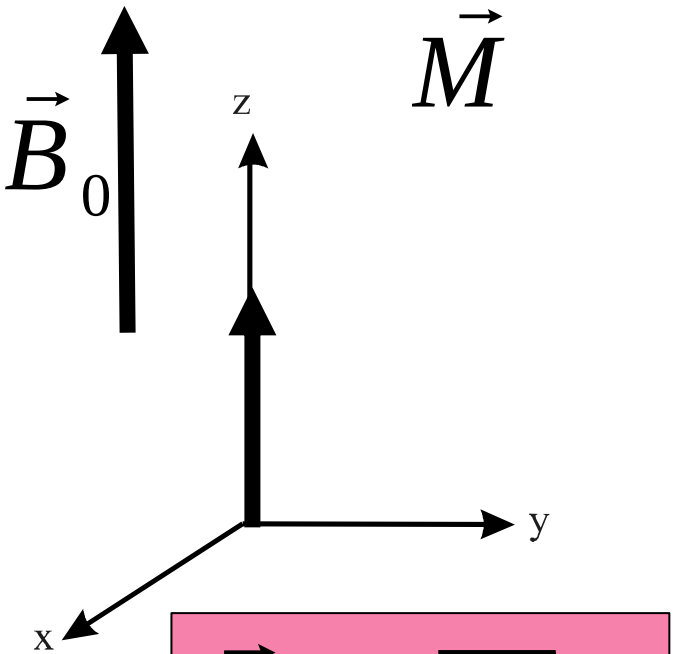

$$\vec{\mathbf{M}} = \sum \vec{\boldsymbol{\mu}}$$

Classical Motion of a Magnet

Classical physics tells us about the motion of a magnet in a magnetic field

$$\frac{d\vec{\mathbf{J}}}{dt} = \vec{M} \times \vec{B}$$

The change in angular momentum per unit time is torque (τ)

This *precession* is very similar to the motion of a spinning gyroscope or top in a gravitational field

$$\frac{d\mathbf{L}(t)}{dt} = \mathbf{r} \times m\mathbf{g}$$

L(t) is the gyroscope's angular momentum, **r** its radius from the fixed point of rotation, m its mass and **g** the force of gravity.

Reminder: Cross Product

$$\vec{a} \times \vec{b} = \begin{matrix} \vec{x} & \vec{y} & \vec{z} \\ a_x & a_y & a_z \\ b_x & b_y & b_z \end{matrix}$$

$$= (a_x b_y - a_y b_x)\vec{z} + (a_y b_z - a_z b_y)\vec{x} - (a_x b_z - a_z b_x)\vec{y}$$

Direction of Precession

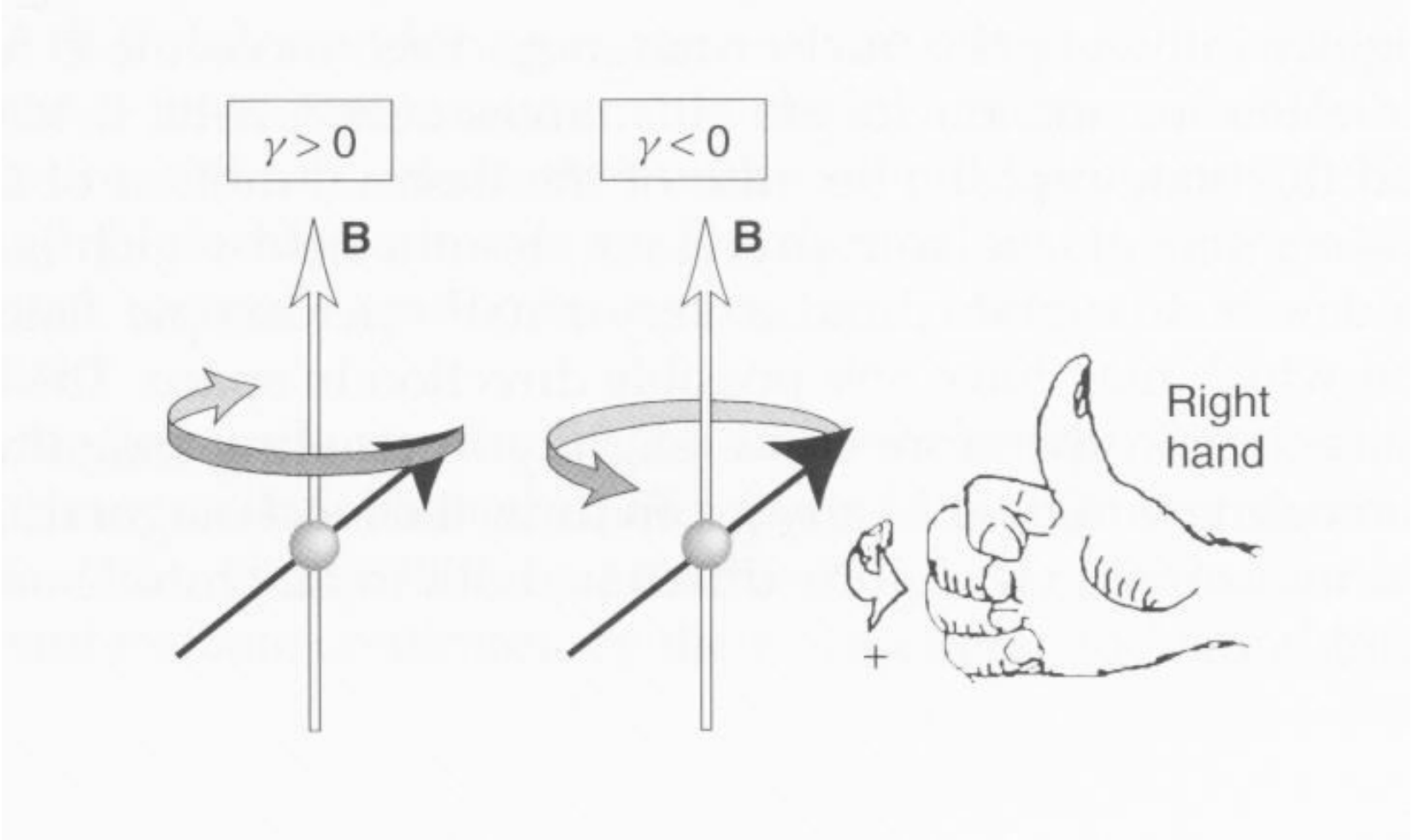

http://instruct1.cit.cornell.edu/courses/biobm730

Classical Motion of a Magnet

$$\frac{d\vec{M}}{dt} = \gamma \vec{M} \times \vec{B}$$

The equations we will be further developing this lecture are known as the "Bloch Equations". They were initially described by Felix Bloch who shared the Nobel prize in Physics in 1952 for this work.

Case 1: At equilibrium in a magnet: $\frac{d\vec{M}}{dt} = 0$

Case 2: After a radiofrequency pulse moves $\vec{M}$ away from equilibrium:

$$M_x = M_\perp \cos \omega_0 t$$

$$M_y = -M_\perp \sin \omega_0 t$$

$$M_\perp = \sqrt{(M_x^2 + M_y^2)}$$

This describes precession in the x-y plane, but there is no mechanism to return the magnetization back to equilibrium along z.

Bloch Equations

In order to allow the system to return to equilibrium, Felix Bloch made the following modifications to the basic equation

$$\frac{d\mathbf{M}(t)}{dt} = \mathbf{M}(t) \times \gamma\mathbf{B}(t) - \mathbf{R}(\mathbf{M}(t) - M_0)$$

Empirical modification in which a "relaxation matrix" **R** acts on magnetization that is different from the equilibrium state, M_0 (cannot be justified with classical physics, need QM).

Bloch Equations

$$\frac{d\mathbf{M}(t)}{dt} = \mathbf{M}(t) \times \gamma \mathbf{B}(t) - \mathbf{R}(\mathbf{M}(t) - M_0)$$

This equation is easiest to understand broken into its matrix components:

$$\frac{dM_z(t)}{dt} = \gamma[M_x(t)B_y(t) - M_y B_x(t)] - \frac{M_z(t) - M_0}{T_1}$$

Magnetization along the z-axis

$$\frac{dM_x(t)}{dt} = \gamma[M_y(t)B_z(t) - M_z B_y(t)] - \frac{M_x(t)}{T_2}$$

Magnetization along the x-axis

$$\frac{dM_y(t)}{dt} = \gamma[M_z(t)B_x(t) - M_x B_z(t)] - \frac{M_y(t)}{T_2}$$

Magnetization along the y-axis

Bloch Equations in the Rotating Frame

Substituting $\Delta\omega=-\gamma B_0-\omega_{rf}$ (where $B_0=B_z$ and is not time-dependent) into the Bloch equations yields:

$$\frac{dM_z(t)}{dt}=\gamma[M_x(t)B_1^y(t)-M_yB_1^x(t)]-\frac{M_z(t)-M_0}{T_1}$$

B_1 refers to the rf field in the rotating frame

$$\frac{dM_x(t)}{dt}=-\Delta\omega M_y(t)-\gamma M_zB_1^y(t)-\frac{M_x(t)}{T_2}$$

$$\frac{dM_y(t)}{dt}=\gamma M_z(t)B_1^x(t)+\Delta\omega M_x-\frac{M_y(t)}{T_2}$$

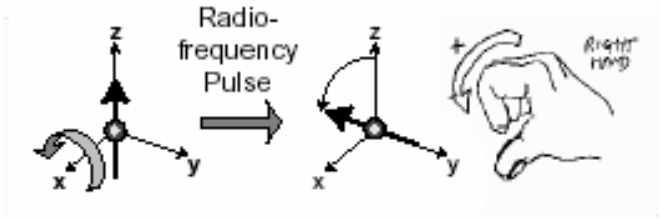

Bloch Equations

$$\frac{dM_z(t)}{dt} = \underbrace{\gamma M_x(t) B_1^y(t)}_{\text{y-axis pulse}} - \underbrace{\gamma M_y(t) B_1^x(t)}_{\text{x-axis pulse}} - \frac{M_z(t) - M_0}{T_1}$$

$$\frac{dM_x(t)}{dt} = -\Delta\omega M_y(t) - \underbrace{\gamma M_z(t) B_1^y(t)}_{\text{y-axis pulse}} - \frac{M_x(t)}{T_2}$$

$$\frac{dM_y(t)}{dt} = \underbrace{\gamma M_z(t) B_1^x(t)}_{\text{x-axis pulse}} + \Delta\omega M_x(t) - \frac{M_y(t)}{T_2}$$

In the Bloch equations, magnetic fields along the x and y axes create B_1 fields or pulses. These are typically applied for short durations, and the length of time the pulse is turned on is adjusted to give a desired rotation (such as 90 or 180 degrees).

Populations of Spin States and RF Pulses

90˚ and 180˚pulses

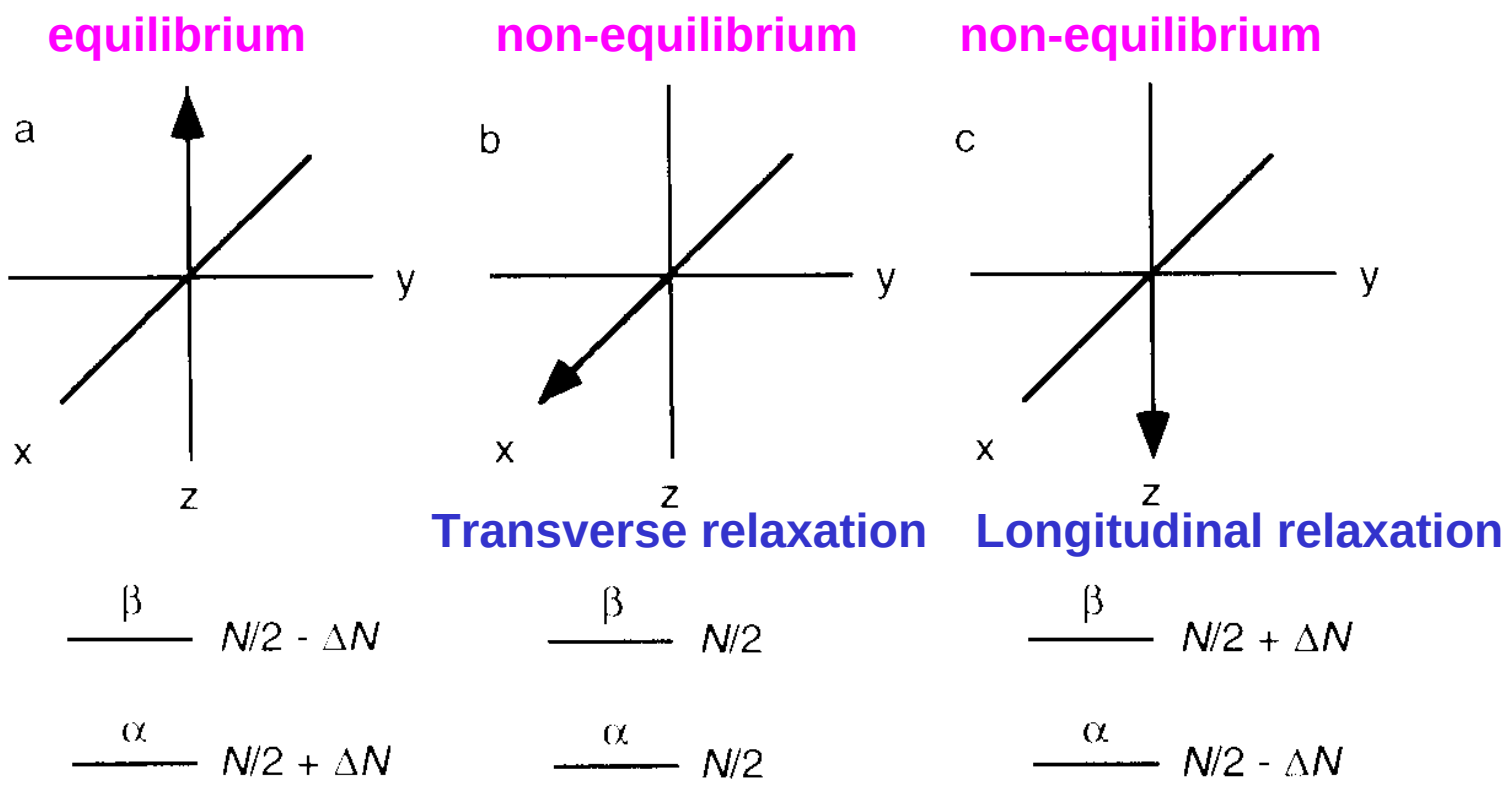

From: J. Cavanagh et al. (1996) Protein NMR spectroscopy

http://instruct1.cit.cornell.edu/courses/biobm730

Precession and Relaxation

In most NMR experiments, the pulses are short and the relaxation times are relatively long. We mainly worry about relaxation after the pulses are applied.

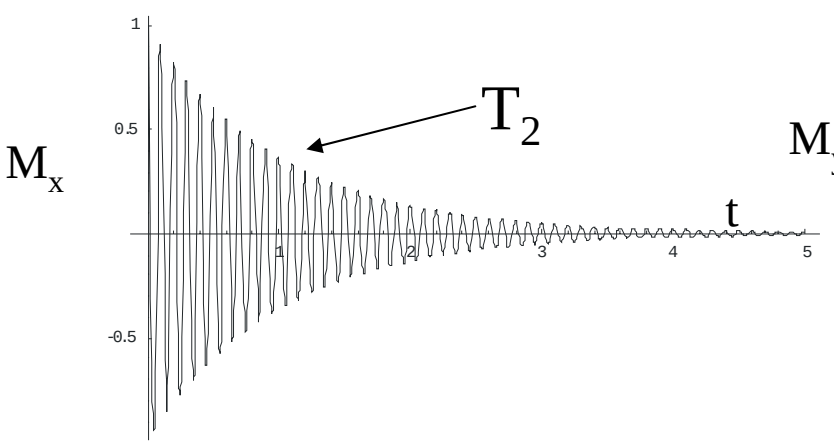

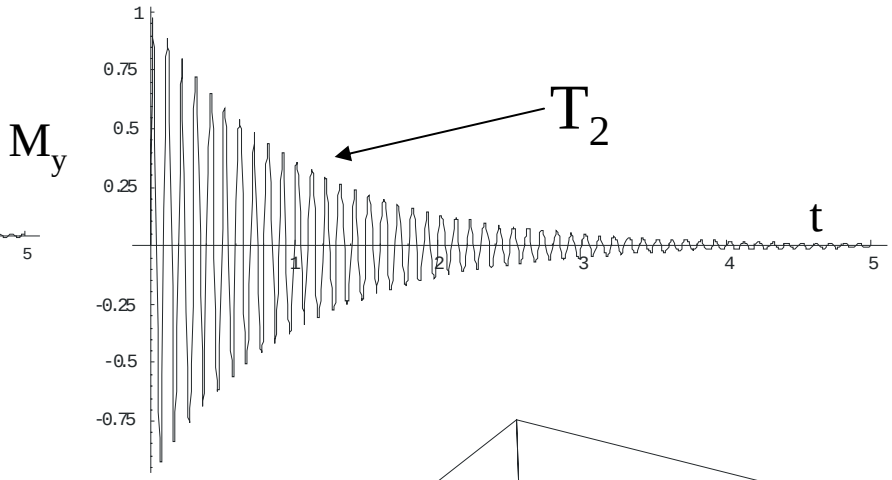

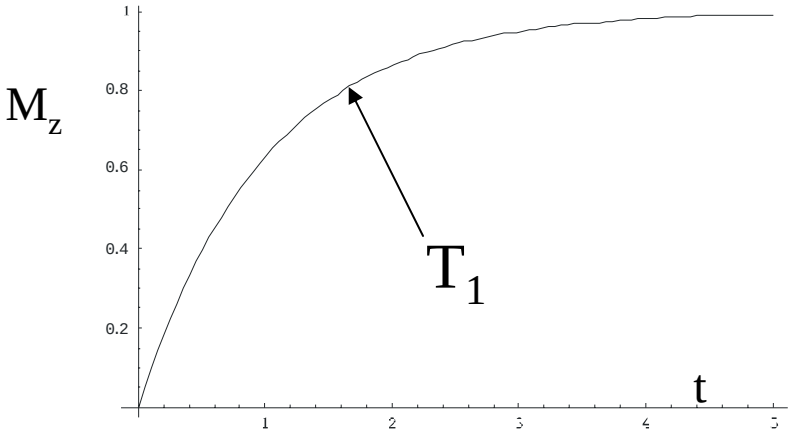

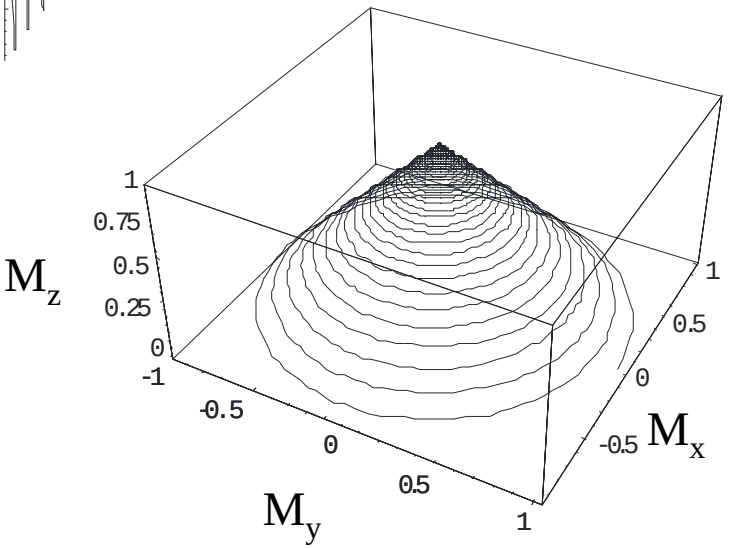

Longitudinal Relaxation (T_1)

- first order rate process

$$\frac{dM_z(t)}{dt} = \frac{\left(M_o - M_z(t)\right)}{T_1}$$

$$M_z(t) = M_o - \left(M_o - M_z(0)\right)e^{-t/T_1}$$

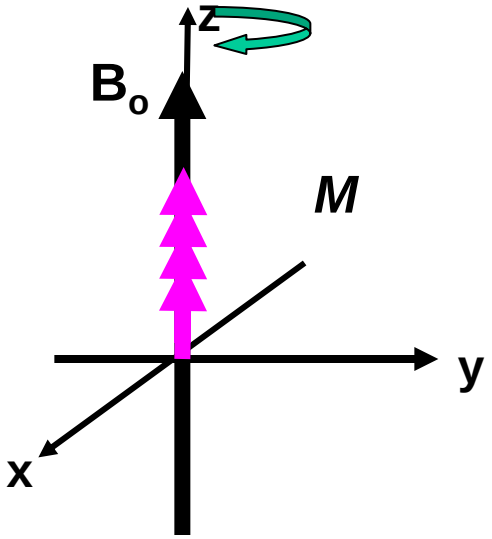

M_o = total magnetization

$M_z(0)$ = magnetization along the *z* axis at t = 0

Longitudinal Relaxation (T_1)

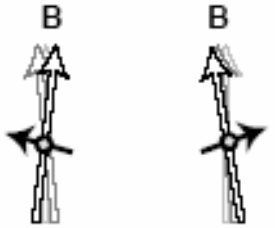

- Incoherent molecular fluctuations on the order of the Larmor frequency
- T_1 has a field dependent inflection point
- Historically called spin-lattice relaxation (heat lost to the surroundings)
- In NMR this is known as longitudinal relaxation due to our frame of reference

Usual experiment to measure T_1:
Inversion-Recovery

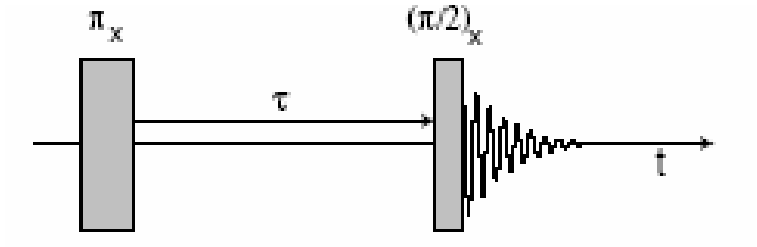

Measured signal

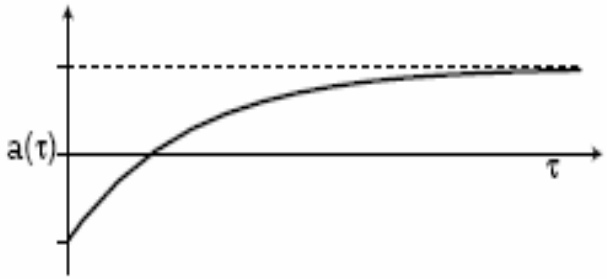

$$M_z(t) = M_0(1-2e^{-\tau/T_1})$$

Longitudinal Relaxation (T_1)

Buildup

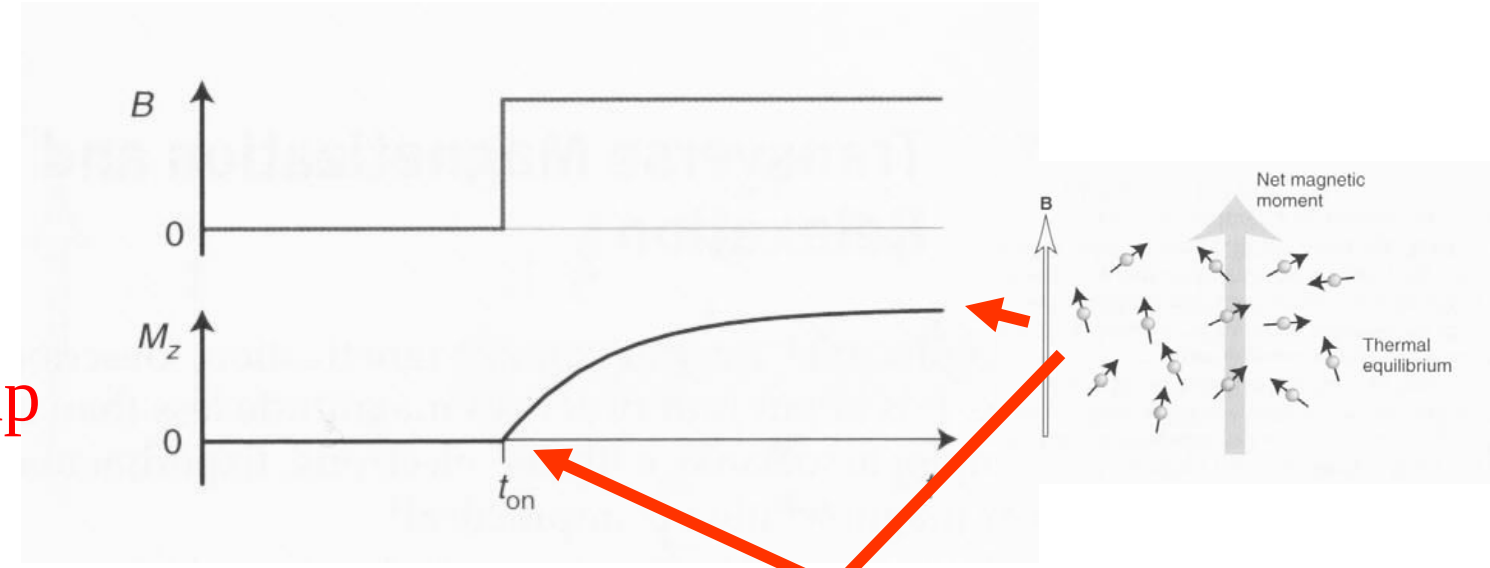

Decay

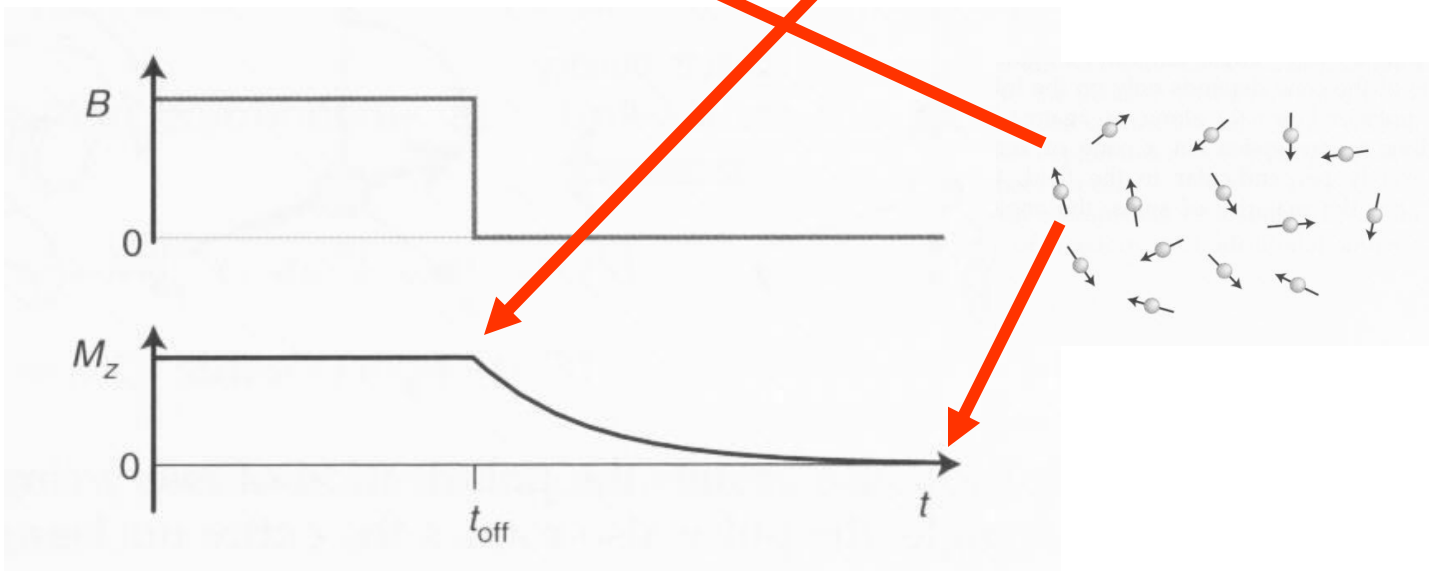

http://instruct1.cit.cornell.edu/courses/biobm730

Longitudinal Relaxation (T_1)

Putting the sample into a magnetic field
Or after the magnetization is in the x-y plane

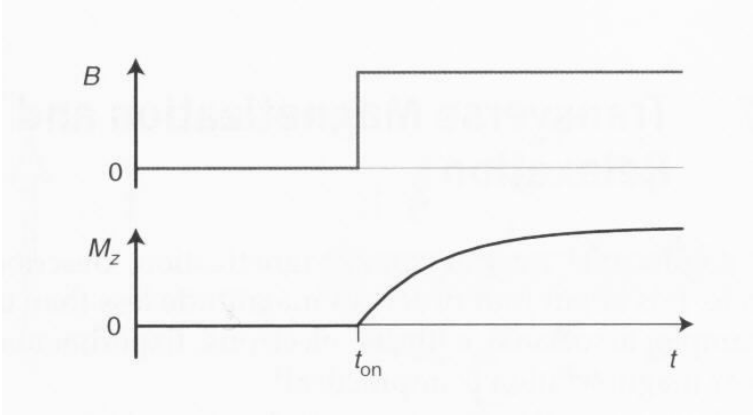

Taking the sample out of a magnetic field

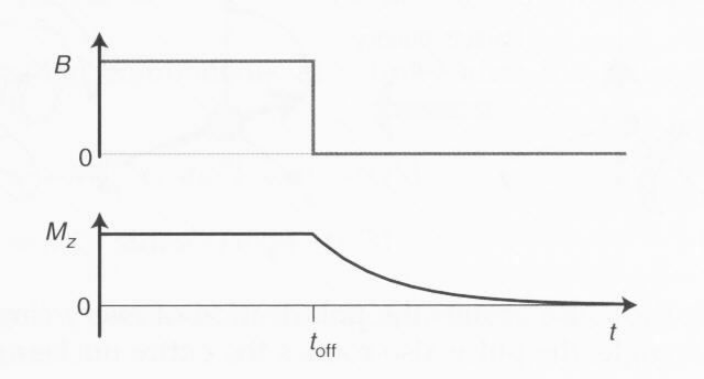

$$M_z(t) = M_{equil}(1 - e^{-t/T_1})$$ → One has to wait ~5xT_1 to get the signal back

- A lot of time in conventional NMR is spent waiting for relaxation.
- Initial experiments to observe NMR signals were hampered by not knowing T_1

Transverse Relaxation (T_2)

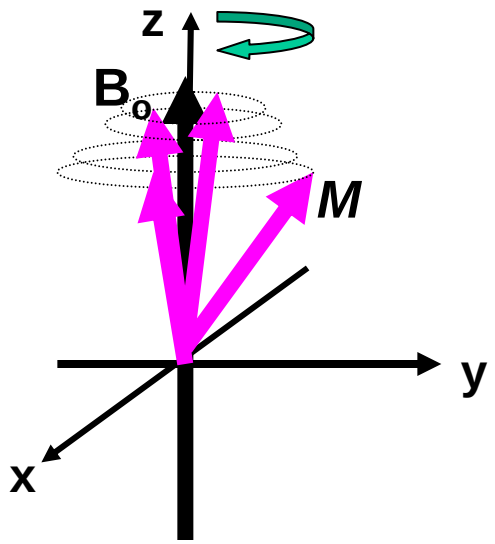

Relaxation back to equilibrium

Transverse Relaxation (T_2)

Inhomogeneous broadening: variations in the *macroscopic* magnetic field

- Instrument limitations
- Magnetic susceptibility

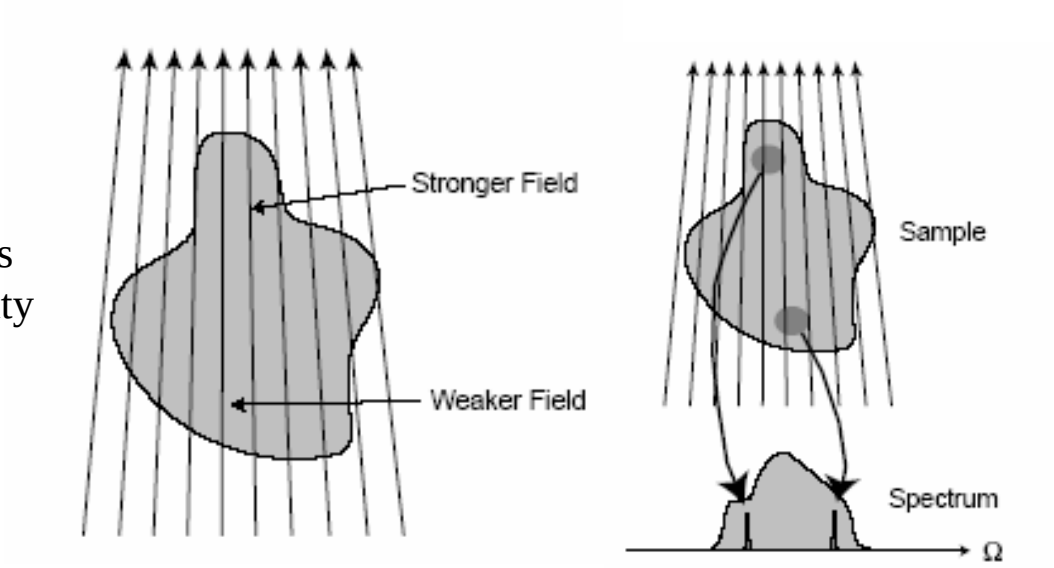

Homogeneous broadening: fluctuating *microscopic* magnetic fields

- Molecular dynamics and spin-spin interactions → more details later
- Chemical exchange
- Historically called spin-spin relaxation
- In NMR we call it transverse relaxation→ loss of signal in the x-y plane

Transverse Relaxation (T_2)

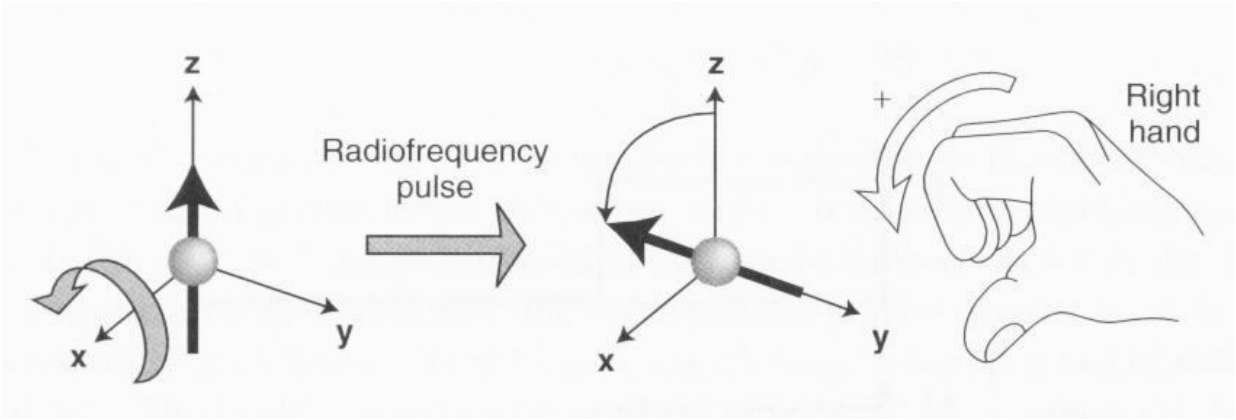

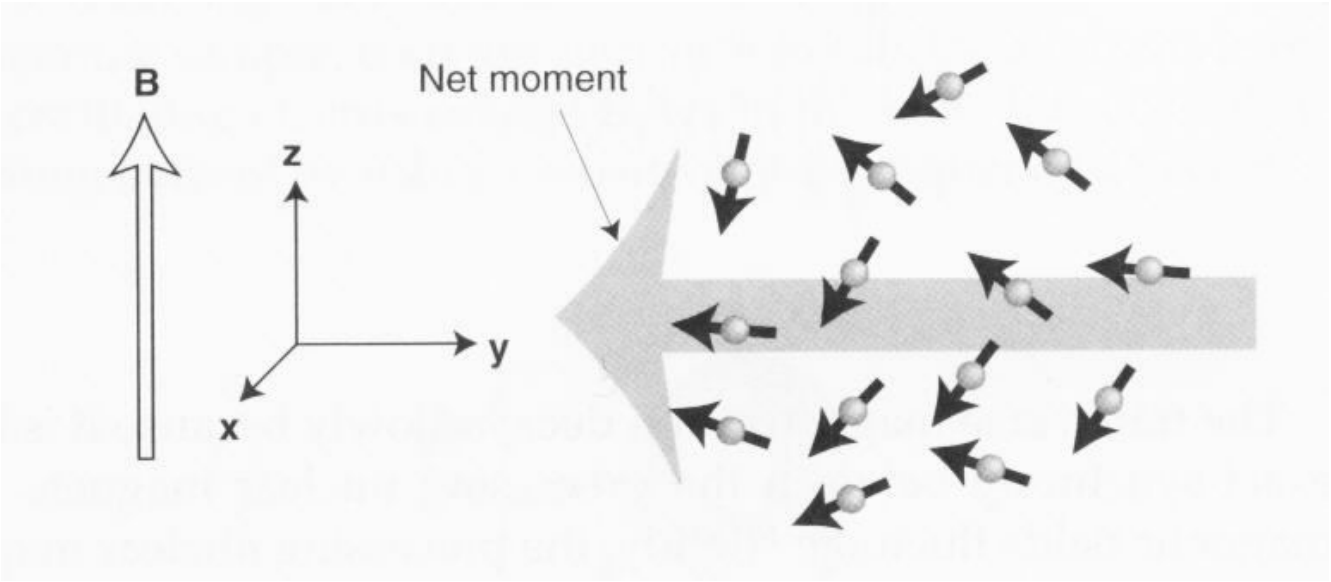

http://instruct1.cit.cornell.edu/courses/biobm730

Transverse Relaxation (T_2)

$$M_x(t) = M_o \cos(\omega_o t) e^{-t/T_2}$$

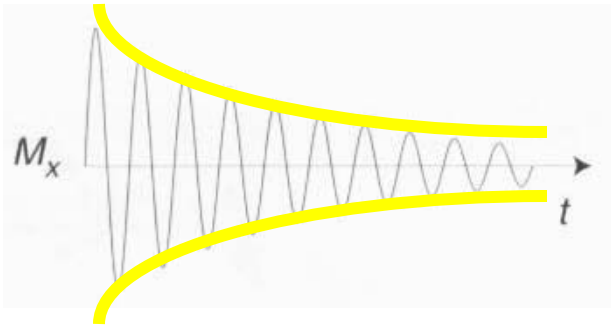

$$M_y(t) = M_o \sin(\omega_o t) e^{-t/T_2}$$

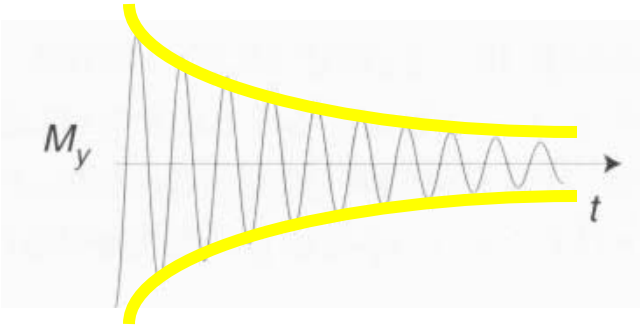

Free Induction Decay

Transverse Relaxation (T_2)

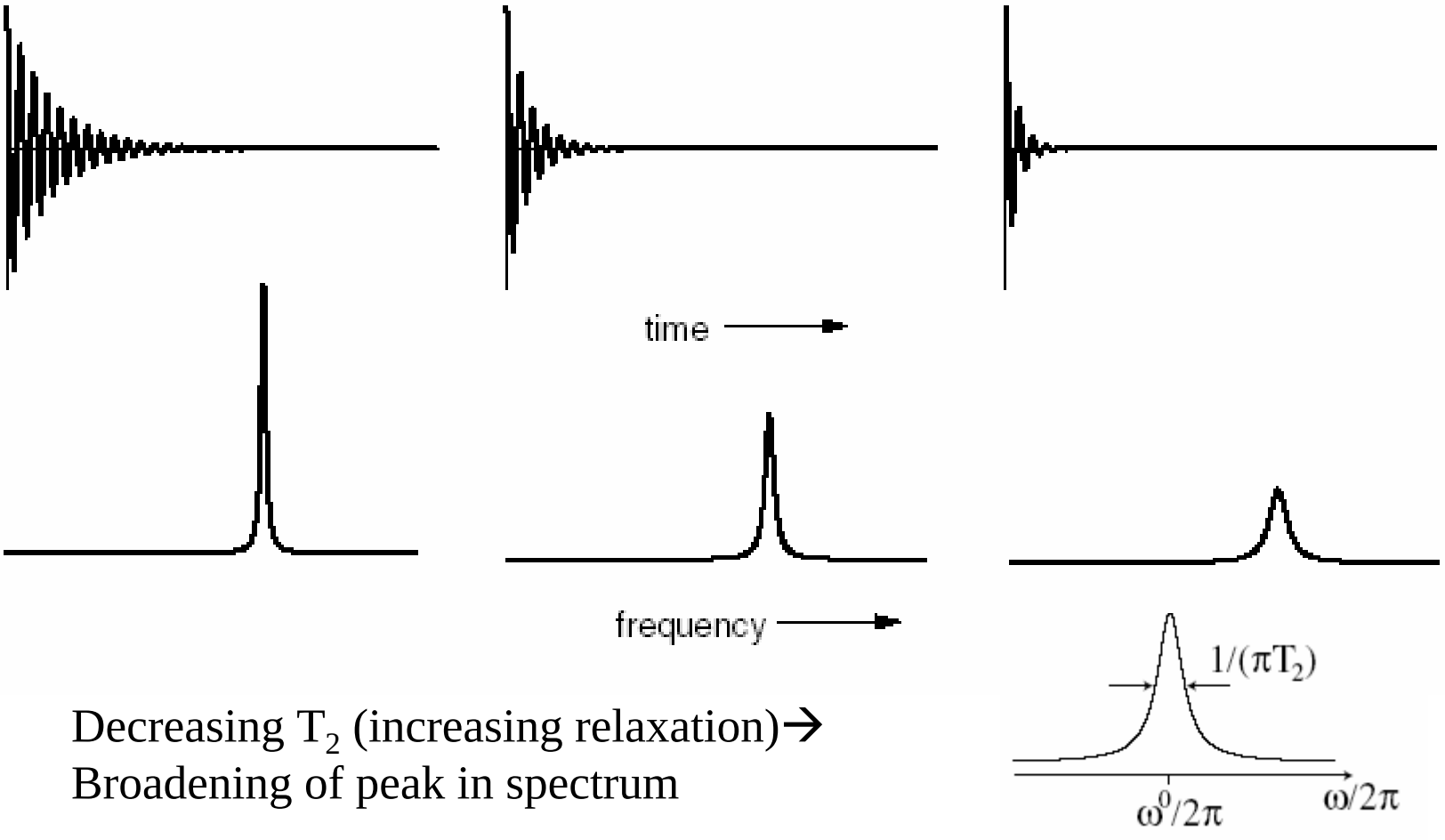

Decreasing T_2 (increasing relaxation)→
Broadening of peak in spectrum

The Biomolecular NMR Experiment

Hardware

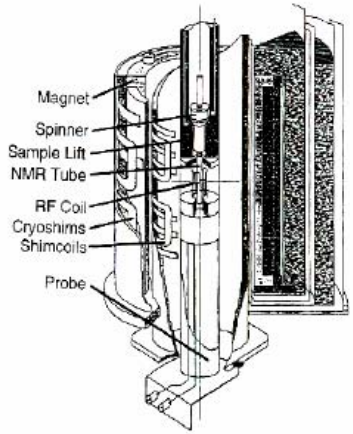

FIGURE 3.2 Cutaway diagram of a superconducting magnet. The probe, sample spinner, and room-temperature shim coils are positioned coaxially in the room-temperature bore of the magnet. The solenoid and cryoshim coils are immersed in liquid helium. The helium dewar is surrounded by a radiation shield and a liquid nitrogen dewar. Diagram courtesy of Bruker Instruments, Inc.

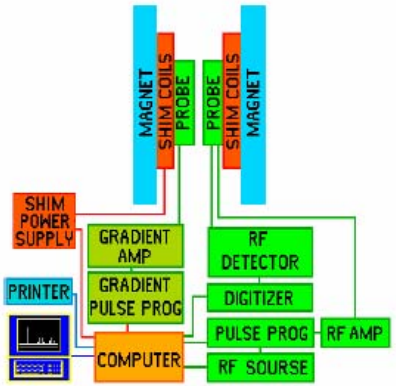

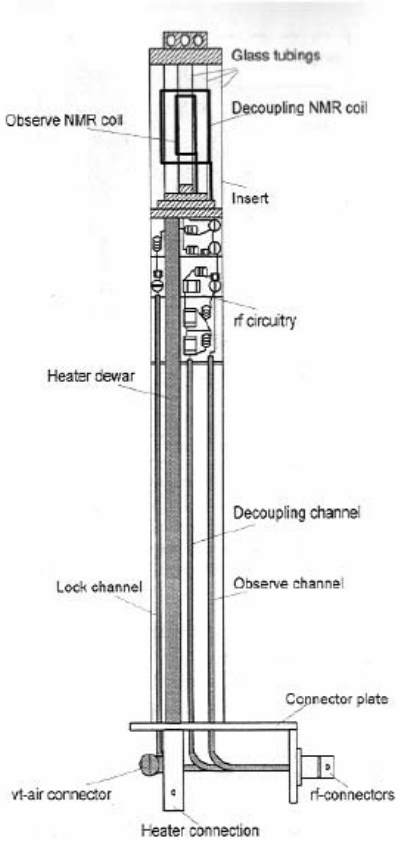

FIGURE 3.3 Probe assembly. Major components of a high-resolution NMR spectroscopy rf probe are illustrated. Diagram courtesy of Bruker Instruments, Inc.

(Cavanagh, et al. "Protein NMR spectroscopy")

magnet (B_0) **spectrometer** **probe (rf + receiver coil)**

Experimental Sensitivity

$$S/N \sim N\ \gamma_{exc}\ \gamma_{det}^{3/2}\ B_0^{3/2}\ NS\ T_2^{1/2}$$

S/N	signal-to-noise	
N	number of spins	→ sample concentration
γ_{exc}	gyromagnetic ratio of excited spins	
γ_{det}	gyromagnetic ratio of detected spins	
B_0	static magnetic field	
	(e.g. 14.1 Tesla or 600 MHz for ^1H)	
NS	number of scans	→ experimental time
T_2	transverse relaxation time	→ line width $\Delta\nu \sim 1/(\pi T_2)$

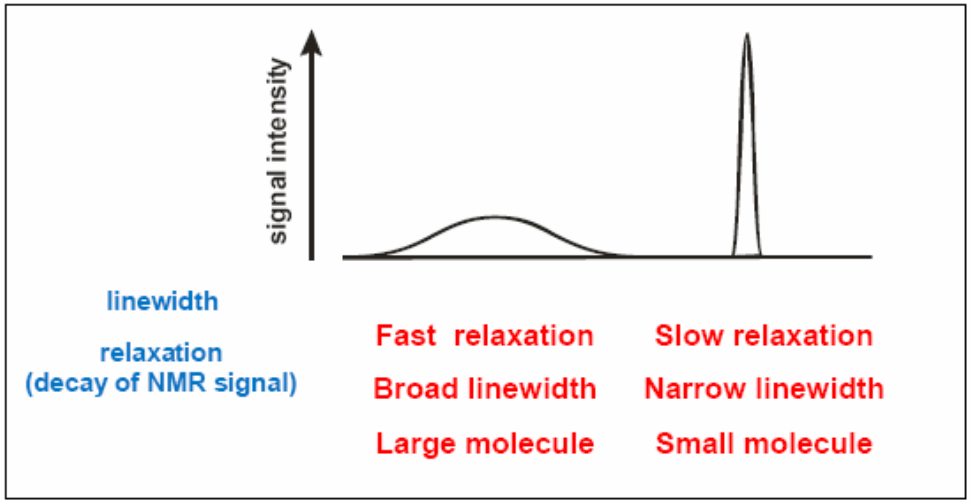

CW vs. FT NMR

CW

FT

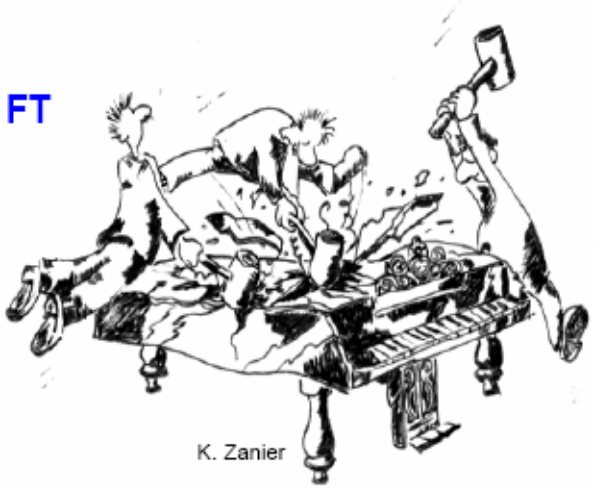

$$f(t) \underset{IFT}{\overset{FT}{\rightleftharpoons}} F(\omega)$$

time domain — frequency domain

Continuous Wave (CW) NMR

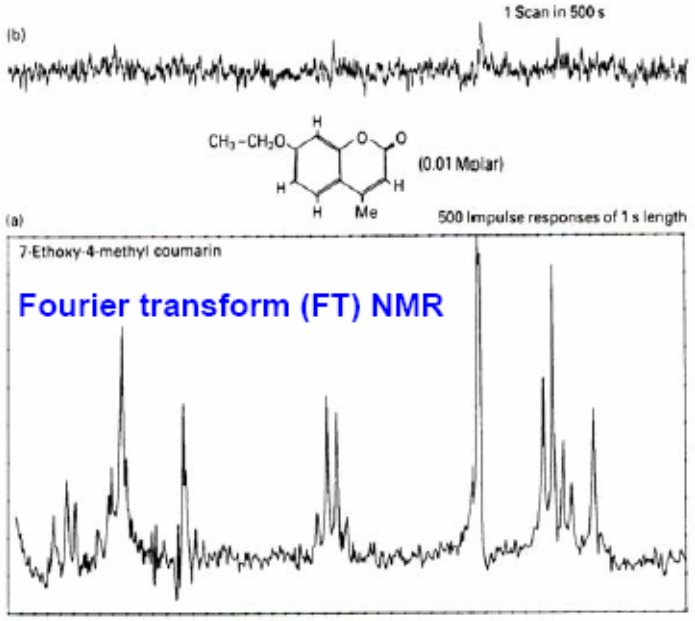

(Ernst, et al. "Principles of Nuclear Magnetic Resonance")

1D NMR

A radio frequency (rf) pulse along x causes the z-magnetization (M) to precess around the x-axis. The pulse is switched off after a 90° rotation leaving the magnetization along the y-axis.

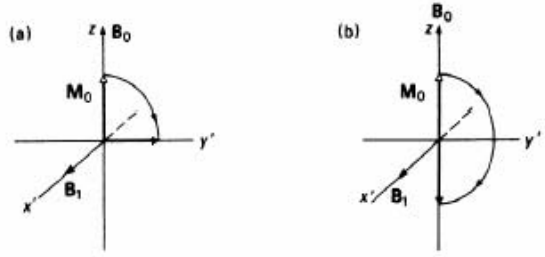

90°(x) pulse

180°(x) pulse

→ In this state, the spin vectors whose population difference gave rise to the z-magnetization before the rf pulse have become phase coherent, e.g. are oriented towards the y-axis.

→ The α- and β-states are equally populated, thus no z-magnetization is left.

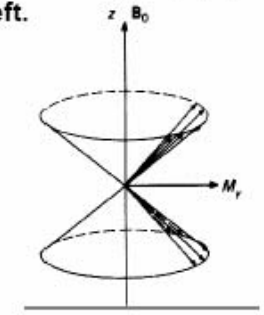

M_y: y-magnetization

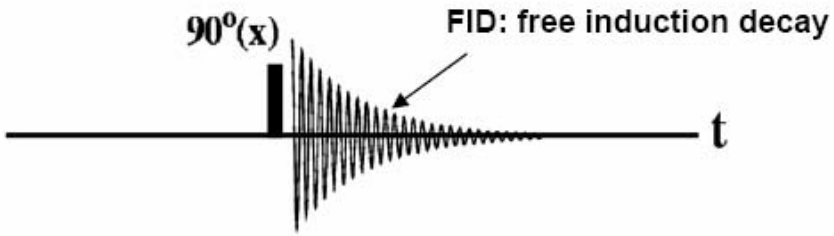

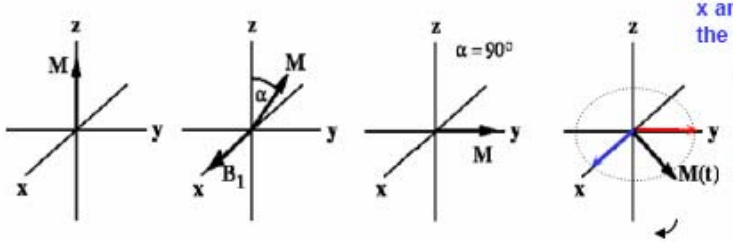

Frequency components along x and y are detected to define the sign of ω.

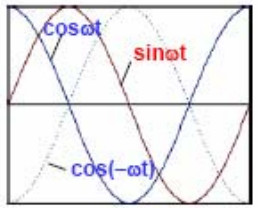

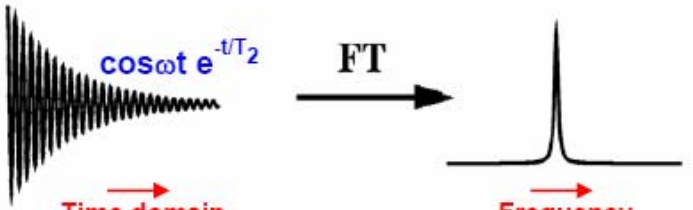

Time domain f(t)

FID

Frequency F(ω)

spectrum

90°(x) = 90° rf pulse along x–axis

FT = Fourier transformation F(t) –> F(ω)

FID = free induction decay

1D Spectrum of a Protein

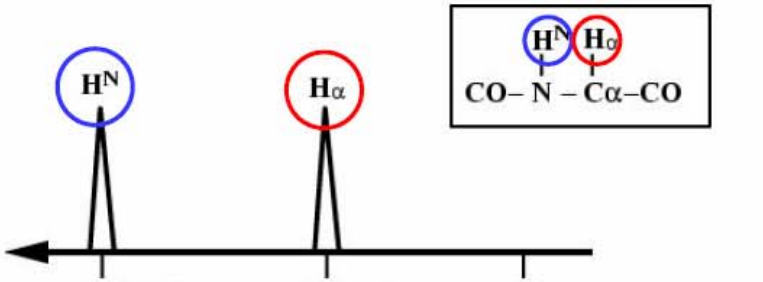

$$\delta(\text{ppm}) = (\Omega - \Omega_{ref})/\omega_0 * 10^6$$

chemical shifts in parts per million [ppm] are *independent* of the field strenght of the static magnetic B_0 field

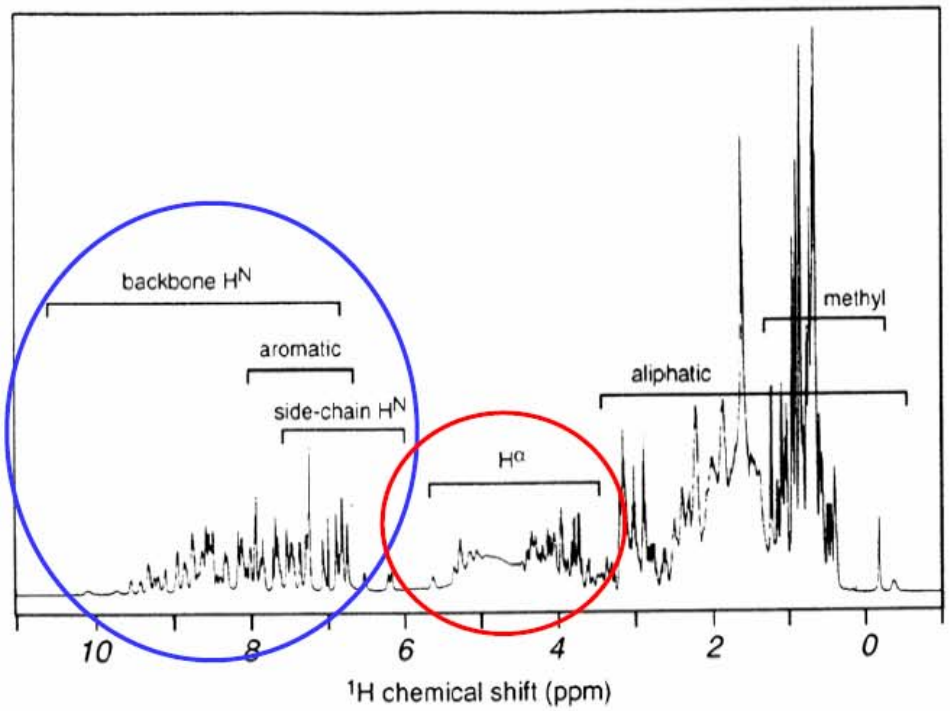

Chemical Shift

Origin: Nuclear Shielding

- Nuclei are shielded by electrons.
- Induced field associated with orbiting electrons.
- Require stronger magnetic field than H_0.
- Increased shielding requires greater applied field strength to achieve resonance.

- A molecule may contain multiple protons that exist in unique electronic environments.
- Therefore not all protons are shielded to the same extent.
- Resonance differences in protons are very small (ppm).
- Measure differences in resonance energy relative to a reference.
- Tetramethylsilane $(CH_3)_4Si$ (TMS) provides highly shielded reference (set to 0ppm).

$$\text{Chemical Shift } (\delta, \text{ppm}) = \frac{\text{Observed chemical shift from TMS (Hz)}}{\text{Spectrometer frequency (MHz)}} = \text{ppm}$$

http://mason.gmu.edu/~bbishop1/chem318.1stlecture.ppt

Chemical Shift

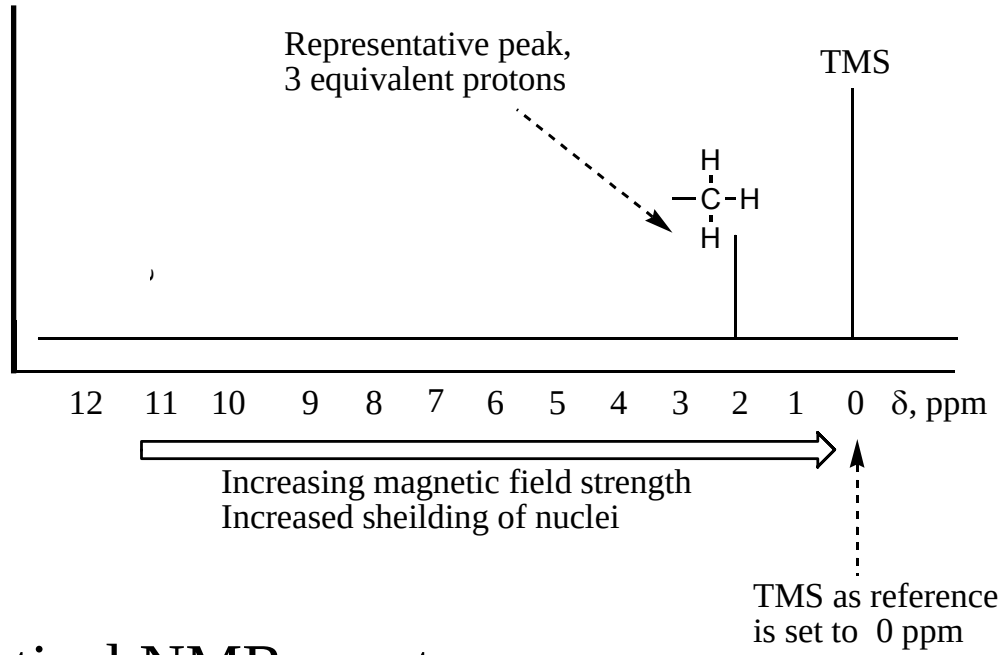

- Hypothetical NMR spectra.
- Shows TMS reference.
- Chemical shifts (δ, ppm) given relative to TMS

http://mason.gmu.edu/~bbishop1/chem318.1stlecture.ppt

Chemical Shift: Equivalency

- Protons in the same environment will have the same chemical shift.
- Protons in different environments have different chemical shifts.
- Protons with the same chemical shift are referred to as chemically equivalent.
- Integrated area of peak is proportional to the number of protons.

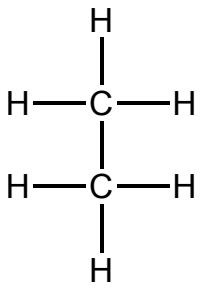

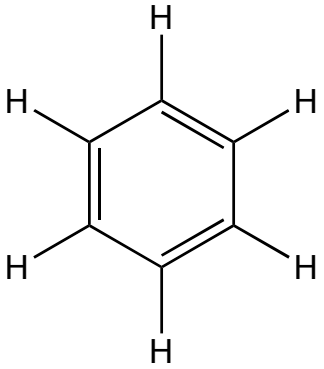

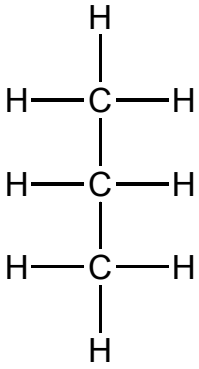

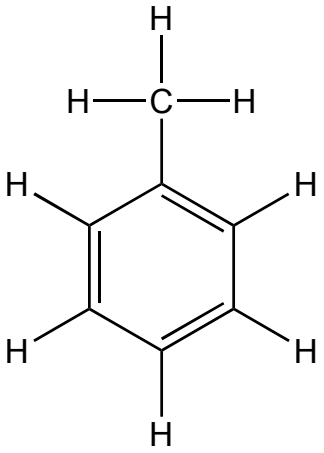

http://mason.gmu.edu/~bbishop1/chem318.1stlecture.ppt

Chemical Shift

Chemical shifts are influenced by the electronic environment. Therefore, they are diagnostic for particular types of molecular structures. The following figure indicates average ranges of chemical shifts for protons in different types of molecules.

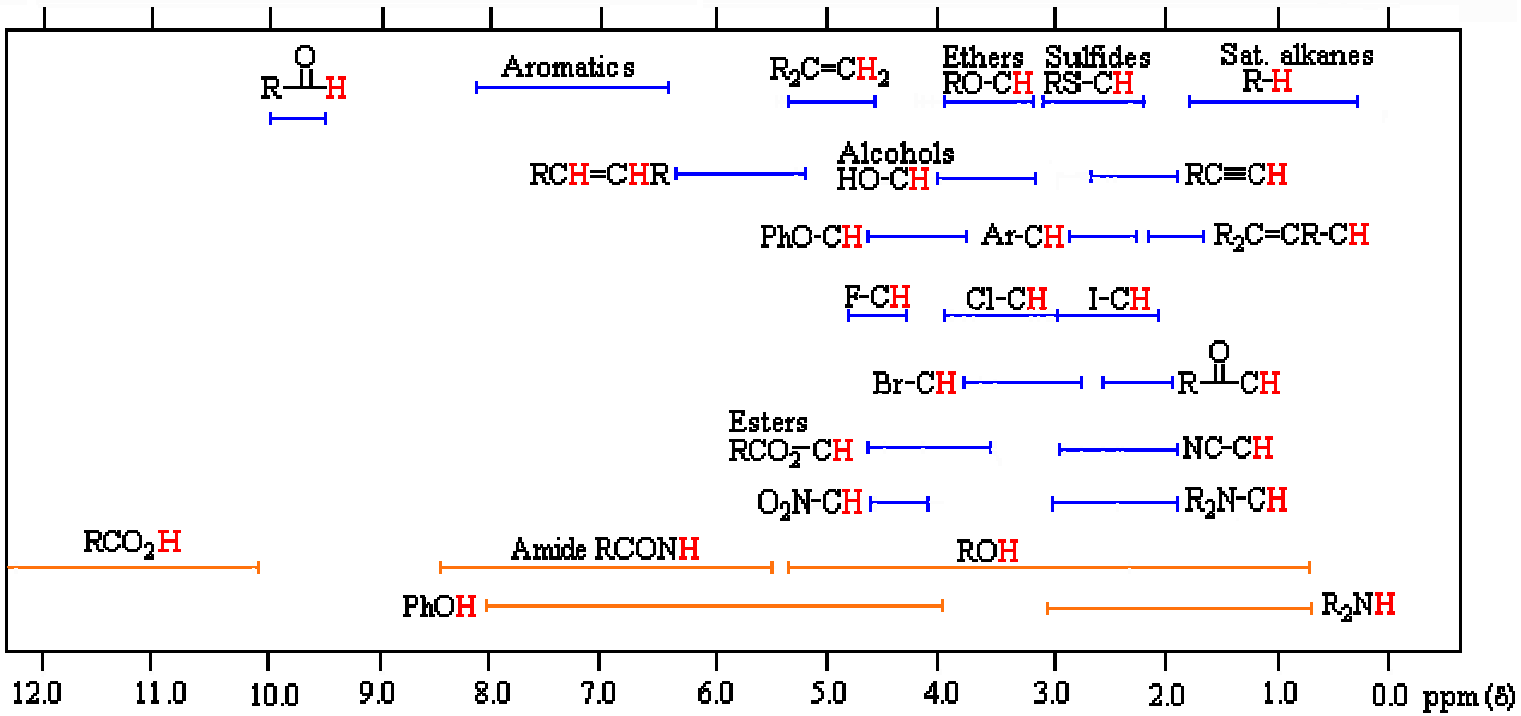

(c) http://www.cem.msu.edu/~reusch/OrgPage/nmr.htm

Chemical Shift: Summary

- intrinsic chemical shifts (depending on amino acid or nucleotide type)

  random coil chemical shifts in proteins (G-G-X-G-G)

- conformational chemical shifts, i.e. secondary chemical shift $\Delta\delta$:

  secondary structure: ^{1}H,^{13}C shifts in proteins → backbone conformation

  tertiary structure: → ring-current shifts

- applications (proteins):

  → secondary structure identification: chemical shifts index, $\Delta\delta$

  → secondary structure prediction combined with database search: TALOS

  → tertiary structure validation and refinement

  → with RDCs: molecular fragment replacement, homology model refinement

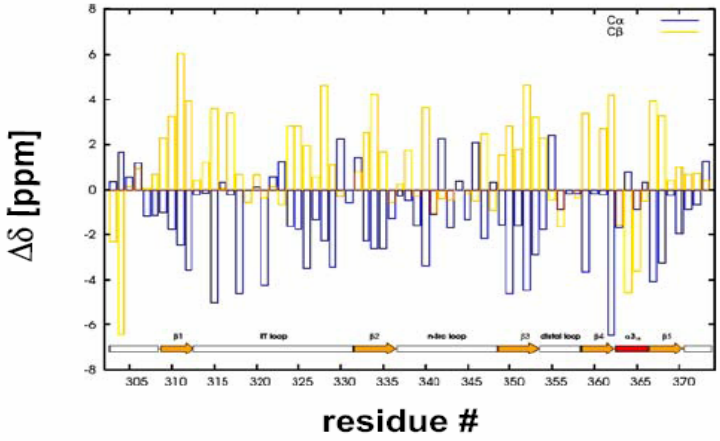

secondary chemical shift $\Delta\delta$

Scalar / J-Coupling

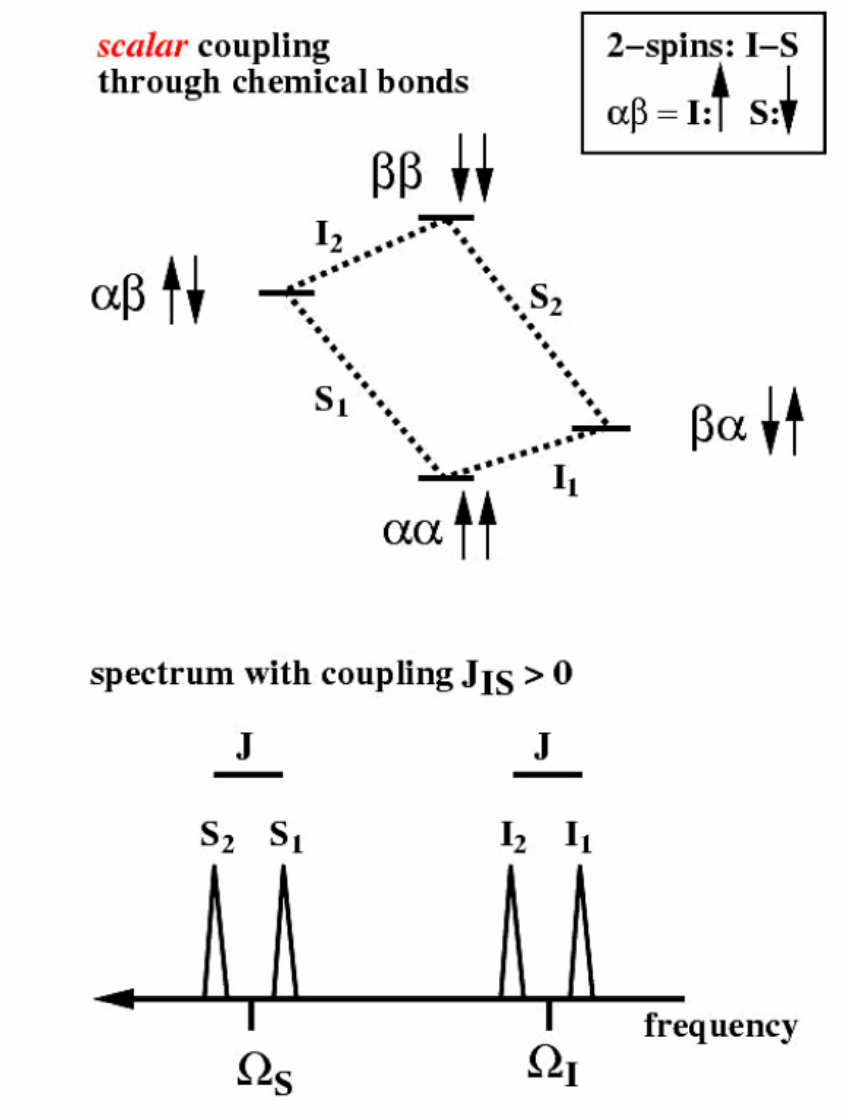

Scalar / J-Coupling

$J_{jk} > 0$

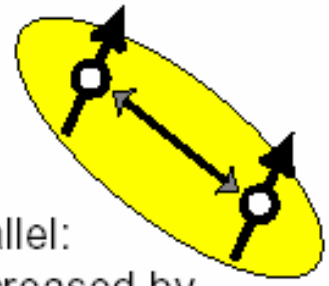

Spins parallel:
Energy increased by
J-coupling

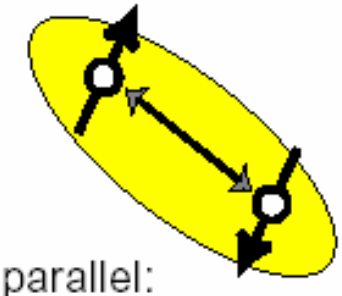

Spins antiparallel:
Energy decreased by
J-coupling

$J_{jk} < 0$

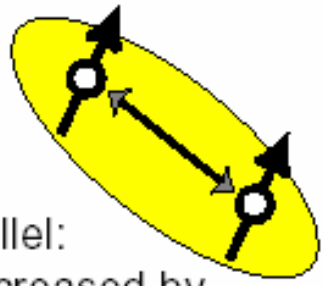

Spins parallel:
Energy decreased by
J-coupling

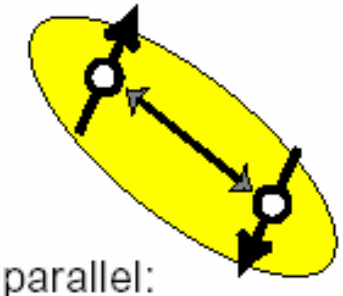

Spins antiparallel:
Energy increased by
J-coupling

Levitt

J-Coupling and Chemical Shift: Example

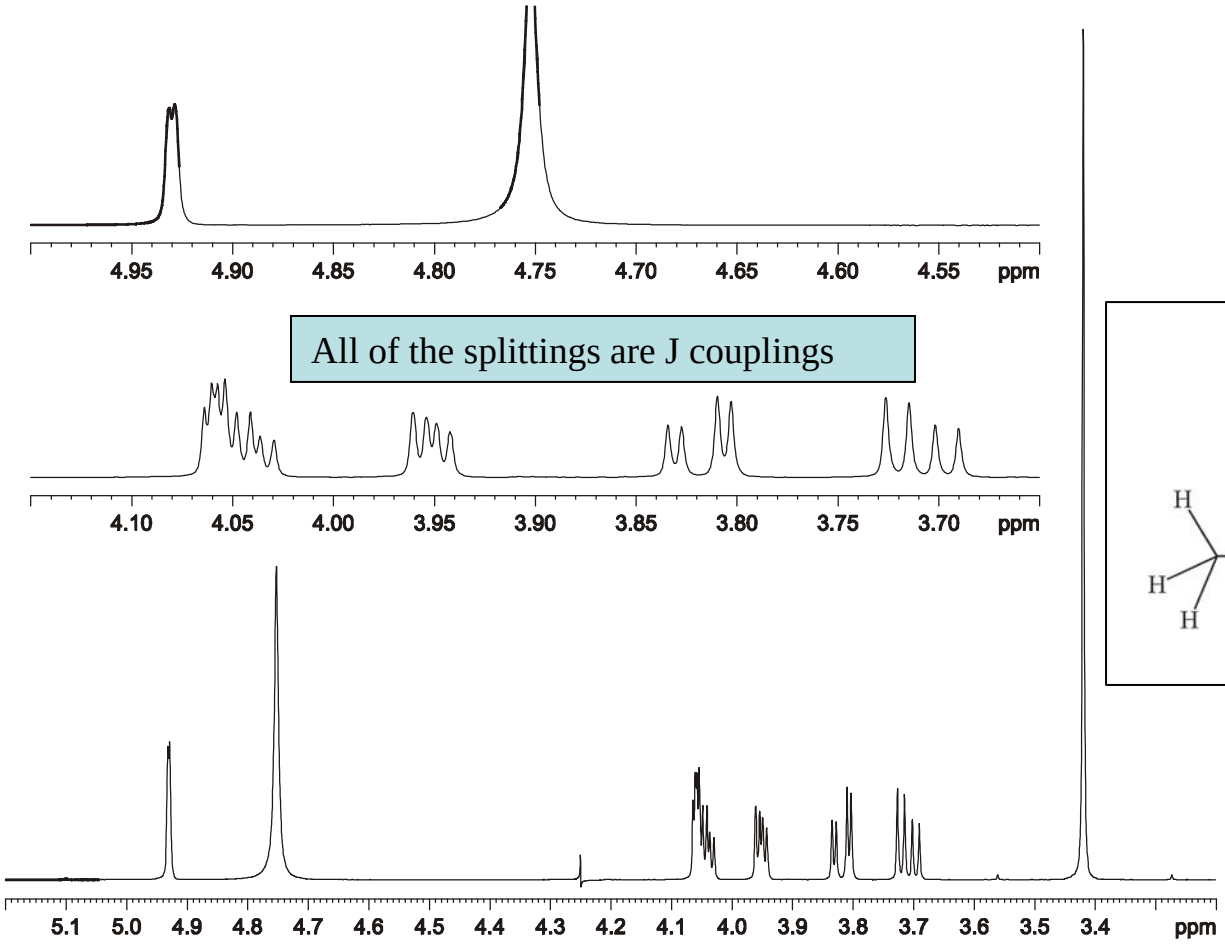

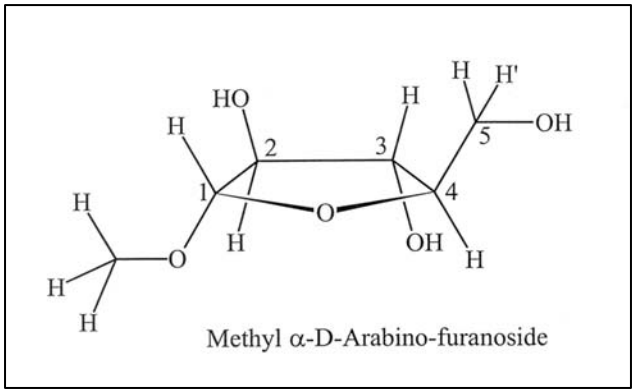

^{1}H NMR 1D spectra of Methyl α-D-Arabinofuranoside in CD_3CN. Collected at 11.7 T by Jim Rocca in AMRIS.

3-Bond J-Couplings

Martin Karplus showed that J from vicinal coupled ^{1}H atoms depends on the dihedral angle between the protons. This relationship can be approximated by the famous **Karplus equation**:

$$J(\theta) = A\cos^2(\theta) + B\cos(\theta) + C$$

A, *B*, and *C* are empirically derived parameters.

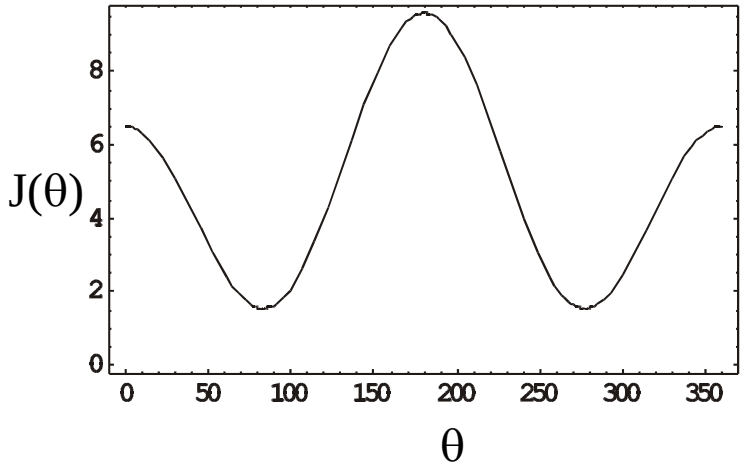

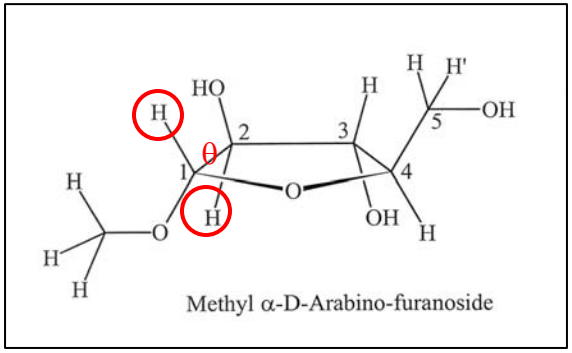

J-couplings provide an estimation of molecular conformation!

Karplus Relation and Peptide Torsion Angle Φ

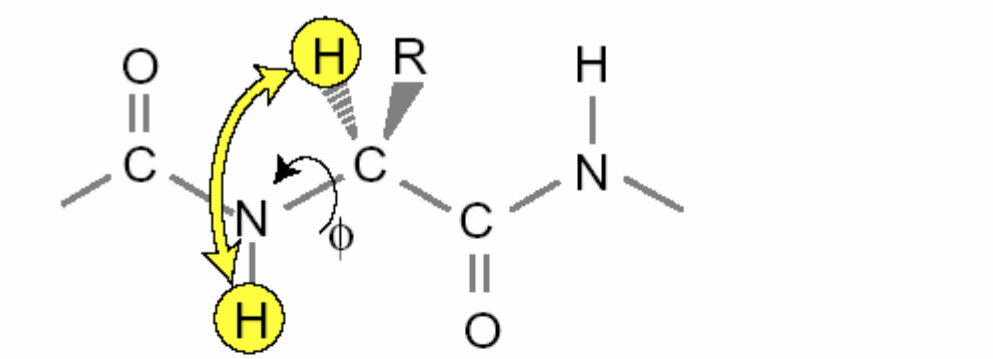

Levitt

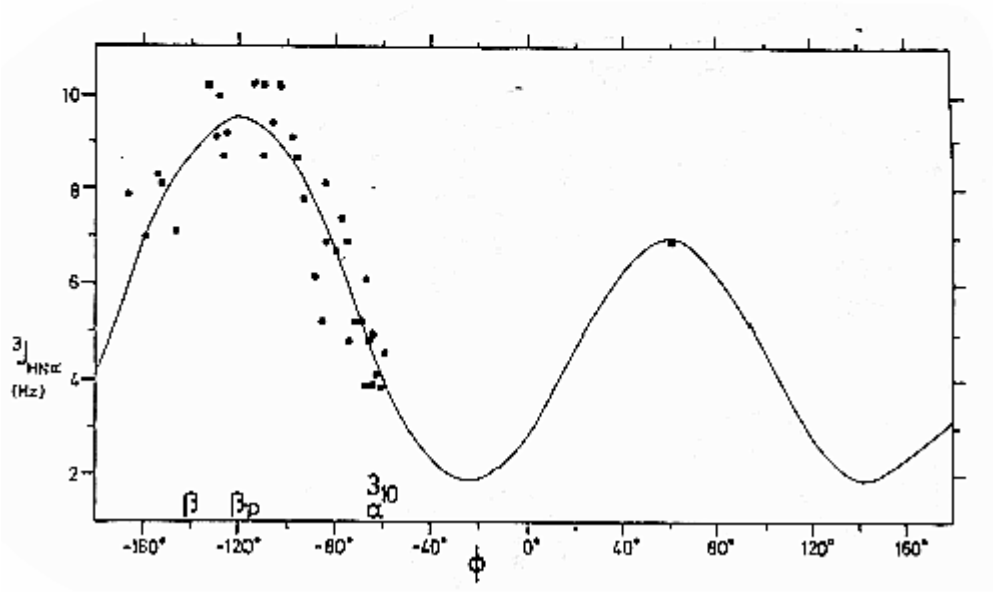

2D NMR: COSY

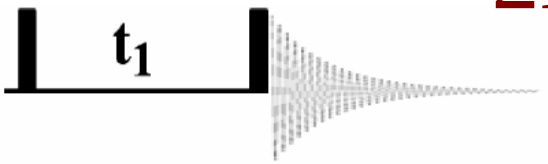

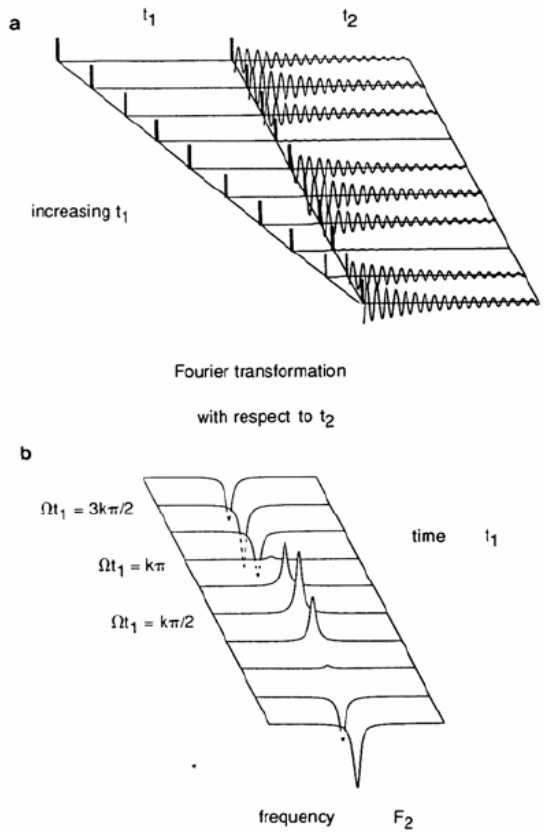

c) 2D FT

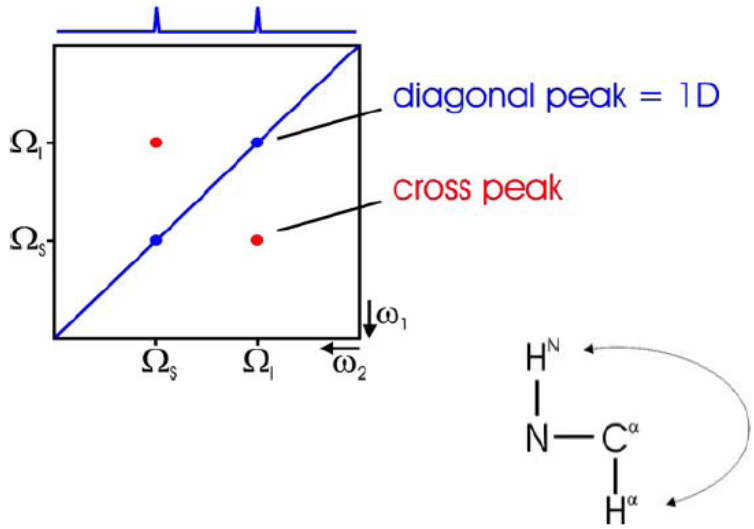

Cross peaks contain new information as a result of magnetization transfer during the 2D experiment.

In a COSY spectrum the scalar J-coupling yields transfer of magnetization from the H^N to the Ha and vice versa which belong to the same scalar coupled spin system. The cross peak therefore provides information about intraresidue $^1H,^1H$ connectivities.

Nuclear Overhauser Effect (NOE)

•The nuclear Overhauser effect (NOE) is in incoherent process in which two nuclear spins "cross-relax". Recall that a single spin can relax by T_1 (longitudinal or spin-latice) or T_2 (transverse or spin-spin) mechanisms. Nuclear spins can also cross-relax through dipole-dipole interactions and other mechanisms. This cross relaxation causes changes in one spin through perturbations of the other spin.

•The NOE is dependent on many factors. The major factors are molecular tumbling frequency and internuclear distance. The intensity of the NOE is proportional to r^{-6} where r is the distance between the 2 spins.

•Since protons have a higher polarization than carbons and the same sign of gamma they increase the observed carbon intensities.

Nuclear Overhauser Effect (NOE)

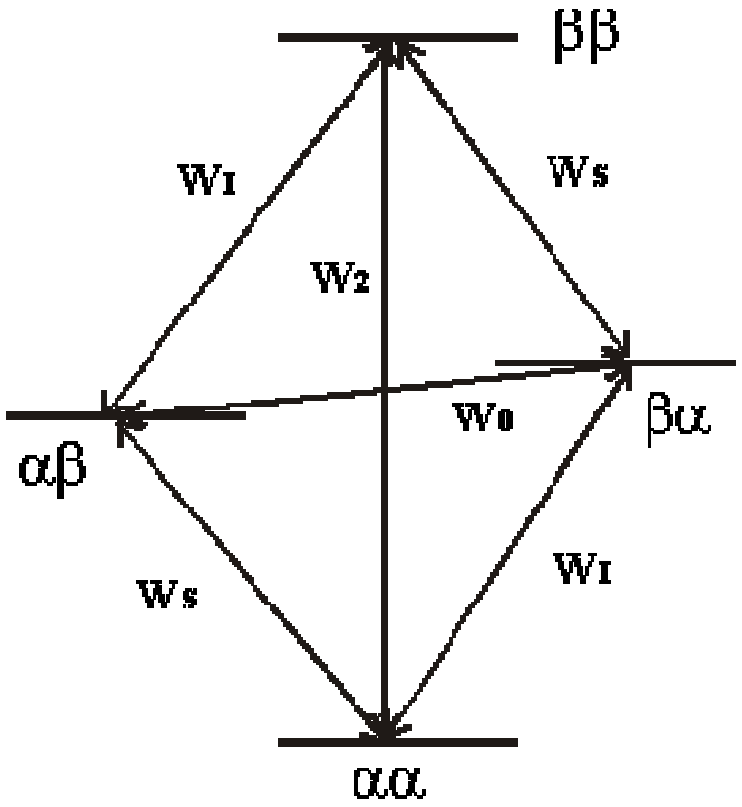

Two nuclear spins within about 5 Å will interact with each other through space. This interaction is called cross-relaxation, and it gives rise to the nuclear Overhauser effect (NOE).

Two spins have 4 energy levels, and the transitions along the edges correspond to transitions of one or the other spin alone. W_2 and W_0 are the cross-relaxation pathways, which depend on the tumbling of the molecule.

Nuclear Overhauser Effect (NOE)

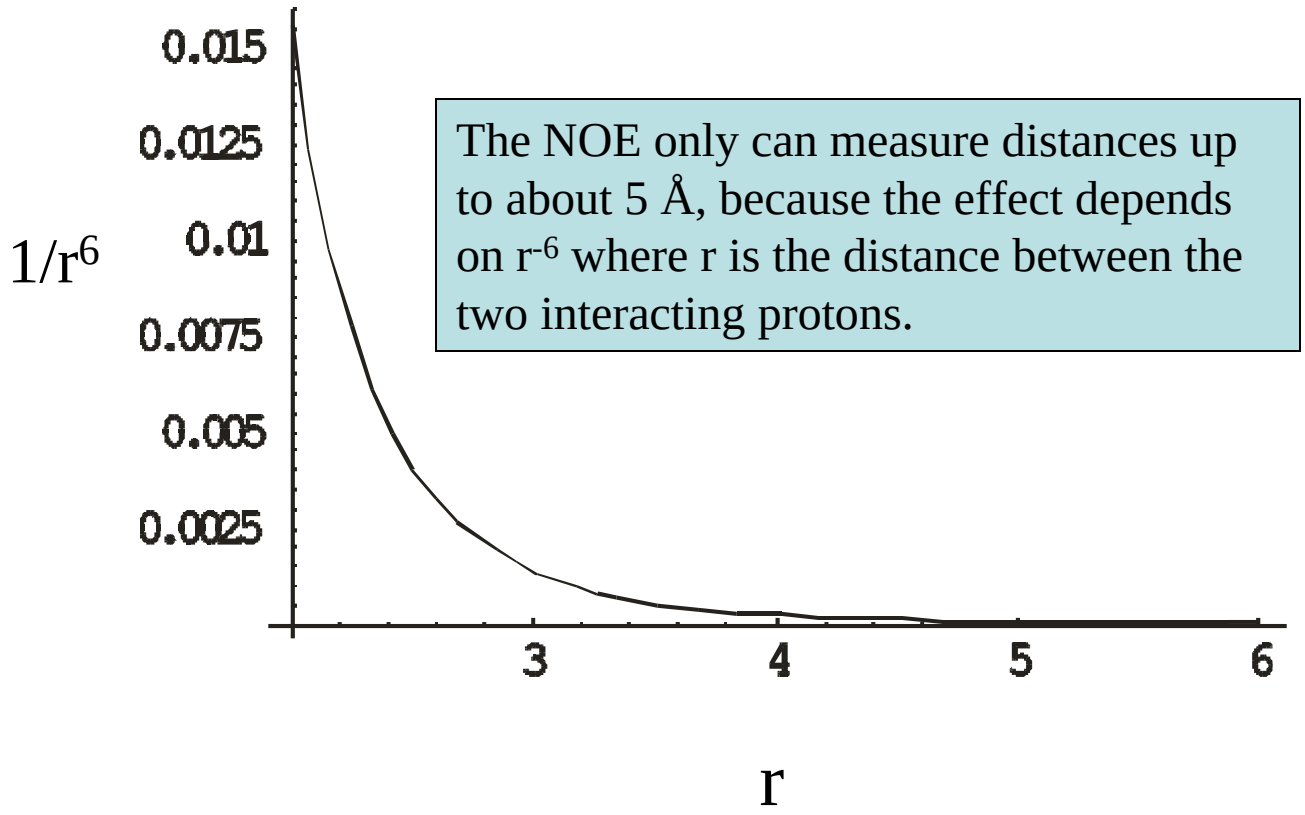

The NOE only can measure distances up to about 5 Å, because the effect depends on r^{-6} where r is the distance between the two interacting protons.

Nuclear Overhauser Effect (NOE)

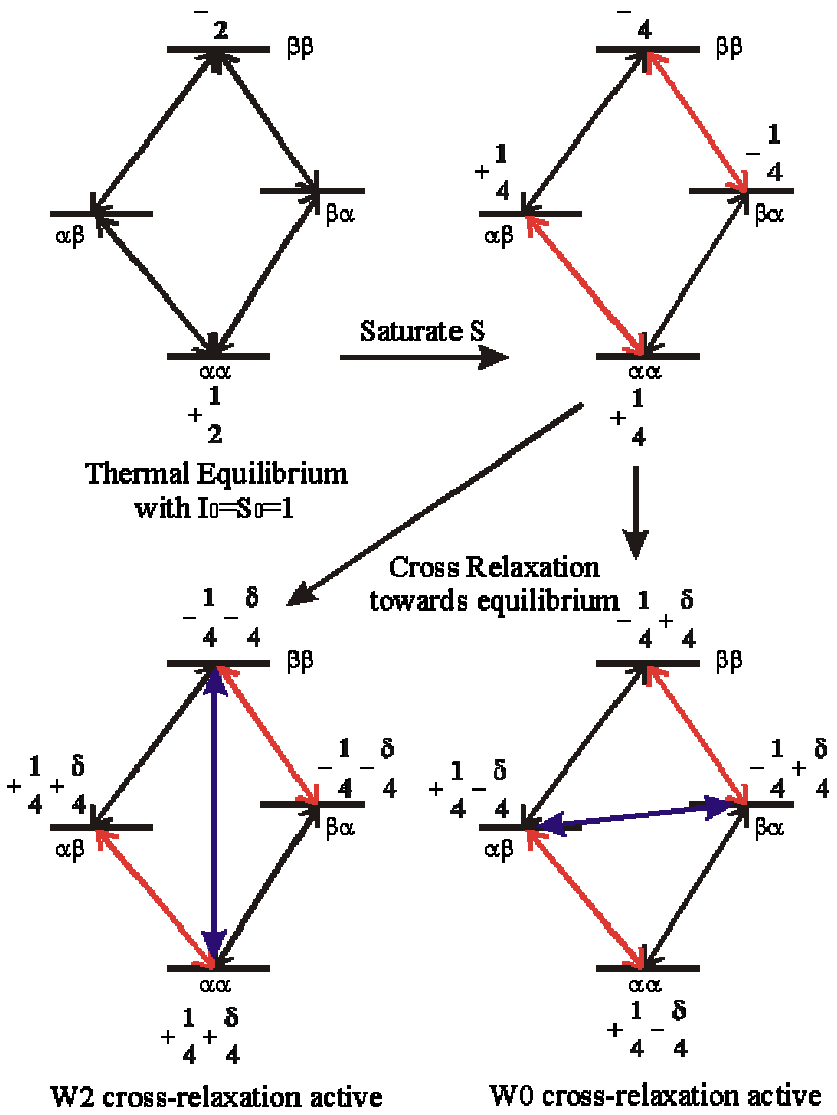

When two nuclear spins are within 5 Å, they will cross-relax. If one spin (S) is saturated (red lines along the edge), the system is not in equilibrium anymore. Magnetization will either flow from the top to the bottom (W_2 active) or from the right to left (W_0 active). The difference in energy between ββ and αα is twice the spectrometer frequency, and molecular motions about that frequency are required for the transition. The difference between αβ and βα is very small, and very slow molecular motions (e.g. proteins) will excite that transition.

Residual Dipolar Couplings

Dipolar couplings are the physical basis for spin-spin cross-talk which causes relaxation and the NOE. The dipolar coupling between two spins depends on the internuclear distance r and its orientation with respect to the static magnetic field B_0.

$$D \sim 1/r^3 \langle 3\cos^2\theta - 1 \rangle$$

In the solid state, this leads to large dipolar splittings and huge linewidths since dipolar couplings, e.g. H-N are in the kHz range. In the liquid state, the orientation dependence and therefore D is averaged to zero.

If a molecule in solution is weakly aligned (10^{-3}) residual dipolar couplings (RDCs) can be reintroduced with a size of a few Hz. Thus, high-resolution spectra are obtained, but the distance and orientation dependence of D is reintroduced and provides valueable structural information.

For example, from the H-N dipolar couplings the projection angles θ and ϕ can be obtained.

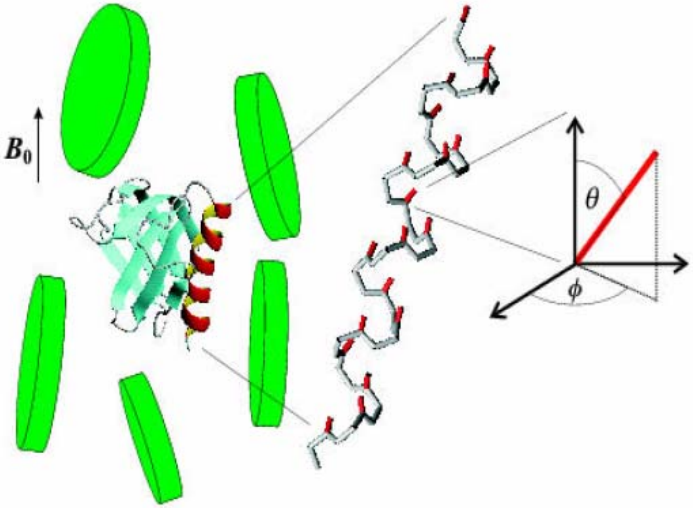

$$RDC = D_a \{(3\cos^2\theta - 1) + 3/2\ R \sin^2\theta \cos 2\phi\}$$

D_a and R describe the alignment tensor.
Biomolecules can be weakly aligned in dilute liquid crystalline media, e.g. bicelles (see figure).

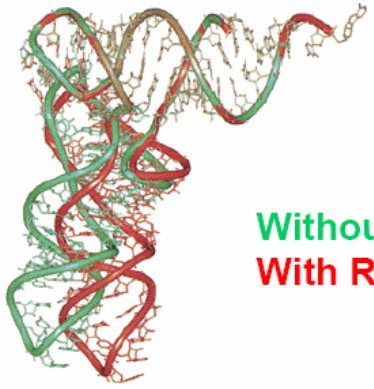

Without RDCs
With RDCs

Exchange

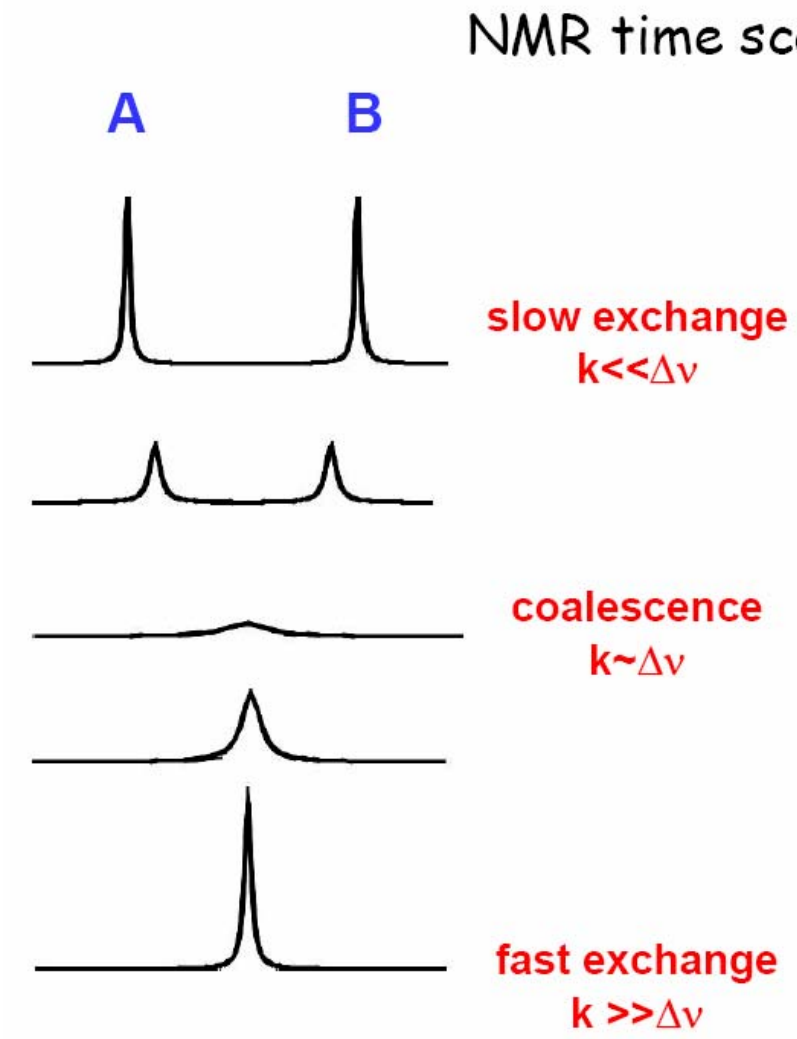

- Chemical or conformational exchange can be analyzed by NMR
- Rate constants can be determined, e.g. for a 2-state chemical reaction or conformational exchange:

$$A \underset{k_{-1}}{\overset{k_1}{\rightleftharpoons}} B \quad k_{ex} = k_1 + k_{-1}$$

NMR Time Scales

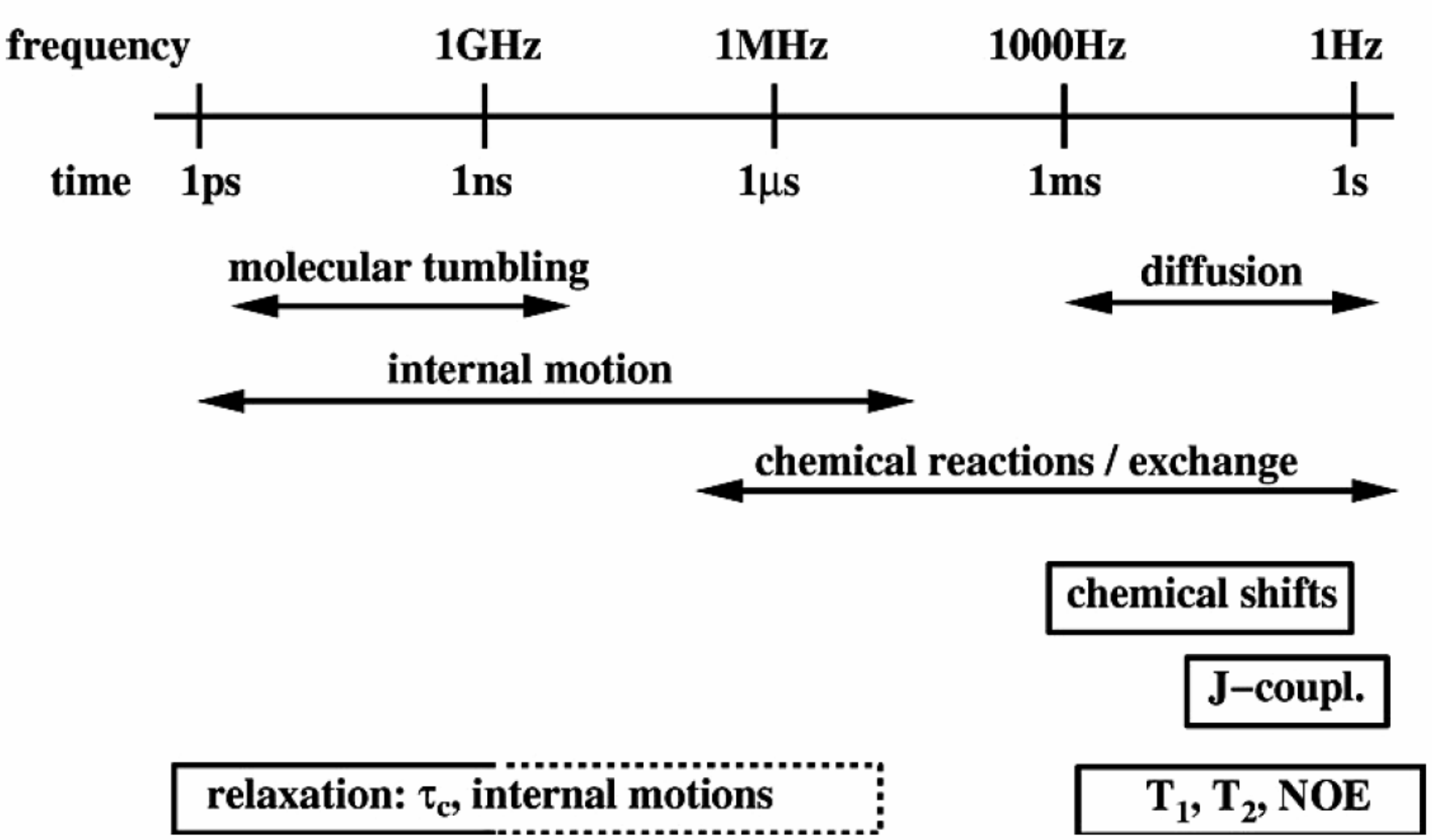

NMR Observables

Observable	Information
• chemical shifts $^{1}H, ^{13}C, ^{15}N, ^{31}P$	assignments, secondary structure
• J-couplings (through bond) $^{3}J(H^{N}, H\alpha)$, $^{3}J(H\alpha, H\beta)$, ...	dihedral angles: ϕ, χ, Karplus curves
• NOE (through space)	interatomic distances (<5Å)
• solvent exchange (HN)	hydrogen bonds
• relaxation / linewidths $^{1}H, ^{13}C, ^{15}N$	mobility, dynamics conform./chem.exchange projection angles (ψ, ...)
• residual dipolar couplings ^{1}H-^{15}N, ^{1}H-^{13}C, ^{13}C-^{13}C, ...	bond projection angles

Structure Determination

NMR Structure Determination

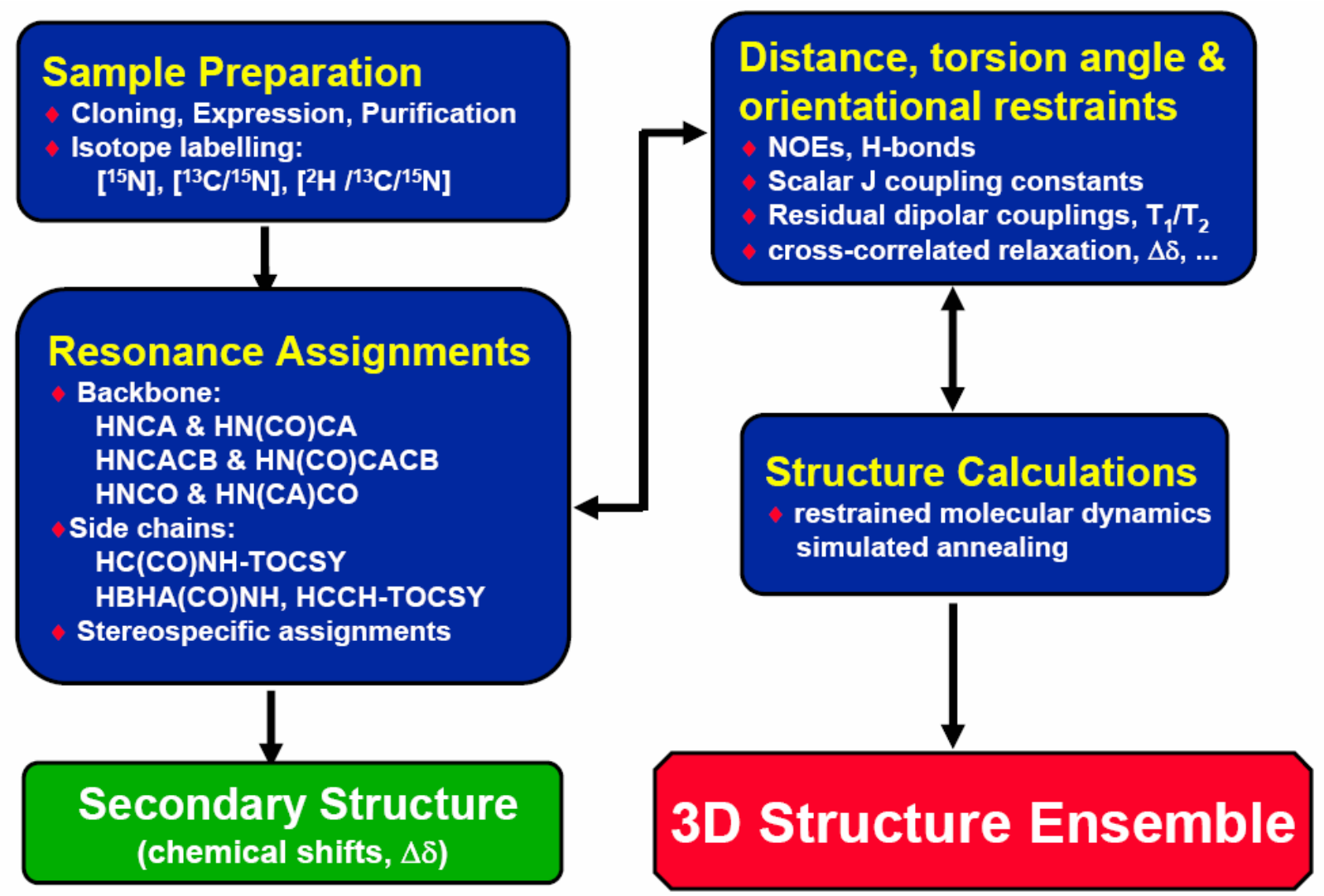

NMR Structure Determination

- The NOE intensities measured in a NOESY spectrum are calibrated and used to derive proton/proton distance restraints (NOE ~ $1/r^6$)
- These are applied in a restrained molecular dynamics / simulated annealing (MD/SA) calculation.
- Different and/or randomized starting structures are used. The result is an ensemble of structures that is consistent with the experimentally derived distance restraints.

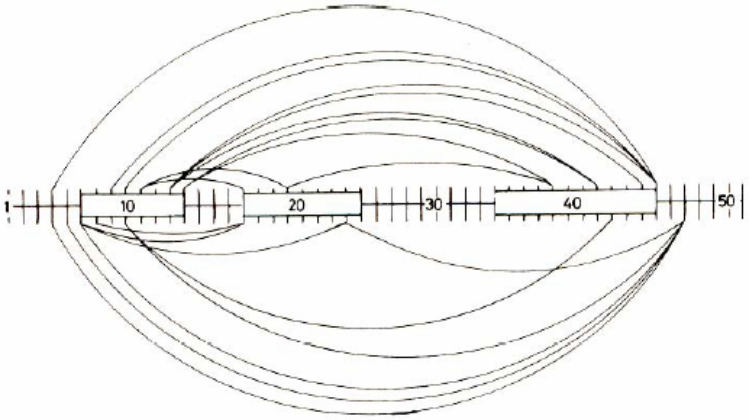

Figure 10.2. Schematic presentation of the amino acid sequence of *lac* headpiece, with three boxes identifying α-helical regions. The curved lines connect residues between which one or several long-range NOE's were observed (from Zuiderweg et al., 1984b).

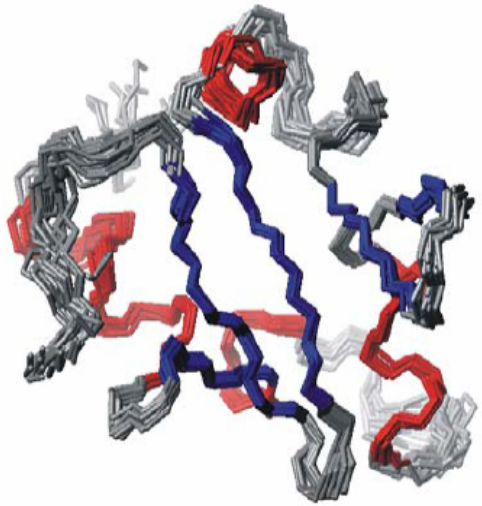

An ensemble of NMR structures obtained from a restrained MD/SA calculation

Distance Restraints

Proton “density” in a 15 kDa protein

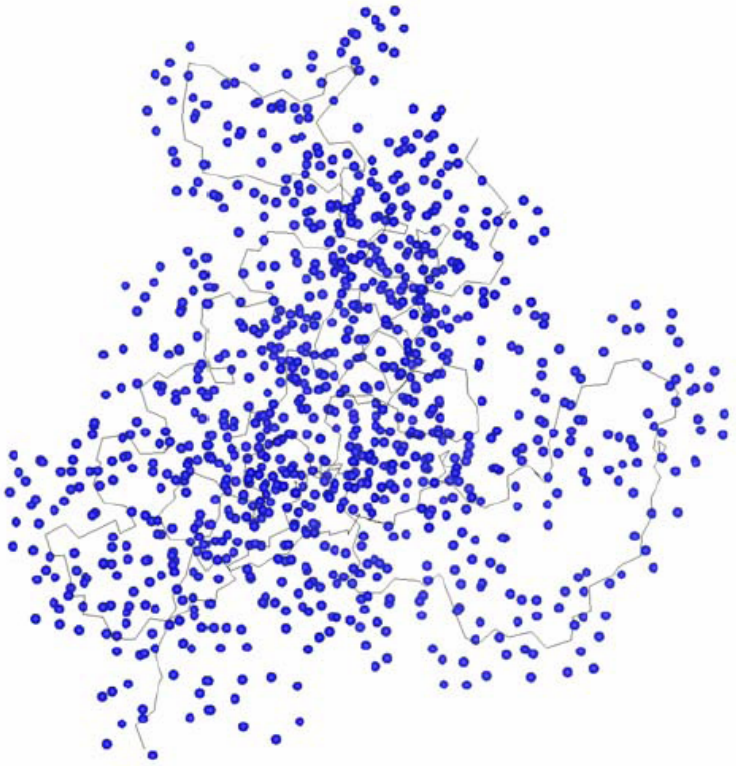

protein/protein NOEs

intermolecular NOEs protein/RNA

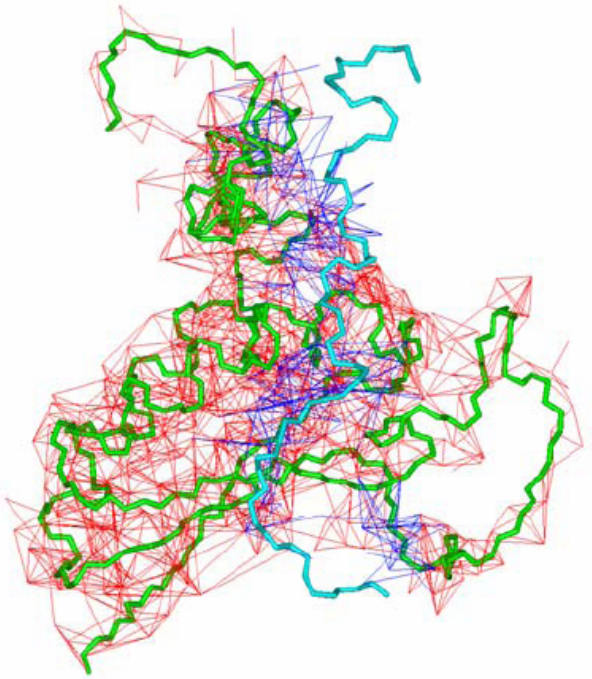

18 kDa protein/RNA complex

Accuracy and Precision

Precision: coordinate rmsd of structure ensemble vs. average structure

Accuracy: coordinate rmsd of structures ensemble vs. "true" structure

Protein

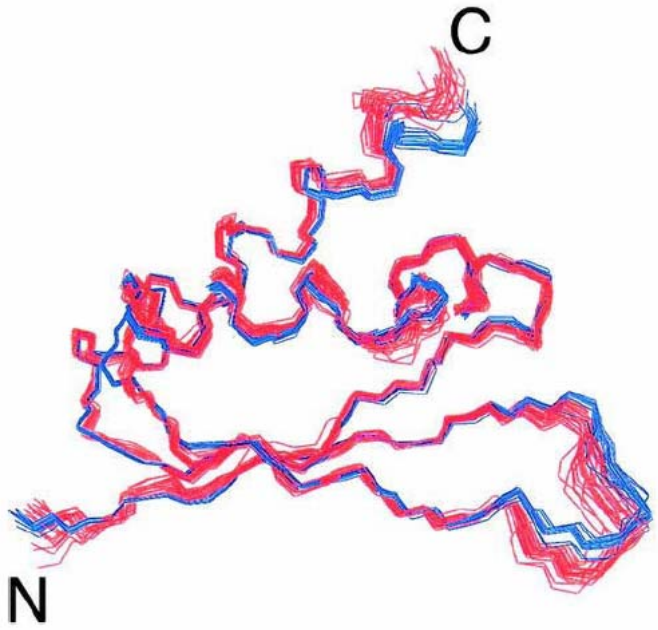

J. Mol. Biol. (1999) 289, 949-962

RNA

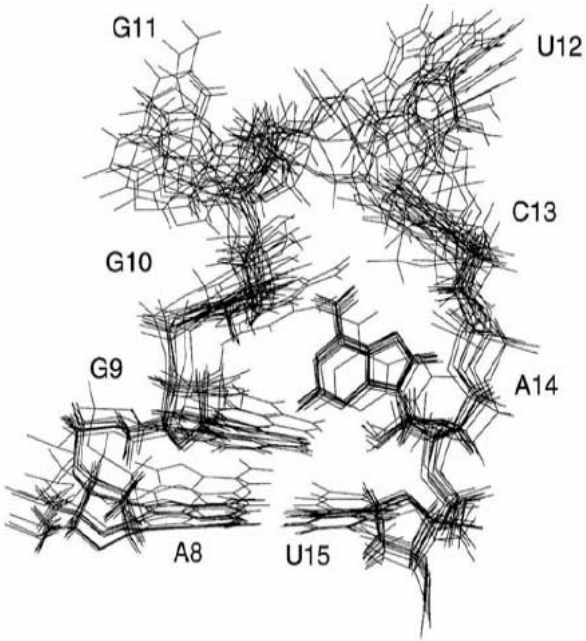

EMBO J. (1998) 17, 7498-7504

Problems with Higher Molecular Weights

- slower tumbling in solution → fast decay of NMR signal → poor signal-to-noise
- larger number of signals → signal overlap in NMR spectra

linewidth $\Delta\nu_{1/2} = 1/\pi T_2$

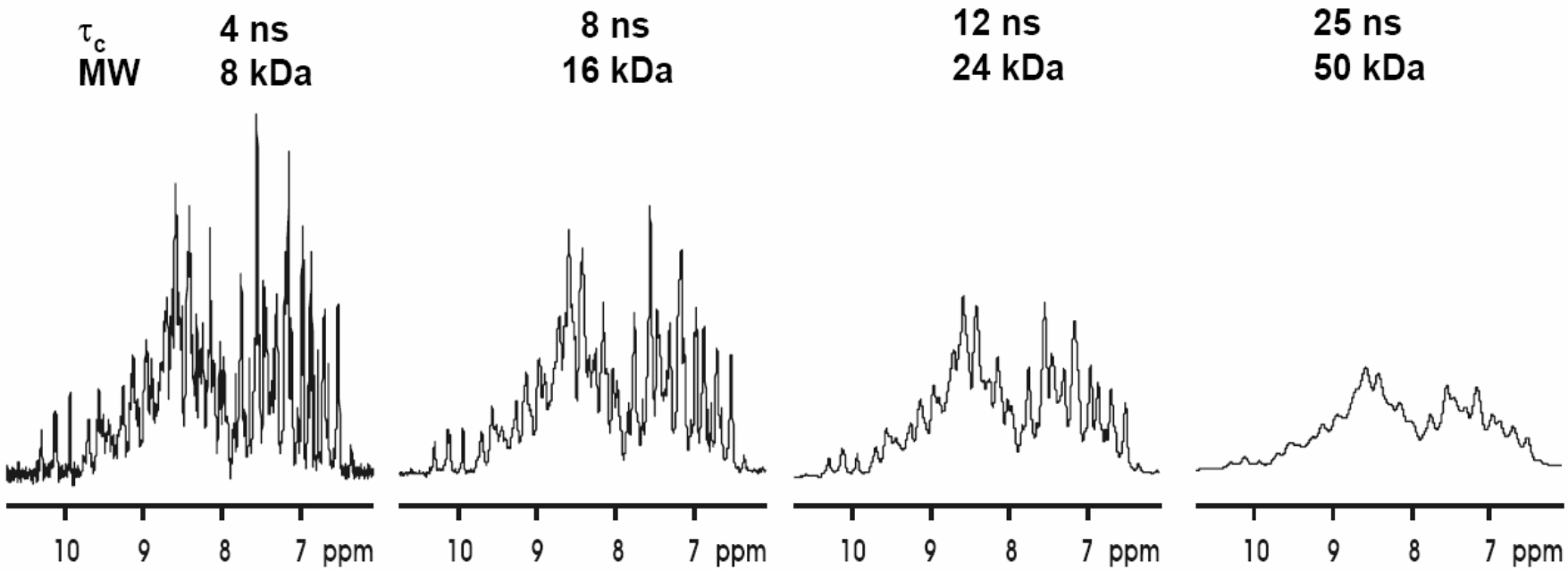

Solutions for Higher Molecular Weights

- improvements in hardware:
  - → higher magnetic fields, cryoprobes
- improved NMR methods: relaxation optimized pulse sequences
  - → TROSY (transverse relaxation optimized spectroscopy), multiple quantum line-narrowing
- novel restraints:
  - → residual dipolar couplings
  - → cross-correlated relaxation
  - → chemical shifts
- isotope labeling, especially deuteration:
  - → residue-specific labeling (amino acid or nucleotide)
  - → ^{2}H-labeling - random fractional (e.g. 50-75%)
    - specific, e.g. with $^{1}H^{\alpha}$- or methyl-selective ^{1}H-labeling
  - → segmental labeling (chemical ligation, intein method, ligases)
  - → subunit specific labeling in molecular complexes

TROSY and ^{2}H-Labeling

Transverse relaxation optimized spectroscopy

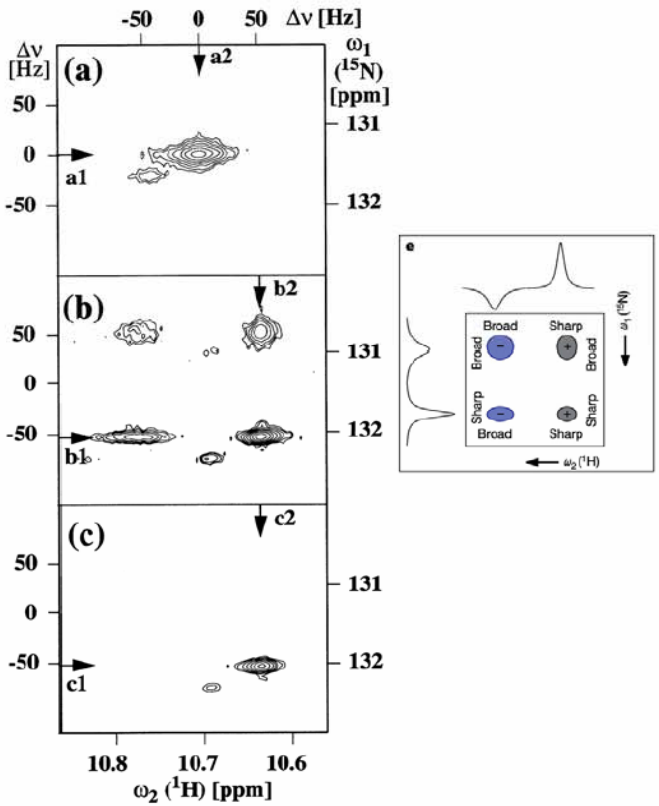

Pervushin et al. PNAS (1997) 94, 12366-71.

^{2}H-labeling

- reduced relaxation (γ_D/γ_H ~ 1 / 6.5)
  - improved signal-to-noise
  - better resolution
- reduced number of cross peaks
- suppression of spin diffusion

^{1}H ↕ ^{13}C dipole/dipole relaxation

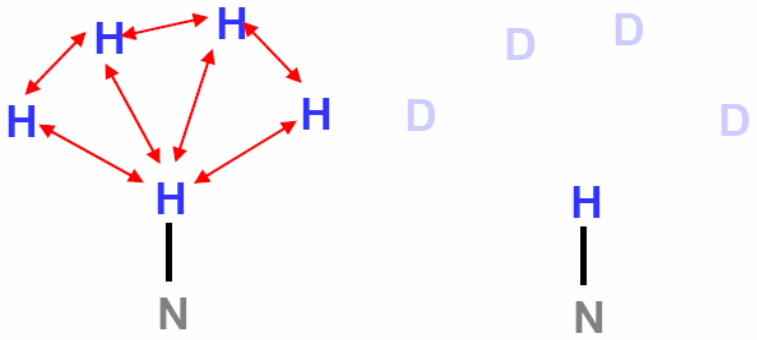

Increase in Molecular Weight

Proteins	7 kDa	15 kDa	30 kDa	50 kDa	100+ kDa

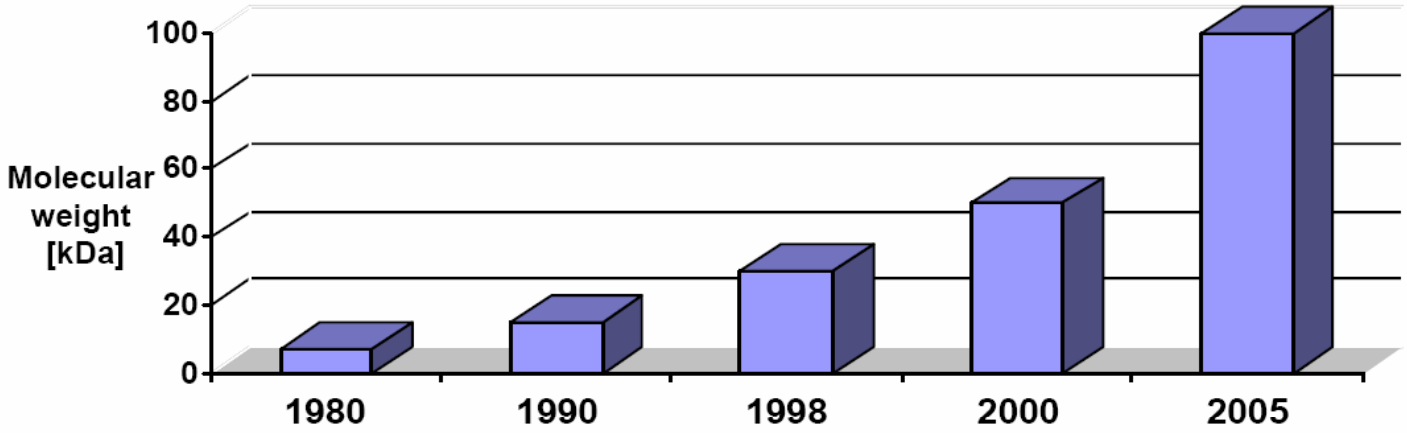

magnets	500 MHz	600 MHz	800 MHz	900 MHz	1 GHz
cryoprobes			500,600	700,800	
NMR	2D	3D/4D	TROSY, residual dipolar couplings cross-correlated relaxation		
		triple resonance, gradients			
Labeling		^{13}C, ^{15}N	$^{2}H/^{13}C/^{15}N$	selective $^{1}H/U\text{-}^{2}H$-labeling segmental labeling	

S/N > 2400:1 @ 900 MHz, spectral resolution
S/N (3-4000:1) @ 600 MHz

higher molecular weights
projection angle restraints
spectral resolution/quality

higher molecular weights

NMR Tools for Protein-Ligand and Protein-Protein Interactions

Two-Site Exchange

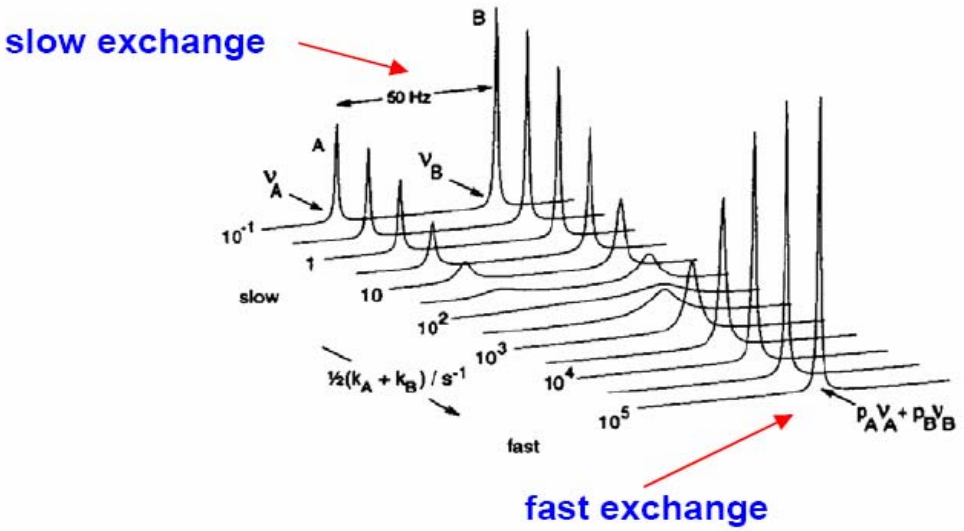

Fig. 4.7 Calculated NMR spectra for a pair of nuclei exchanging between two sites A and B with populations in the ratio $p_B/p_A = 2$ (unsymmetrical two-site exchange). Spectra are shown for a range of values of the average exchange rate $\frac{1}{2}(k_A + k_B)$, where $k_A/k_B = 2$. The difference in resonance frequencies of the two sites, $\delta\nu$, is 50 Hz. The linewidths in the absence of exchange are 1 Hz.

$$P + L \underset{k_{on}}{\overset{k_{off}}{\rightleftharpoons}} PL$$

$K_{diss} = [P][L] / [PL] = k_B/k_A$
$k_A = k_{on}\,[L] \quad k_B = k_{off}$
B = protein-ligand complex PL
A = free protein P

This can be extended directly to study protein-ligand interactions.

Limit	Rates	Populations	Line broadening
Slow	$k_{A,B} << (\nu_A - \nu_B)$	$p_A/p_B = area_A/area_B$	$\Delta\nu_A = k_A/\pi = 1/(\pi\,\tau_A)$
Fast	$k_{A,B} >> (\nu_A - \nu_B)$	$p_A = (\nu - \nu_B)/(\nu_A - \nu_B)$	$\Delta\nu = 4\pi p_A p_B\,(\nu_A - \nu_B)^2/(k_A + k_B)$

NMR Titrations

Equilibrium Binding Constants from the Langmuir Isotherm

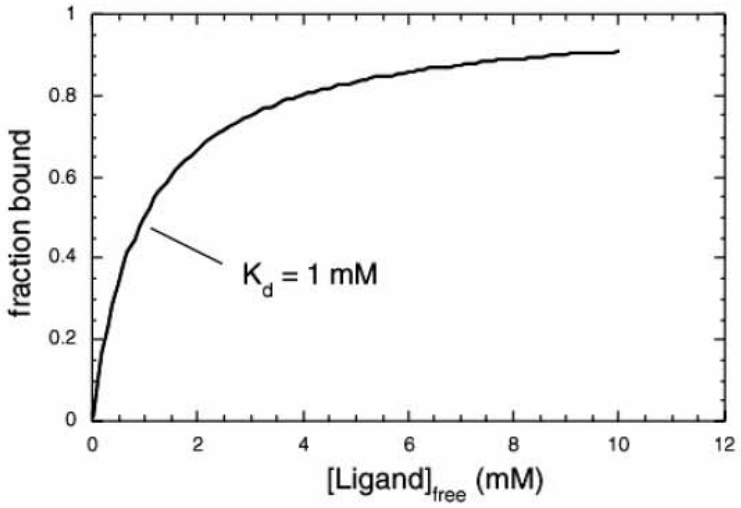

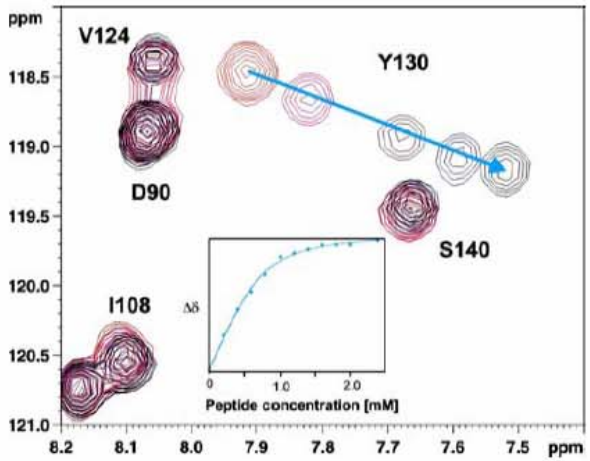

$$\Delta\delta = \delta_{obs} - \delta_f = f([L_{tot}])$$

$$\mathbf{P + L \leftrightarrow PL} \qquad K_d = \frac{[P]\,[L]_{free}}{[PL]}$$

$$f_b = \frac{\nu_{obs} - \nu_{free}}{\nu_{bound} - \nu_{free}} \text{ (fast)} \qquad f_b = \frac{area_{bound}}{area_{bound} + area_{free}} \text{ (slow)}$$

$$f_b = \frac{[L]_{free}}{K_d + [L]_{free}}$$

- In the fast exchange regime, chemical shift changes $\Delta\delta$ which induced upon adding the ligand are proportional to the mole fraction c of ligand-bound protein.
- Dissociation constants are obtained by least-square fitting of $\Delta\delta$ as a function of ligand concentration L_{total}.

NMR in Drug Research

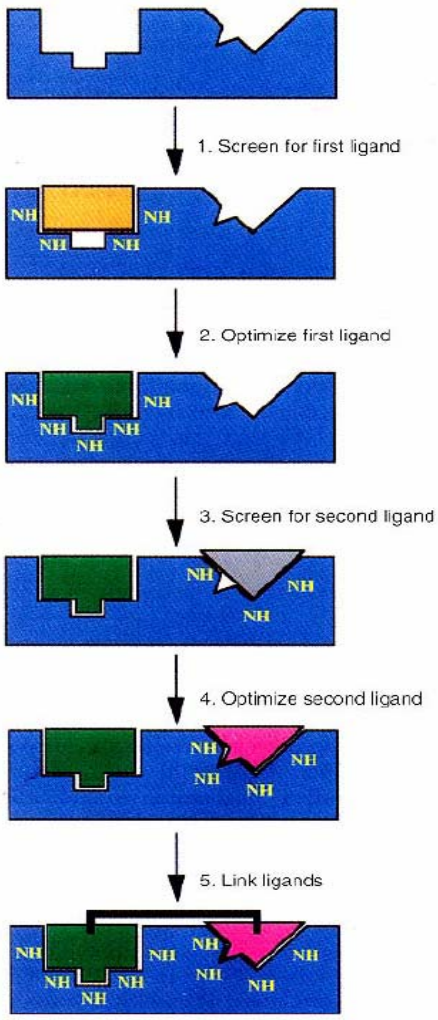

Fig. 1. An outline of the SAR by NMR method.

Structure-Activity Relationships (SAR) by NMR

Science (1996) 274, 1531

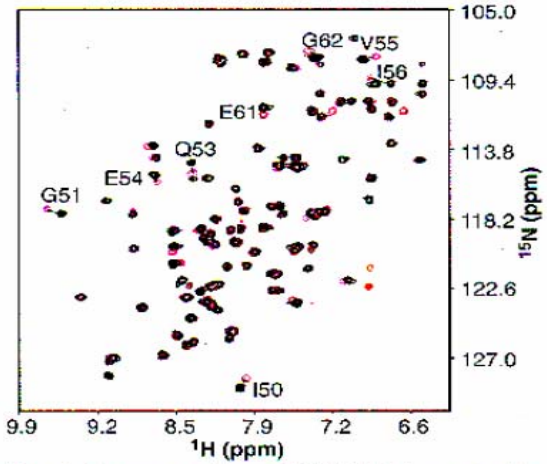

Fig. 2. A superposition of ^{15}N-HSQC spectra for FKBP in the absence (magenta contours) and presence (black contours) of compound **3**. Both spectra were acquired in the presence of saturating amounts of **2** (2.0 mM). Significant chemical shifts changes are observed for labeled residues.

SAR by NMR ...

... is a nuclear magnetic resonance (NMR)-based method in which small organic molecules that bind to proximal subsites of a protein are identified, optimized, and linked together to produce high-affinity ligands. The approach is called "SAR by NMR" because structure-activity relationships (SAR) are obtained from NMR. With this technique, compounds with nanomolar affinities for a target protein can be rapidly discovered by tethering two ligands with micromolar affinities. The method reduces the amount of chemical synthesis and time required for the discovery of high-affinity ligands and is particularly useful in target-directed drug research.

GroEL/ES Subunit Labeling

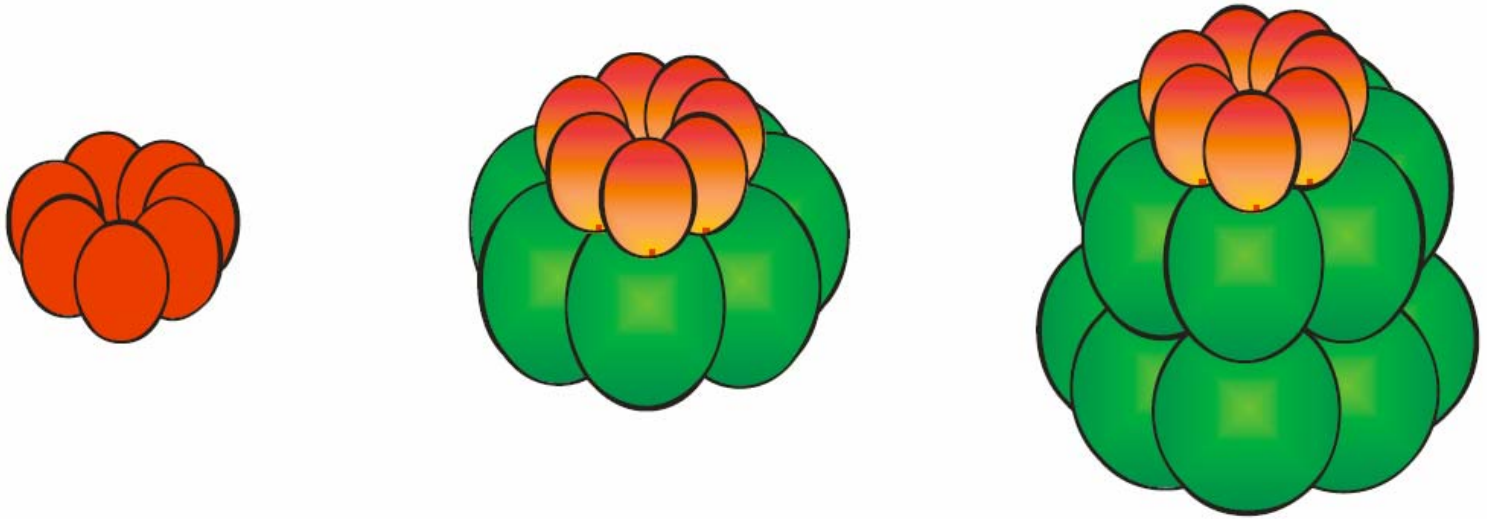

GroES
72 kDa

GroES/SR1
472 kDa

GroES/GroEL
872 kDa

Fiaux J, Bertelsen EB, Horwich AL, Wüthrich K (2002) Nature 418, 207-211.

Molecular Interface Mapping

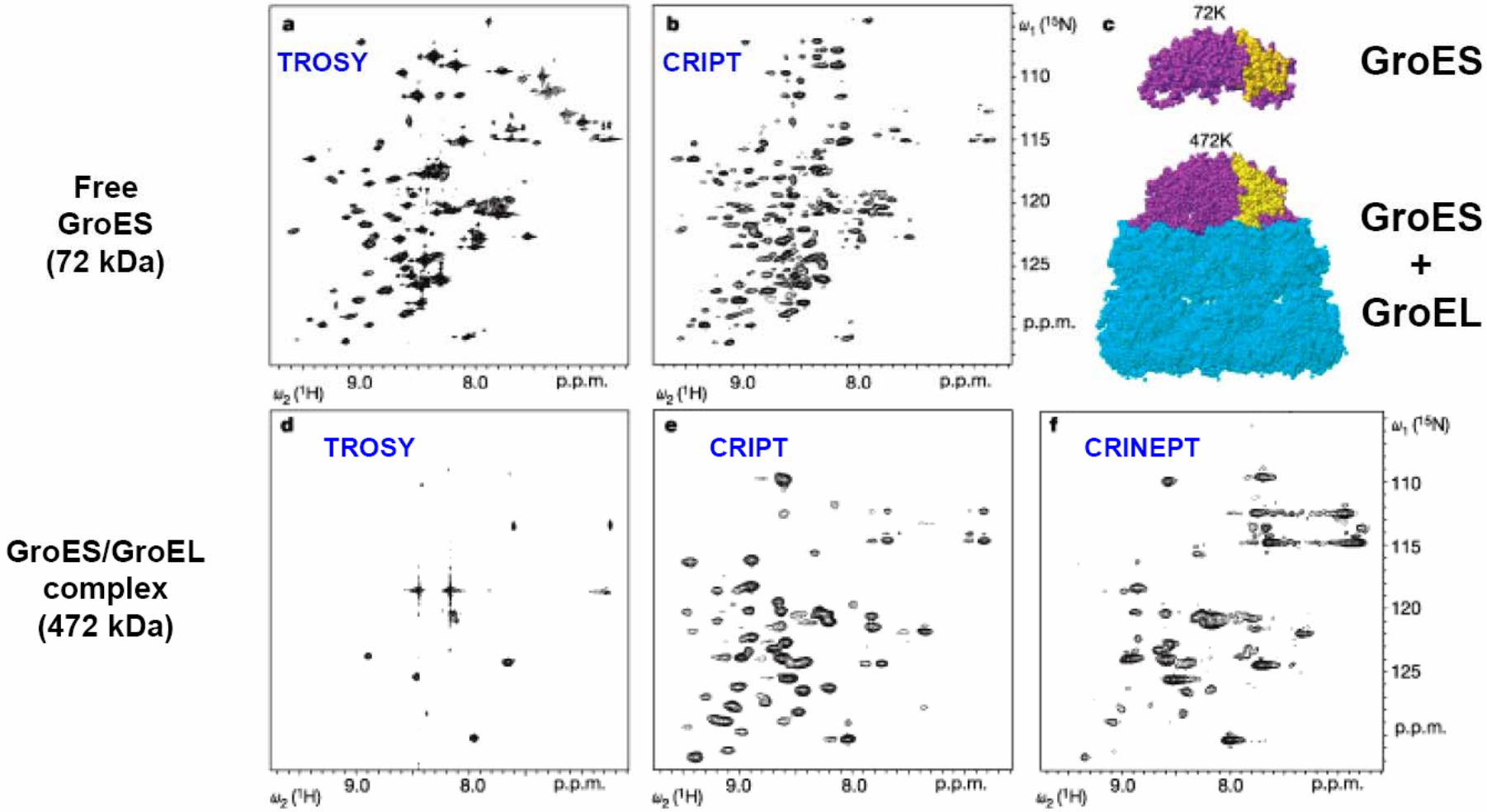

Molecular Interface Mapping

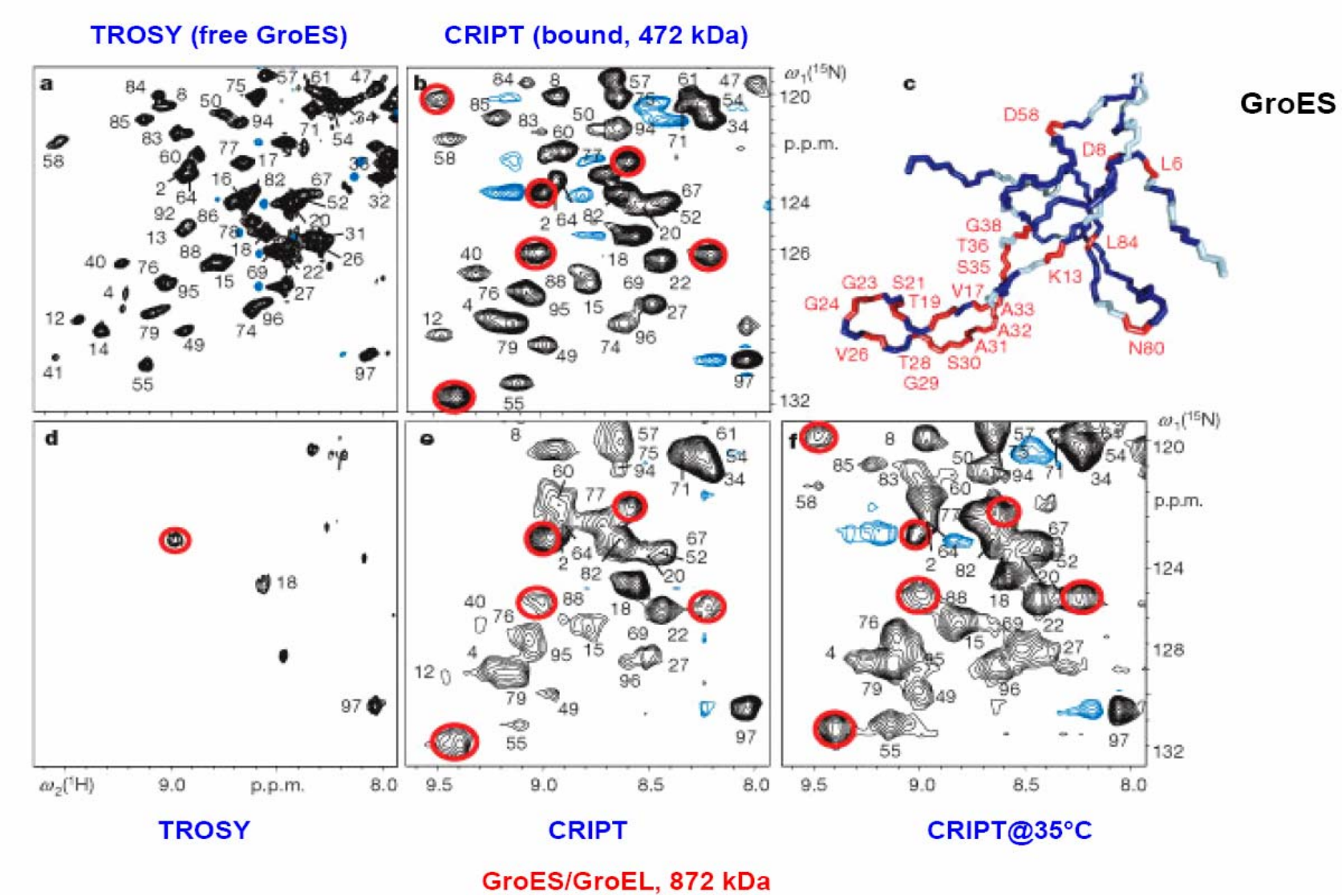

Characterizing Protein Dynamics

Backbone Dynamics – Multidomain Proteins

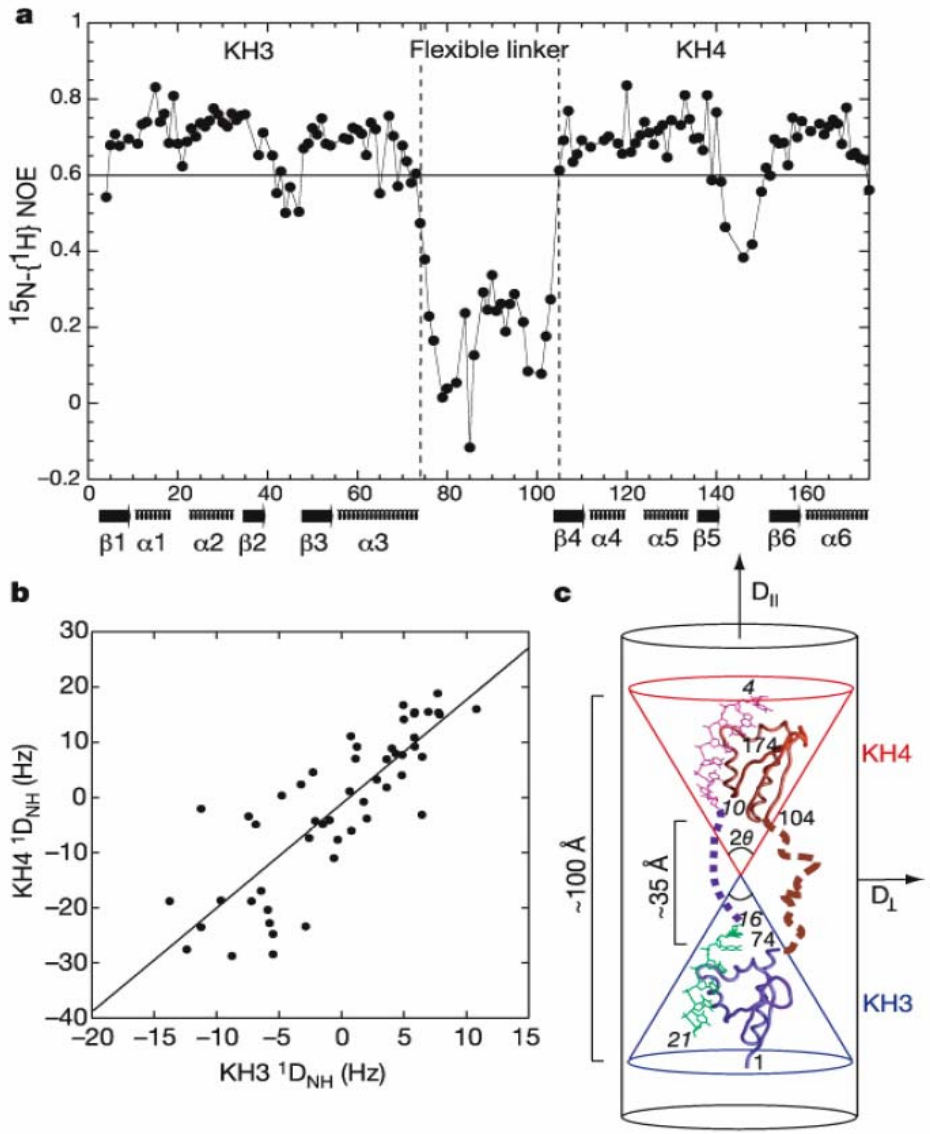

Interdomain motion in the FBP3/4-M29 ssDNA complex

Even when the ssDNA is bound the linker connecting the two KH domains remains flexible as determined by NMR relaxation measurements.

Nature (2002) **415**, 1051-6.

Enzyme Dynamics During Catalysis

- Cyclophilin A catalyses cis/trans isomerization of Xxx-Pro peptide bonds.
- Conformational fluctuations of the active site are found that occur on a time scale of hundreds of μs.
- The rates of conformational dynamics of the enzyme strongly correlate with the microscopic rates of substrate turnover.

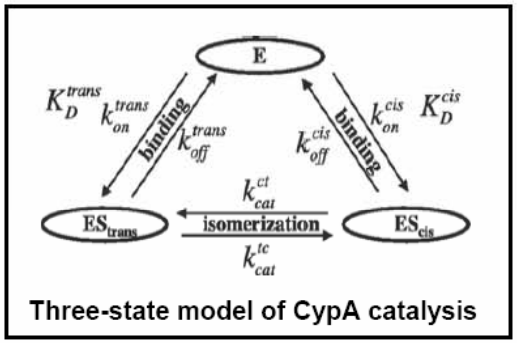

Three-state model of CypA catalysis

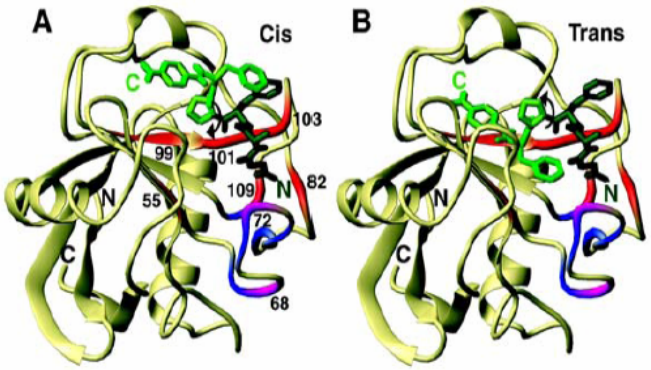

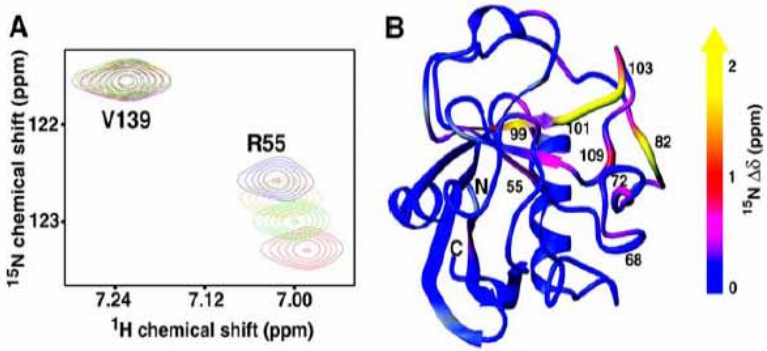

Chemical shift changes of the N-H signals in CypA upon titration with substrate map to the active site

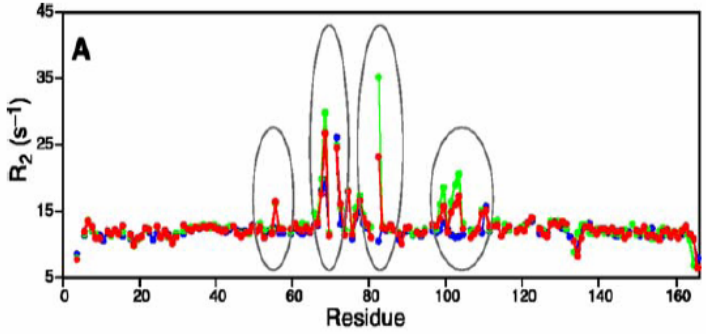

R_2 relaxation rate constants of CypA at different substrate substrate concentrations

Science (2002) 295, 1520-1523.

Enzyme Dynamics During Catalysis

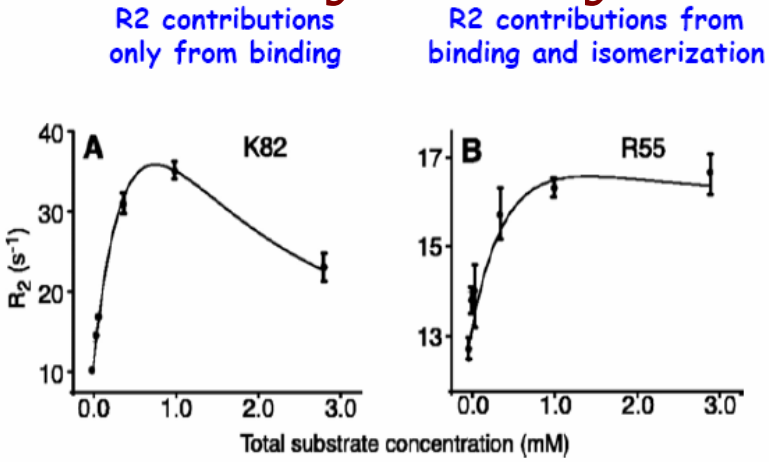

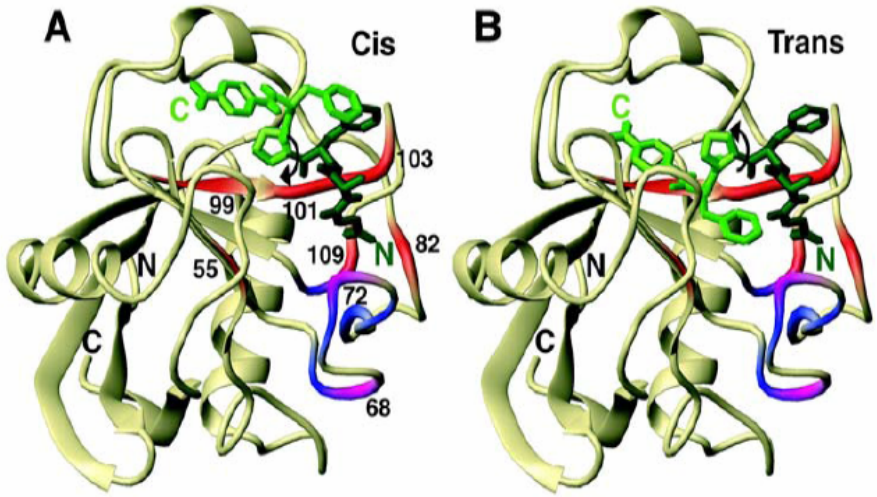

Quantification of exchange dynamics in CypA during catalysis. R_2 rate constants are plotted as a function of total substrate concentration.

(A) R_2 data for K82. The continuous line indicates the fitted Eq. 2, including contributions only from binding. K_D^{obs} = 1.18 mM; k_{off} = 11,100 s^{-1}; $\delta\omega$ = 1450 s^{-1} (3.8 ppm).

(B) R_2 data for R55. The continuous line indicates a fit according to the full three-state model, including contributions from both binding and isomerization; using K_D^{obs} = 1.19 mM, then k_{off}^{trans} = 13,000 s^{-1}; k_{off}^{cis} = 10,000 s^{-1}; k_{cat}^{ct} = 9000 s^{-1}; k_{cat}^{tc} = 5100 s^{-1}; $\delta\omega$ = 440 s^{-1} (1.2 ppm); $\delta\omega_{ct}$ = 640 s^{-1} (1.7 ppm).

Residues in CypA exhibiting microsecond time scale dynamics during catalysis.

(A) Structure of the cis conformation of the substrate Suc-Ala-Phe-Pro-Phe-4-NA (green) bound to CypA, based on the x-ray structure of CypA complexed with the cis form of Suc-Ala-Ala-Pro-Phe-4-NA (1RMH) (21). CypA residues with chemical exchange in both the presence and absence of substrate are color coded in blue (F67, N71, G74, S77, and S110). **Residues in red exhibit chemical exchange only during turnover (R55, K82, L98, S99, A101, N102, A103, and G109).** Residues shown in magenta exhibit chemical exchange in the absence of substrate, but increase in its presence (T68 and G72).

(B) Suggested trajectory of the enzymatic pathway based on the dynamics results. CypA catalyzes prolyl isomerization by rotating the part COOH-terminal to the prolyl peptide bond by 180° to produce the trans conformation of the substrate. In this model, the observed exchange dynamics for residues in strand 5 can be explained.

Science (2002) 295, 1520-1523.

Protein Folding

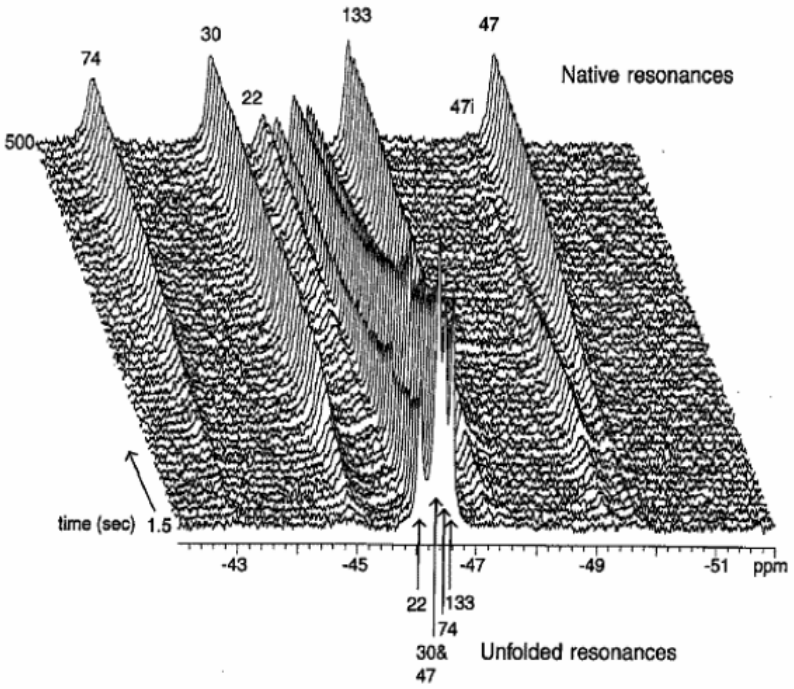

Stopped-flow ^{19}F NMR spectra of the refolding of 6-^{19}F-tryptophan labeled Escherichia coli dihydrofolate reductase following dilution from 5.5 to 2.75 M urea at 5 °C in the presence of 3.8 mM NADP+.

The disappearance of the five resonances of the unfolded state, clustered between -46.0 and -46.6 p.p.m., and the growth of the more widely dispersed native peaks are clearly seen in this well-resolved set of spectra. Each spectrum represents the sum of 41 separate rapid dilution experiments. The kinetics and chemical shifts suggest the formation of an intermediate that is unable to bind NADP+ strongly, having a native-like side chain environment in the regions around tryptophans 30, 47 and 133, and little if any native side chain environment around tryptophans 22 and 74. The resonance labeled 47i is that of Trp 47 in the intermediate.

NMR Supplement II, *Nature Struct. Biol.* (1998) **5**, 504 - 50

Protein Folding

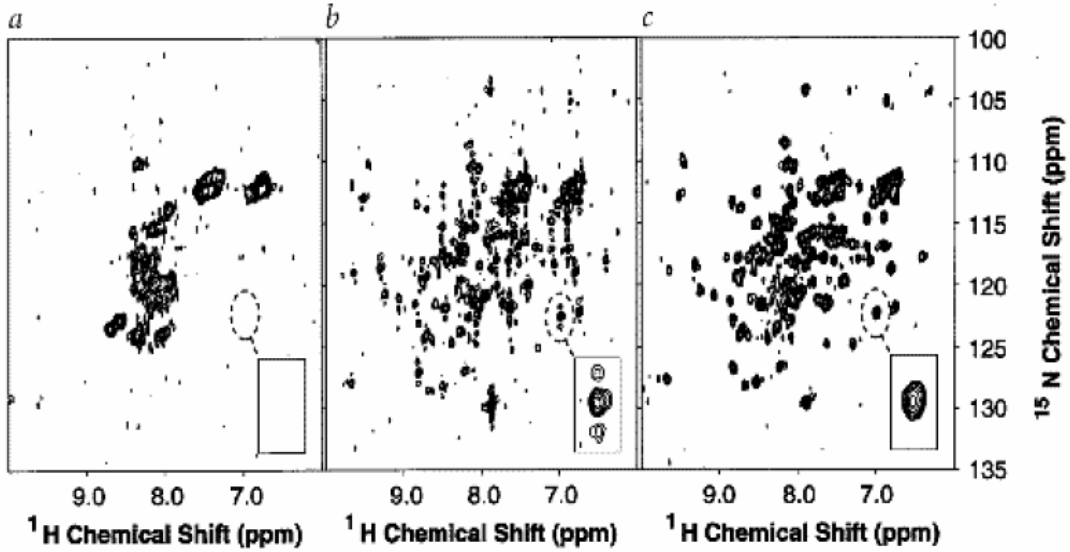

^{1}H-^{15}N HSQC spectra of bovine lactalbumin at 3 °C during different stages of the folding process.

a, Poorly resolved spectrum of the denatured state (A-state) at pH 2.0 recorded before the initiation of refolding.
b, Kinetic spectrum accumulated during folding (30 min).
c, Well resolved spectrum of the native (N) state at pH 7.0 recorded after the refolding reaction.
The insets show enlargements of the region containing the Val 92 resonance of the N-state. The lower intensity of this resonance in spectrum (b) compared to (c), and the negative features above and below the central peak contain information on the local rate of formation of native structure.

NMR Supplement II, *Nature Struct. Biol.* (1998) **5**, 504 - 50

Resources and Further Reading

WWW:
http://www.embl.de/nmr/sattler/teaching

NMR theory:
• Spin dynamics - basics of nuclear magnetic resonance
Malcolm H. Levitt, Wiley 2001
• Protein NMR spectroscopy – Principles and Practice. Cavanagh, Fairbrother, PalmerIII, Skelton. Academic Press (1996)
• Multidimensional NMR in liquids - Basic principles and experimental methods. van de Ven, VCH (1995)
• Nuclear Magnetic Resonance Spectroscopy. Harris. Longman (1983)
• Principles of NMR in one and two dimensions. Ernst, Bodenhausen, Wokaun. Oxford (1989)

Biomolecular NMR:
• NMR of Proteins and Nucleic Acids. Wüthrich. Wiley (1986)
• Nature Struct. Biol. (1997) 4, 841-865 & 5, 492-522 (NMR supplement I & II)
• NMR spectroscopy of large molecules and multimolecular assemblies in solution. Wider, Wüthrich Curr. Op. Struct. Biol. (1999) 9, 594-601